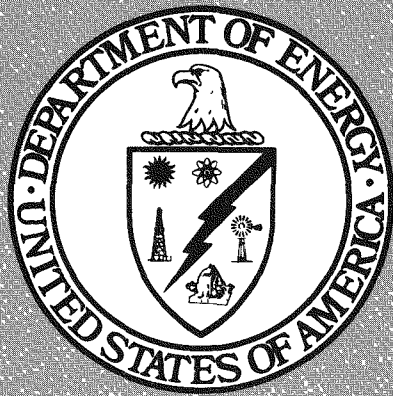


DR. 2773



COO-4299-032

**ORGANIC RANKINE KILOWATT ISOTOPE POWER SYSTEM**

**Final Phase I Report**

July 15, 1978

**Work Performed Under Contract No. EN-77-C-02-4299**

**Sundstrand Energy Systems  
Rockford, Illinois**

**TECHNICAL INFORMATION CENTER  
UNITED STATES DEPARTMENT OF ENERGY**

## **DISCLAIMER**

**This report was prepared as an account of work sponsored by an agency of the United States Government. Neither the United States Government nor any agency Thereof, nor any of their employees, makes any warranty, express or implied, or assumes any legal liability or responsibility for the accuracy, completeness, or usefulness of any information, apparatus, product, or process disclosed, or represents that its use would not infringe privately owned rights. Reference herein to any specific commercial product, process, or service by trade name, trademark, manufacturer, or otherwise does not necessarily constitute or imply its endorsement, recommendation, or favoring by the United States Government or any agency thereof. The views and opinions of authors expressed herein do not necessarily state or reflect those of the United States Government or any agency thereof.**

## **DISCLAIMER**

**Portions of this document may be illegible in electronic image products. Images are produced from the best available original document.**

## NOTICE

This report was prepared as an account of work sponsored by the United States Government. Neither the United States nor the United States Department of Energy, nor any of their employees, nor any of their contractors, subcontractors, or their employees, makes any warranty, express or implied, or assumes any legal liability or responsibility for the accuracy, completeness or usefulness of any information, apparatus, product or process disclosed, or represents that its use would not infringe privately owned rights.

This report has been reproduced directly from the best available copy.

Available from the National Technical Information Service, U. S. Department of Commerce, Springfield, Virginia 22161.

Price Paper Copy \$8.00  
Microfiche \$3.00

**FINAL PHASE I REPORT  
ORGANIC RANKINE  
KILOWATT ISOTOPE POWER SYSTEM**

**by**

**SUNDSTRAND ENERGY SYSTEMS  
ROCKFORD, ILLINOIS**

**Prepared for the  
U. S. DEPARTMENT OF ENERGY  
UNDER CONTRACT EN-77-C-02-4299**

**JULY 15, 1978**

## TABLE OF CONTENTS

---

<u>Title</u>	<u>Section No.</u>
Introduction . . . . .	1.0
Summary . . . . .	2.0
Flight System Conceptual Design (FSCD) . . . . .	3.0
3.1 FSCD Configuration	
3.2 Component Configuration	
3.2.1 Heat Generation System	
3.2.2 Radiator	
3.2.3 FSCD Power Conversion System (PCS)	
3.2.4 FSCD Ground Support Equipment (GSE)	
3.3 Flight System Performance	
3.3.1 Flight System Size	
3.3.2 Flight System Efficiency	
3.3.3 Performance Characteristics	
3.3.4 Prelaunch Handling	
Ground Demonstration System (GDS) . . . . .	4.0
4.1 GDS	
4.1.1 Comparison of GDS with FSCD Configuration	
4.2 Component Configuration	
4.2.1 Heat Generation System	
4.2.2 Radiator	
4.2.3 GDS Power Conversion System	
4.2.4 GDS Ground Support Equipment	
4.3 GDS Test Results	
Quality, Reliability, and Safety . . . . .	5.0
Recommended Follow-on Program . . . . .	6.0
6.1 Ground Qualification Program	
6.2 Technology Verification Program	

---

## LIST OF FIGURES

---

<u>Title</u>	<u>Figure No.</u>
SECTION 1.0 – INTRODUCTION	
KIPS Phase I Schedule . . . . .	1-1
SECTION 2.0 – SUMMARY	
Ground Demonstration System . . . . .	2-1
SECTION 3.0 – FLIGHT SYSTEM CONCEPTUAL DESIGN (FSCD)	
KIPS Baseline Flight System . . . . .	3-1
FSCD Schematic . . . . .	3-2
KIPS Typical Operating Conditions . . . . .	3-3
KIPS Isotope Heat Source Assembly (HSA) . . . . .	3-4
System Mount Schematic . . . . .	3-5
MHW Heat Source . . . . .	3-6
MHW Vent Design . . . . .	3-7
Boiler Tube Configuration . . . . .	3-8
KIPS Radiator . . . . .	3-9
FSCD Regenerator Configuration . . . . .	3-10
Jet Condenser . . . . .	3-11
Internal View of Jet Condenser Injector Passages . . . . .	3-12
Jet Condenser Orifice Tubes . . . . .	3-13
Redundant Bellows Configuration . . . . .	3-14
Flight System Turbine . . . . .	3-15
Turbine Nozzle Configuration . . . . .	3-16
KIPS Turbine Blade Profile . . . . .	3-17
Swept Vane Pump Impeller . . . . .	3-18
Alternator . . . . .	3-19
Turbine Bearing . . . . .	3-20
Pump Bearing . . . . .	3-21
KIPS Block Diagram . . . . .	3-22
FSCD Fluid Loop Controls . . . . .	3-23
KIPS Turbine Loop Flow Control Valve . . . . .	3-24
Control System Block Diagram . . . . .	3-25
KIPS Alternator Controller . . . . .	3-26
KIPS FSCD Controller . . . . .	3-27
Noncondensable Gas Separator . . . . .	3-28
Noncondensable Gas Separator . . . . .	3-29
FSCD Centrifugal Separator . . . . .	3-30
Flight System Start Module . . . . .	3-31
Flight System Envelope . . . . .	3-32
Output Power and Jet Condenser Inlet Pressure as a Function of Rotational Speed . . . . .	3-33
Performance Summary . . . . .	3-34
KIPS Loading and Assembly Station . . . . .	3-35

## LIST OF FIGURES (CONTINUED)

---

<u>Title</u>	<u>Figure No.</u>
SECTION 4.0 – GROUND DEMONSTRATION SYSTEM (GDS)	
Ground Demonstration System . . . . .	4-1
Typical GDS Operating Conditions . . . . .	4-2
GDS Schematic . . . . .	4-3
System Comparison . . . . .	4-4
Electrical Heat Source Installation . . . . .	4-5
Electrical Heat Source Assembly . . . . .	4-6
Electrical Heater . . . . .	4-7
Electrical Heater Schematic . . . . .	4-8
GDS Boiler Fin Tube Heat Exchanger . . . . .	4-9
Boiler Tube Penetration Assembly Installation . . . . .	4-10
Ground Demonstration System Radiator Assembly . . . . .	4-11
GDS Radiator . . . . .	4-12
GDS Radiator Extrusion/Adapter to Header Termination . . . . .	4-13
GDS Radiator Tube Extrusion . . . . .	4-14
Relationship of Radiator Weight of Tube and Header Probability . . . . .	4-15
System Comparison . . . . .	4-16
Regenerator Configurations . . . . .	4-17
Jet Condenser Configurations . . . . .	4-18
Accumulator Configurations . . . . .	4-19
GDS Combined Rotating Unit . . . . .	4-20
GDS Combined Rotating Unit . . . . .	4-21
Combined Rotating Units . . . . .	4-22
GDS Pump . . . . .	4-23
Flow Control Valve . . . . .	4-24
Radiator Bypass Valves . . . . .	4-25
GDS Controller . . . . .	4-26
GDS Start Module Schematic . . . . .	4-27
Heat Source Auxiliary Cooling Schematic . . . . .	4-28

## SECTION 5.0 – QUALITY, RELIABILITY, AND SAFETY

## SECTION 6.0 – RECOMMENDED FOLLOW-ON PROGRAM

KIPS Phase II Schedule . . . . .	6-1
KIPS Program Plan Schedule - Phase III . . . . .	6-2

## LIST OF TABLES

---

<u>Title</u>	<u>Table No.</u>
SECTION 1.0 – INTRODUCTION	
SECTION 2.0 – SUMMARY	
SECTION 3.0 – FLIGHT SYSTEM CONCEPTUAL DESIGN (FSCD)	
KIPS Characteristics . . . . .	3-A
Flight System Radiator Design Performance Criteria and Design Constraints . . . . .	3-B
Expected Load Environments . . . . .	3-C
Jet Condenser Geometry and Performance . . . . .	3-D
Blade Geometry at Pitch Line . . . . .	3-E
KIPS GDS Alternator Insulation System . . . . .	3-F
Radial Bearing Geometry . . . . .	3-G
Thrust Bearing Geometry . . . . .	3-H
Pivot Design . . . . .	3-I
Flight System Weight Breakdown . . . . .	3-J
Flight System Design Point . . . . .	3-K
System Performance as a Function of Turbine Inlet Temperature . . . . .	3-L
Startup Times . . . . .	3-M
SECTION 4.0 – GROUND DEMONSTRATION SYSTEM (GDS)	
GDS Radiator Design Performance Requirements and Design Constraints . . . . .	4-A
Summary of KIPS Phase I Test Results . . . . .	4-B
SECTION 5.0 – QUALITY, RELIABILITY, AND SAFETY	
SECTION 6.0 – RECOMMENDED FOLLOW-ON PROGRAM	
Phase II Task Summary . . . . .	6-A

## LIST OF ABBREVIATIONS

---

### SYSTEM

AC	Alternating current
AWG	American wire gauge
BOM	Beginning of mission
CRU	Combined rotating unit
DC	Direct current
DOE	Department of Energy
ECM	Electro chemical machining
EDM	Electrical discharge machining
ECS	Emergency cooling system
EHDS	Emergency heat dump system
EHS	Electrical heat source
EOM	End of mission
FSA	Fuel sphere assembly
FSCD	Flight system conceptual design
GDS	Ground demonstration system
GIS	Graphite impact shell
GSAR	Ground safety analysis report
GSE	Ground support equipment
HSA	Heat source assembly
IHS	Isotope heat source
IHSA	Isotope heat source assembly
IUS	Interim upper stage
ID	Inner diameter
KIPS	Kilowatt isotope power system
L/D	Length to diameter ratio
MHW	Multi hundred watt
NCGS	Non condensable gas separator
OD	Outer diameter
PCS	Power conversion system
PICS	Post impact containment shell
PLR	Parasitic load resistor
PRD	Pressure relief device
PWM	Pulse width modulated
QD	Quick disconnect
RA	Radiator assembly
RTG	Radioisotope thermo electric generator
UV	Ultra violet
VCO	Voltage controlled oscillator

### UNITS

Amps	amperes
Btu	British thermal unit
db	decibel
deg	degree
°F	degrees Fahrenheit

## LIST OF ABBREVIATIONS (CONT'D)

---

ft	foot
g	gravitational acceleration units (32.2 ft/second <sup>2</sup> )
grms	root mean square acceleration units
gpm	gallons per minute
hr	hour
hz	hertz (cycles/second)
in	inch
kVA	kilo volt amperes
kw	kilowatt
lbm	pound mass
lbs	pound
M	mach number
mil	1/1000 inch
msec	1/1000 second
oct	octave
OD	outer diameter
psi	pounds/inch <sup>2</sup>
psia	pounds/inch <sup>2</sup> absolute pressure
psid	pounds/inch <sup>2</sup> differential pressure
psig	pounds/inch <sup>2</sup> gauge pressure
Ph	radiator header probability of non-puncture
P <sub>(o)</sub>	overall probability of non-puncture of radiator
PT	radiator tube probability of non-puncture
rad/sec	radians per second
Re <sub>D</sub>	Reynolds number based on diameter
rpm	revolutions per minute
sec	second
sq. in	square inches
torr	millimeters of mercury pressure
VAC	volts — alternating current
VDC	volts — direct current
W(e)	watts — electrical
W(t)	watts — thermal
Watts <sub>e</sub>	watts — electrical
$\alpha_s$	solar absorptance
$\epsilon_h$	hemispherical emittance

**SECTION 1.0**  
**INTRODUCTION**

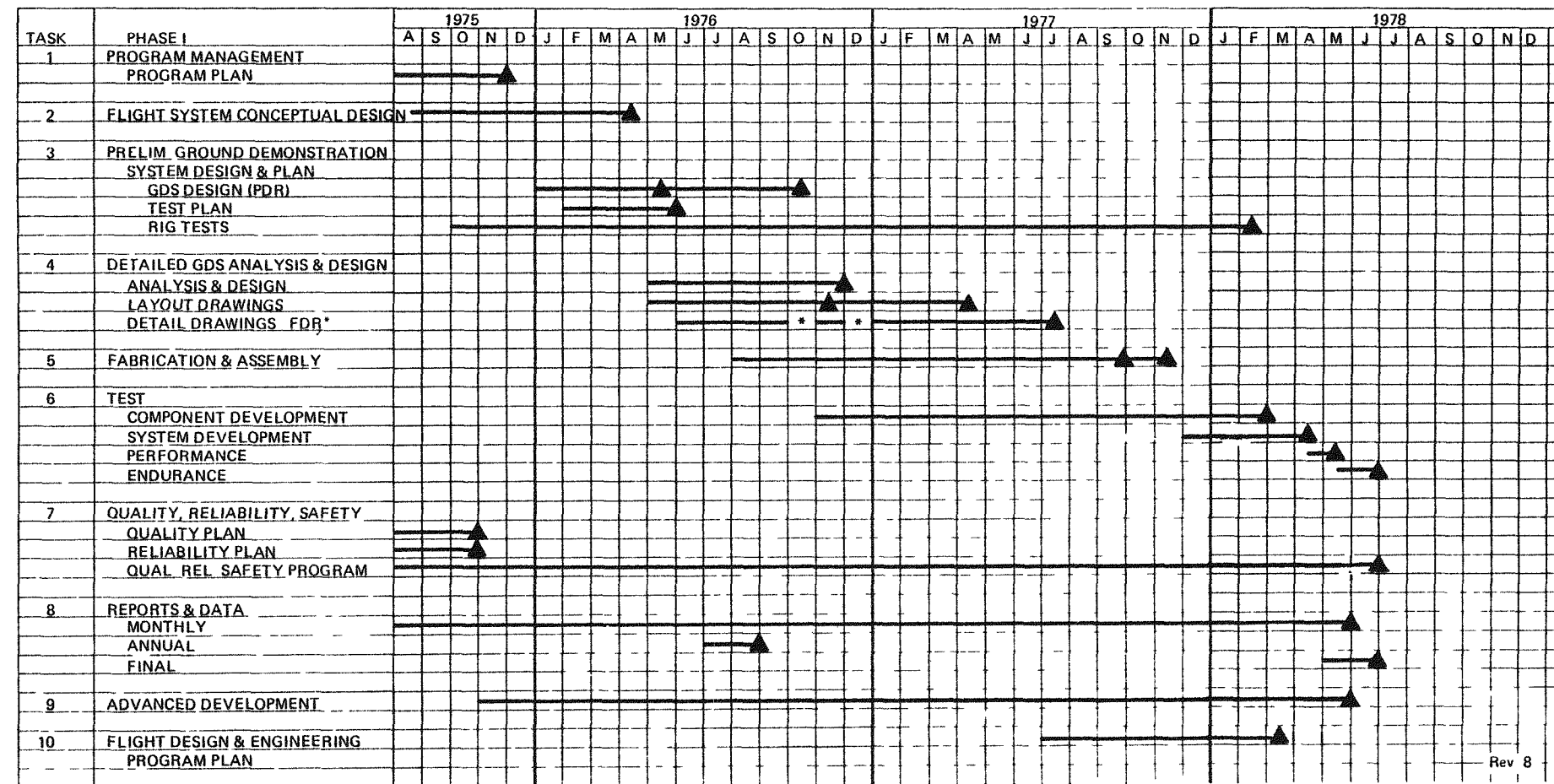


**Figure 1-1 KIPS Phase I Schedule**

**SECTION 2.0**

**SUMMARY**

## **SECTION 2.0**

### **SUMMARY**

---

The principal Phase I program objectives were met and are summarized below:

- Flight System Conceptual Design (FSCD) — The FSCD presented in this report is the original design updated to incorporate the pertinent results of testing and continuing analysis. The flight weight goal of 450 pounds for a 1300 watt system still appears to be realistic. However, for lower risk, first generation flight hardware, a 475 pound system is proposed.
- Ground Demonstration System (GDS) — The GDS which was designed, fabricated, and tested in Phase I is shown in Figure 2-1. As discussed in this report, this GDS is highly prototypic of the proposed flight system. The notable difference being the use of electric heaters to simulate the multihundred watt isotope heat source and the use of bolted flanges in lieu of welding to facilitate disassembly and reassembly during development testing.
- GDS Test Results — The GDS demonstrated a system efficiency of over 15 percent. Development areas have been identified that make over 18 percent a realistic goal. The 1000 hour endurance test on the final GDS configuration was completed.

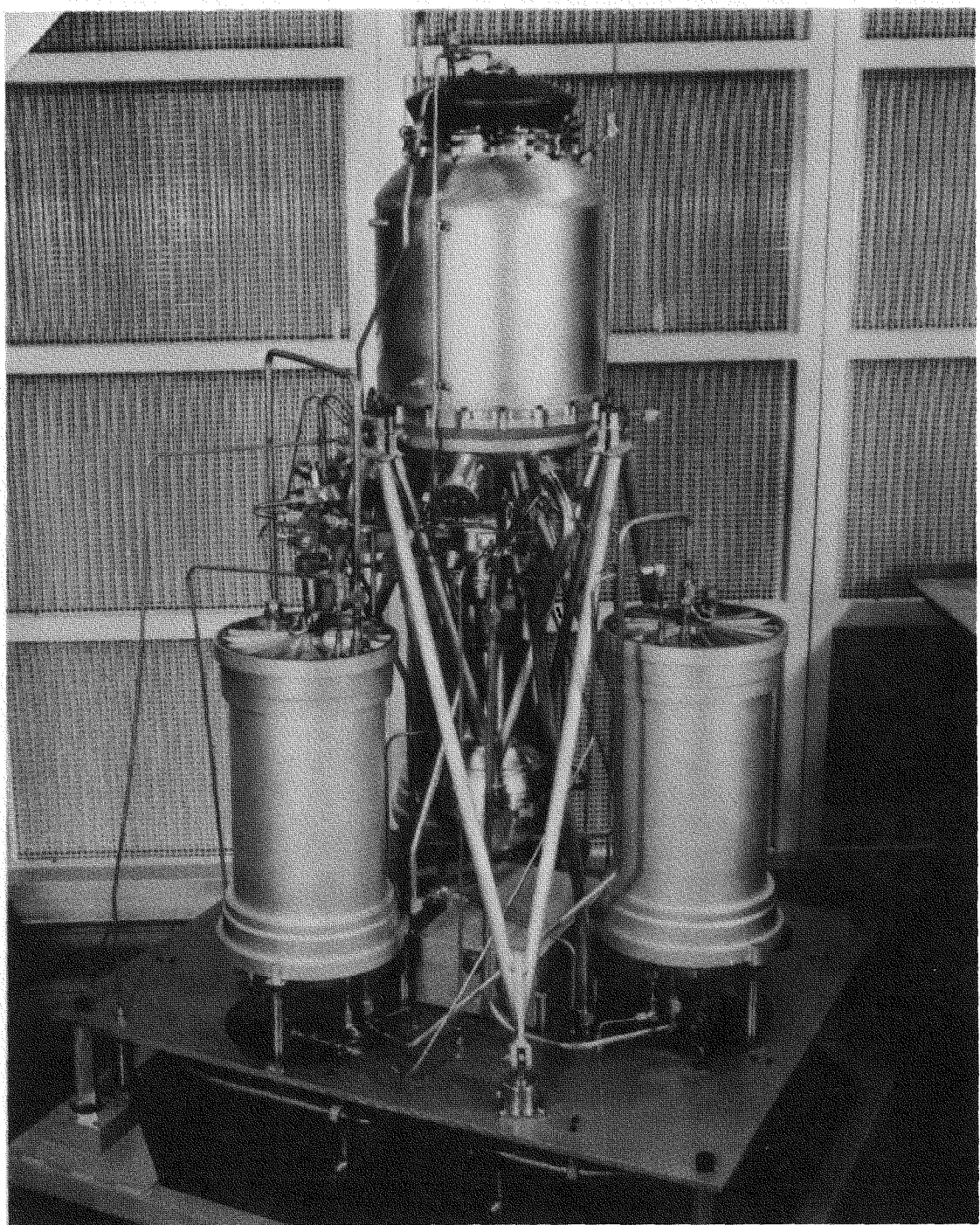


**Figure 2-1 Ground Demonstration System**

**SECTION 3.0**

**FLIGHT SYSTEM CONCEPTUAL DESIGN (FSCD)**

## SECTION 3.0

### FLIGHT SYSTEM CONCEPTUAL DESIGN (FSCD)

---

The KIPS Flight System Conceptual Design (FSCD) is illustrated in Figure 3-1.

The heat source assemblies are located symmetrically around the power conversion system and at the base of the radiator assembly which is mounted to the spacecraft bulkhead.

The major subsystems are:

#### Power Conversion System (PCS)

- Combined Rotating Unit (CRU) - turbine, alternator, pump and bearings
- Electrical and fluid controls
- Regenerator, jet condenser and accumulator

#### Heat Source Assembly (HSA)

- Multi Hundred Watt (MHW) heat source
- Boiler and auxiliary cooler
- Emergency Heat Dump System (EHDS)
- Structure/Insulation system

#### Radiator Assembly (RA)

- Radiator
- Auxiliary cooler
- Bypass valve

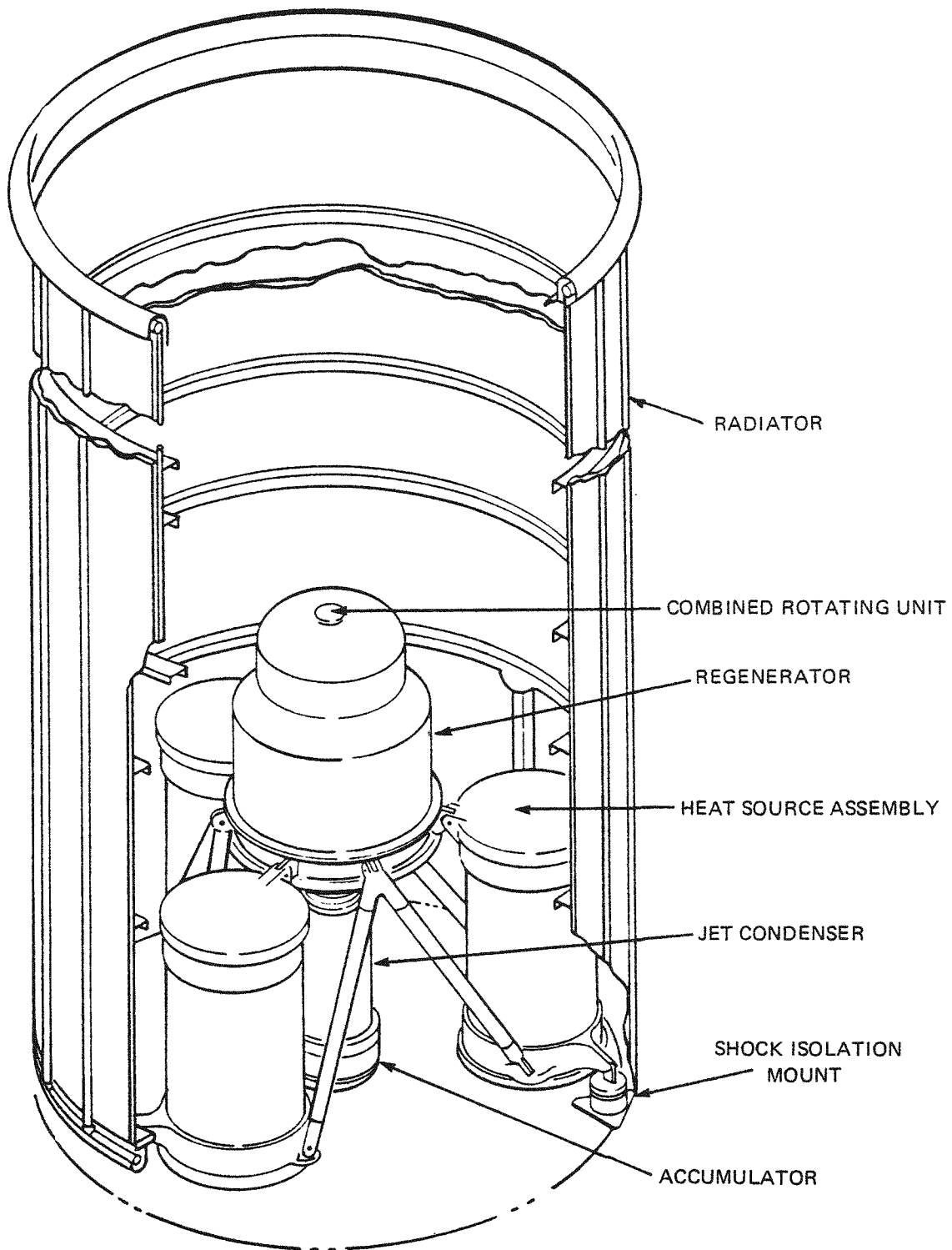


Figure 3-1 KIPS Baseline Flight System

Key features of the KIPS design are radioisotope heat source assemblies, a supersonic axial impulse turbine, homopolar inductor alternator, centrifugal pump, working fluid lubricated fluid film bearings, once-through radiantly heated boiler, jet condenser, liquid working fluid pumped radiator, and electronic controller.

Figure 3-2 is a schematic of the KIPS. The KIPS uses an organic working fluid, Dowtherm A – high purity eutectic of biphenyl and phenyl ether, in a Rankine thermodynamic cycle. It consists of two working circuits, the power loop and the heat rejection loop.

In the first loop, three radioisotope heat source assemblies provide energy to Dowtherm working fluid. This energy preheats and boils the fluid, creating a vapor which drives the turbine. The alternator, mounted directly on the turbine shaft, provides electrical power for the spacecraft. After the vapor leaves the turbine, it passes through a regenerator where the remaining superheat is used to preheat the liquid which is entering the heat source assemblies (boilers). The desuperheated vapor then passes through a condenser, changing to a liquid, and then to the pump, which pressurizes the liquid to the point necessary to complete the cycle.

In the heat rejection loop, a liquid circuit transfers the heat of condensation to the radiator, where the heat is rejected to space. This liquid then returns to the condenser, where the cold liquid provides the heat sink for the vapor condensation to take place in the jet condenser. The liquid of this circuit is mixed with the power loop fluid in the jet condenser before passing through the system pump.

The controls of the system are simple. A flow control valve maintains constant temperature at the turbine inlet as the radioisotope decays slightly over the seven year lifetime; a radiator bypass valve maintains a constant temperature of the liquid into the jet condenser as the spacecraft cycles from light to dark conditions in the space environment; the electronic controller provides voltage and speed control as the electrical load demand on the KIPS is changed.

Three units of ground support equipment will be used. The start module is used to start the power system either for a ground start or a space start. The preferred mode of operation is a ground start. In this case, the start module would be disconnected prior to launch and the KIPS would be operating and producing partial power as required during launch and orbit transfer. The heater temperature control support module is used for cooling during the period between heat source assembly and power system startup. It is also used as emergency cooling for the heat source while the system is in the Space Shuttle. This cooling is supplied by a ground module for the Titan III and the launch vehicle for the Space Shuttle. The heat rejection support module is used for on-the-pad cooling prior to launch for Titan III applications and continuously while in the Shuttle bay. These support modules are decoupled after performing their function and are not part of the KIPS/Spacecraft system that is injected into operational orbit.

Figure 3-3 is a block diagram of the system illustrating typical operating conditions. As described above, the liquid outlet from the pump is split into two loops. The power loop passes liquid through the regenerator to extract energy from the turbine exhaust vapor. At the energy source, additional heat is transferred to the working fluid which is vaporized to drive the turbo-pump alternator. The cooling loop passes liquid flow through the radiator to reject waste heat and then to the jet condenser to condense the vapor emanating from the regenerator. The combined liquid is returned through the accumulator to the pump. As indicated in Figure 3-3, the organic Rankine cycle KIPS has a maximum power conversion system temperature of only 650°F which allows design with common materials as presented in this section.

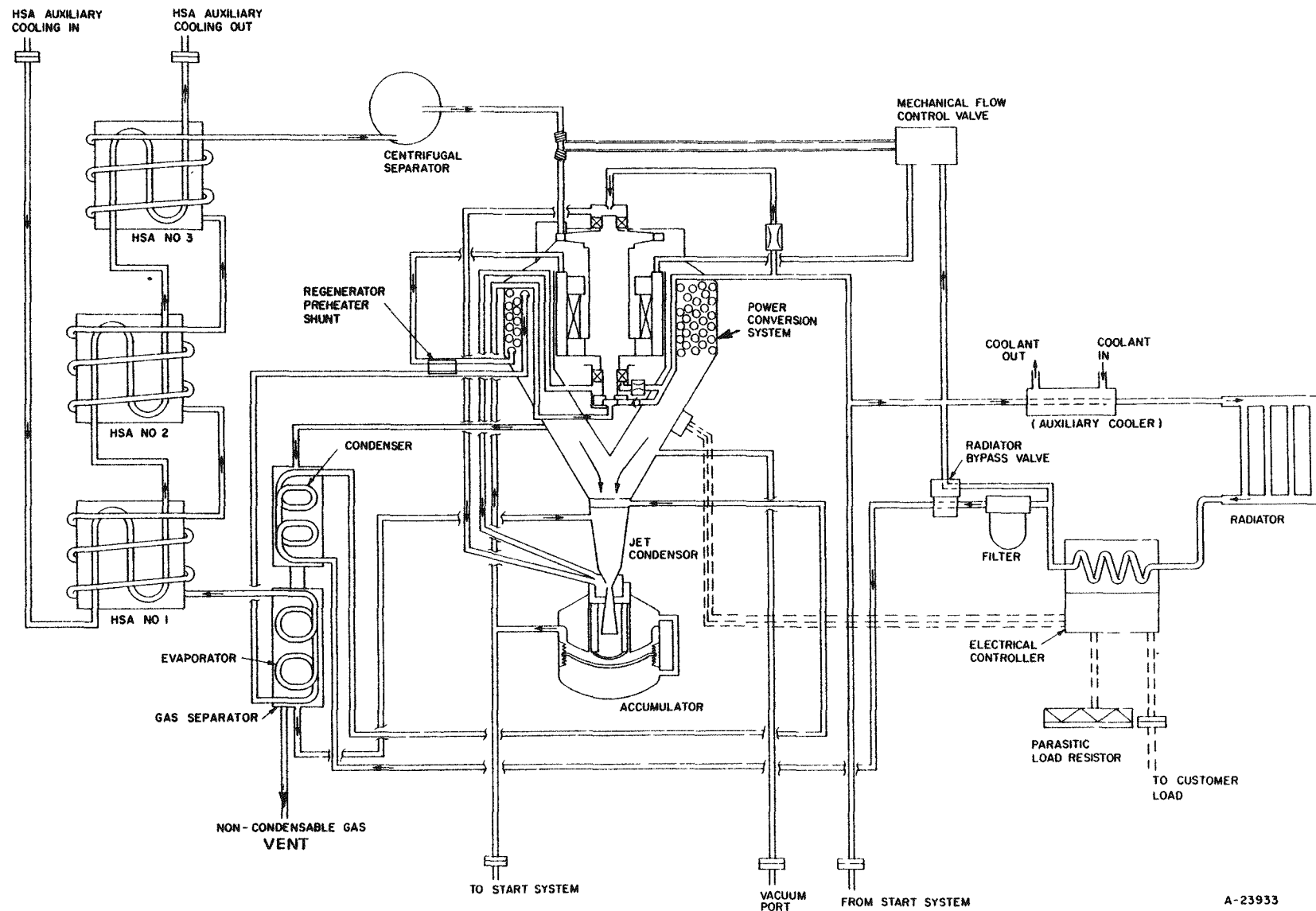


Figure 3-2 FSCD Schematic

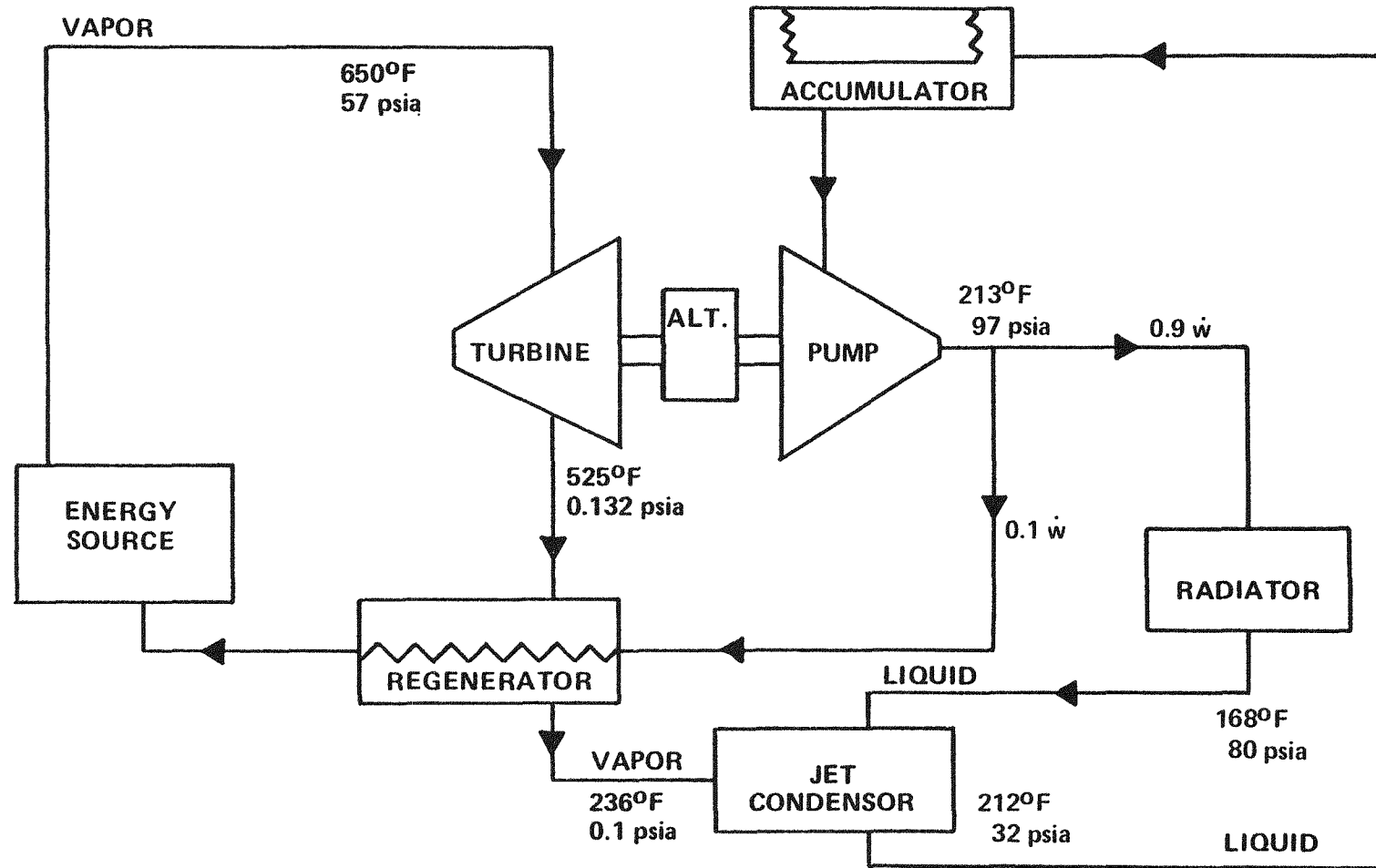


Figure 3-3 KIPS Typical Operating Conditions

Table 3-A is a summary of performance indicating the overall characteristics of the KIPS for the seven year life and five year mean mission duration. Total wet weight is 475 pounds. This system has not yet been fully weight optimized. The 450 pound goal is considered to be realistic for KIPS. A comprehensive weight reduction effort is planned for Phase II. For 1300 watts of electrical power at beginning of mission, the overall efficiency of the 28 VDC  $\pm$  2% system is 18.1%. Overall dimensions are 52 in. diameter by 96 in. long which is the result of optimizing the radiator as a function of liquid side delta P and weight. These dimensions can be changed to accommodate booster or spacecraft constraints. The KIPS is designed to be operating and generating power during launch, parking orbit and orbital transfer to final orbit.

In addition to meeting the basic performance requirements of efficiency, speed control, quality of output power, weight and size, the KIPS is designed to accommodate Isotope Heat Source (IHS) cooling, spacecraft integration, and launch requirements on the Space Shuttle as well as the Titan IIIC. Appropriate cooling provisions have been designed into the IHS and the radiator to provide heat rejection to secondary fluids with both the system operating and nonoperating. After the system has been started, power conversion system (PCS) operation is completely self-controlling. If the constant speed mode of operation is selected, the electrical speed control system will automatically transfer excess electrical output capacity to the dissipative load bank as required to keep speed constant.

When the speed control circuit is disabled for launch, the combined rotating unit (CRU) operates at design point speed at maximum load and at a higher rotative speed at low load. In either mode of operation, a voltage regulator keeps output voltage constant at any customer applied load from zero to rated load.

The radiator can be excessively cooled without affecting system operation because system heat rejection is controlled by the radiator bypass valve. This feature permits auxiliary cooling of the radiator during system checkout or prelaunch operation.

Table 3-A KIPS Characteristics

Rated Output Power	1300W(e) BOM
Optional Ratings	500 to 2000W(e)
Input Power @1300W(e), Beginning of Mission (BOM)	7200 W (t)
Overall Thermal Efficiency (1)	18.1% rectified to 28 VDC
Peak Working Fluid Temperature	650°F
Total Weight(2)	475 pounds
Envelope Dimensions for 1300W(e) BOM <sup>(3)</sup>	52 inches Diameter 96 inches Length
Design Point Output Voltage	28 VDC ± 2%
Response - Variable Output Power - 0 to 100%	Milliseconds
Partial Output Power Capability	On Pad Launch to Parking Orbit Orbital Transfer to Final Orbit
Output Power Capability -0 to 100%	Spin Stabilized Spacecraft
Lifetime	7 years
Capable of Stable Operation with Unbalanced Solar Input	
Resistant to Natural & Induced Radiation	
(1)	With RTG topping, system efficiency can be increased to 22.1% or higher.
(2)	Based on updated flight system design utilizing conventional materials, weight reductions (such as alternate radiator configuration and CRU housing machining) to approach the 450 pound goal will be studied in the Phase II design phase.
(3)	Flexible in design for both size and shape to fit the specific spacecraft.

### 3.1 FSCD CONFIGURATION

---

The total system comprises a cylindrical radiator, a PCS, three isotope HSAs, and several minor additional components. The three major components are configured so that they can all be mounted to the spacecraft through three mount points, a fully determinant mounting arrangement. An isometric drawing of the system mounting arrangement is shown in Figure 3-1.

Each HSA is mounted to one of the shock isolation mounts through which the system is attached to the spacecraft. The PCS in turn is connected to each HSA via both a short linkage to the bottom of the HSA and direct attachment at the top of each HSA cylinder. The radiator is independently mounted to the three HSAs. This structural configuration results in high rigidity, in both bending and torsional modes, and light weight.

For shipping, ground checkout operation of the system with electric heat sources and for isotope fuel loading, the system will be mounted to a ground handling fixture which duplicates the spacecraft mounting locations and provides the necessary mount rigidity. In order to manipulate the system for the isotope fuel loading and for subsequent attachment to the spacecraft, three secondary mounting points are provided. These mount points are located in the top of each HSA and are accessible through the top of the radiator.

There are several major advantages to this system support configuration. The most important is that only three points of attachment are required to the spacecraft, allowing great flexibility in selection of mission. The fact that the components are mounted through the shock isolation mounts greatly reduces structural loading, particularly of the radiator, and means that no large differential motions occur between components. The use of the rigid HSA cylinders as load bearing members allows significant weight reduction from alternate mounting schemes.

Other system components, such as the electronic controller, parasitic load resistors, and radiator auxiliary heat exchanger are mounted to the radiator. All interfaces between the system and ground support equipment are located in one quadrant of the radiator. The electrical interface with the spacecraft is located in the same area. This location is flexible and can be varied to meet spacecraft requirements.

All component interconnecting and intraconnecting plumbing is appropriately supported to prevent vibration problems.

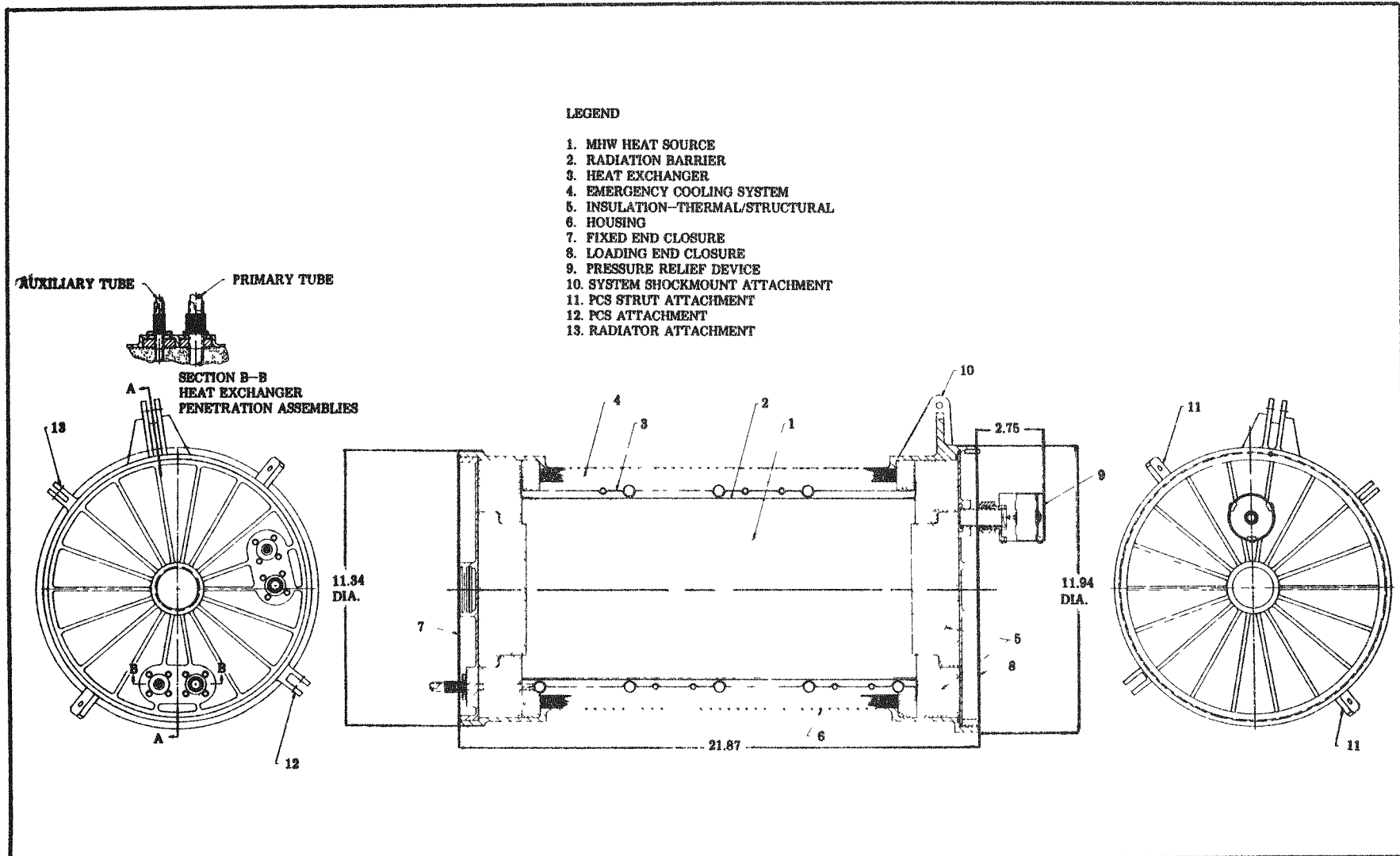


Figure 3-4 KIPS Isotope Heat Source Assembly (IHSA)

## 3.2 COMPONENT CONFIGURATION

---

The following subsections describe the major system components of the Flight System Conceptual Design.

### 3.2.1 HEAT GENERATION SYSTEM

The nuclear isotope generates heat and transfers it to the organic working fluid in three Heat Source Assemblies (HSA). Each HSA comprises a Multi Hundred Watt (MHW) type Isotope Heat Source (IHS), a fin-tube heat exchanger, a heat source structural support system, emergency cooling system, insulation and a gas management device.

#### 3.2.1.1 Isotope Heat Source Assembly (IHSA)

The Isotope Heat Source Assembly (IHSA) is a right circular, stepped cylinder which measures 11.34 in. diameter at the nonloading end, 10.13 in. diameter at the midpoint, 11.94 in. diameter at the loading end, 24.62 in. overall length from the fixed end of the housing to the pressure relief device and weighs 73.5 pounds (see Figure 3-4). There are three HSAs in the flight system, each supplying 2400 W<sub>(t)</sub> input to the flight system for conversion to output power.

Each IHSA serves as the mounting structure for a portion of the power conversion system (PCS) and is attached to the spacecraft structure by means of a single shockmount (see Figure 3-5). Inlet and outlet connections to the heat exchanger tubes are made at the fixed end of the unit while loading of the MHW heat source takes place through the loading end, which is at the opposite end of the unit. HSA fueling operations can be accomplished without having to disturb either of the heat exchanger tube connections.

To facilitate on-site ground checkout of the flight system prior to launch, the HSA is initially assembled using an electrical heater as the power source. After successful checkout, the electrical heater, center insulation disc and lower cover are removed and replaced with the MHW heat source, flight-type insulation disc, and end cover.

Loading of the MHW heat source takes place in a facility designed for this operation, using conventional fueling techniques and tooling.

Each of the IHSAs in the flight system is identical except for the heat exchanger centerbody. The major components of an IHSA are the MHW heat source, radiation barrier, heat source heat exchanger, emergency cooling system, fibrous insulation, heat exchanger tube penetration fitting assemblies, upper and lower end covers, housing and pressure relief device.

**3.2.1.1.1 MHW HEAT SOURCE (IHS):** The MHW heat source (Figure 3-6) is in the shape of a right circular cylinder measuring 7.42 in. diameter and 16.53 in. in length and weighs approximately 42 pounds. The primary heat source element is the Fuel Sphere Assembly (FSA) which is a self-contained modular fuel element. The FSAs are arranged in six (6) planes of four (4) spheres each; adjacent planes are rotated 45° to achieve nesting and to minimize length. The FSAs are held in place in groups of eight (8) by segmented graphite retaining rings with conical seats. Woven graphite cloth compliance pads are positioned between each FSA plane to achieve a tight fit without tight tolerance control. Three (3) FSA/retaining ring subassemblies are inserted into the

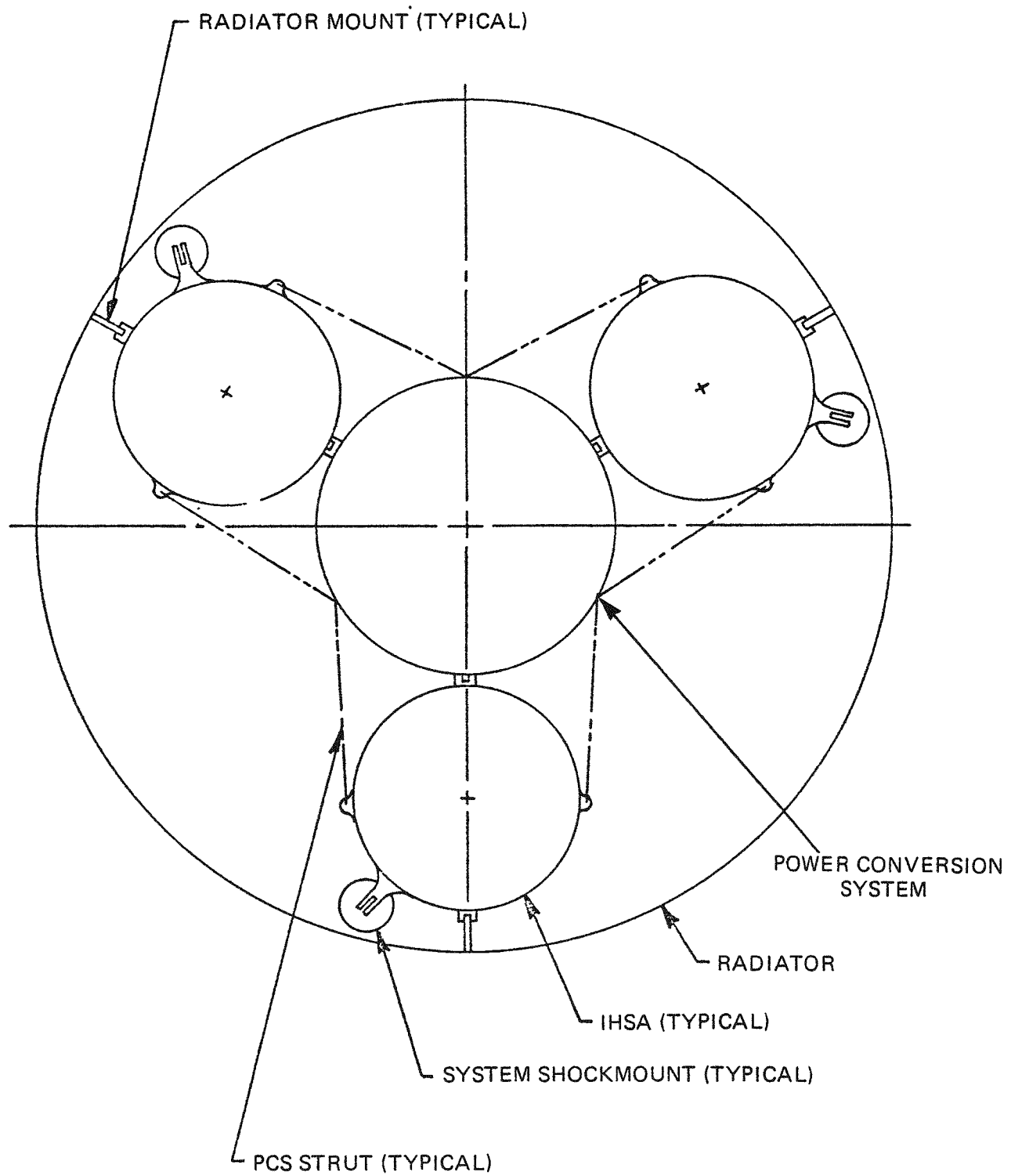


Figure 3-5 System Mount Schematic

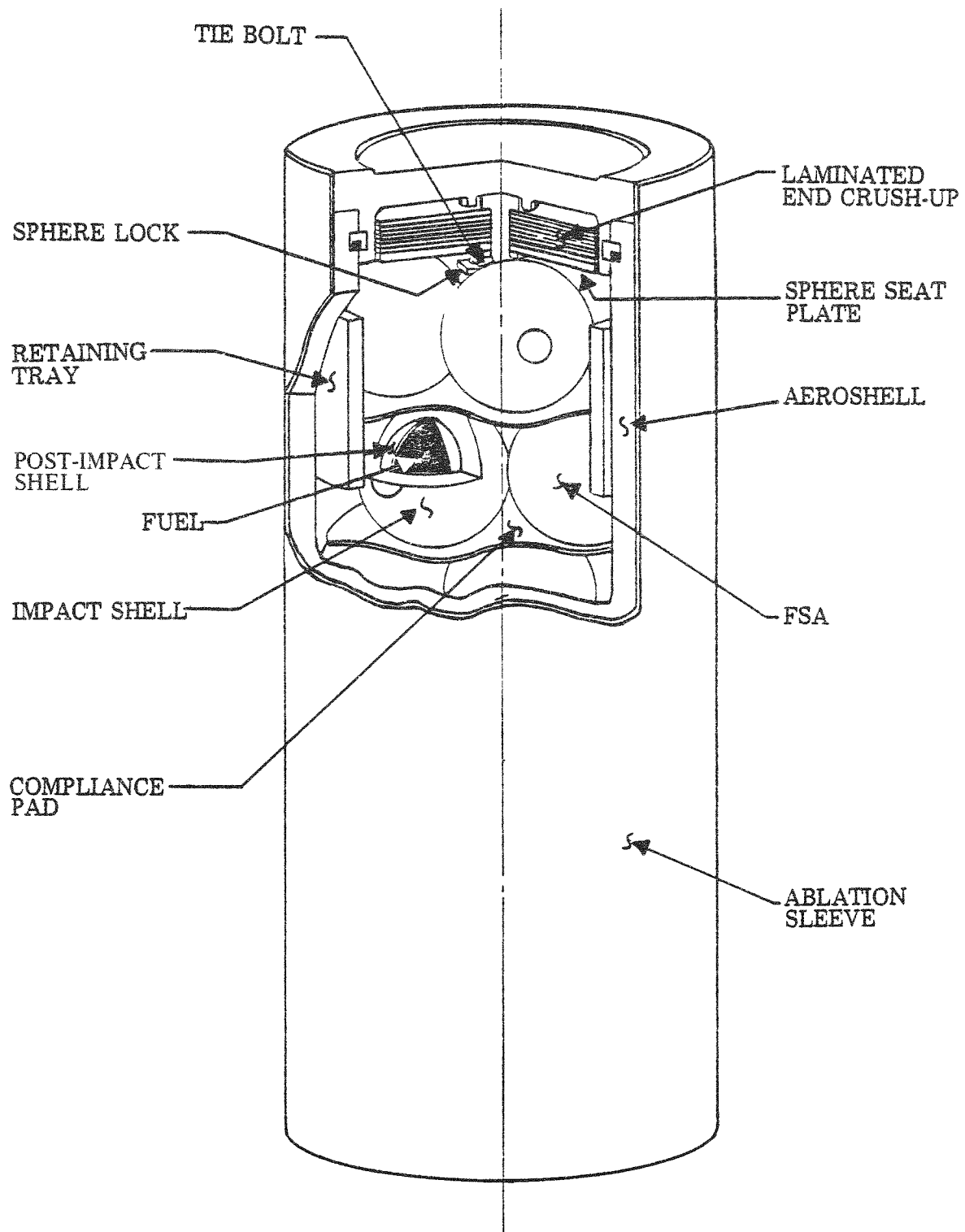


Figure 3-6 MHW Heat Source

graphite crush-up material which is provided at both ends for additional FSA impact protection, graphite end caps, which are captivated by an expandable ring, complete the assembly. A woven graphite emissivity sleeve is placed over the cylindrical portion of the aeroshell.

The Fuel Sphere Assembly (FSA) is the basic heat source fuel element. The FSA is comprised of the fuel sphere, the Post Impact Containment Shell (PICS), two vent hole filter subassemblies, a weld shield, and the Graphite Impact Shell (GIS). The FSA is designed to provide impact protection and post-impact containment for the fuel.

Each fuel sphere contains an initial thermal inventory of 100 watts nominal. A total of 24 spheres provides a nominal thermal power of 2400 watts for the heat source at beginning of life. The physical form of the fuel is a sphere shaped, solid ceramic compact of plutonium dioxide,  $\text{PuO}_2$ . The individual sphere diameter is 1.465 in.

The Post Impact Containment Shell (PICS) consists of two welded, 0.024 thick, 1.550 in. internal diameter, iridium hemispheres, which encapsulate the fuel sphere. Each PICS is designed with the following: (1) vent hole (0.005 in. diameter) and vent hole filter subassembly in each hemisphere which permits the helium gas to vent but prevents release of particulates from the interior of the PICS; (2) a burst disc, which is welded over the vent hole to seal the PICS hermetically, thus permitting decontamination after fuel encapsulation; and (3) a weld shield, mounted on one hemisphere of the set, to provide thermal protection to the fuel during closure welding and to prevent contamination of the weld by the fuel. The vent hole filter subassembly is welded around its periphery to the hemisphere; the weld shield is attached to one of the hemispheres by welding at its three tabs. When assembled, these components (the iridium hemispheres with vent holes, the vent hole filter subassemblies, the burst discs, and the weld shield) comprise the Post Impact Containment Shell (PICS); all components of the PICS are made of iridium. The hemispheres are grit blasted on their exterior surface to increase emissivity and thus enhance radiative heat transfer.

Figure 3-7 shows the arrangement of the vent hole filter subassembly. The filter medium is a frit of iridium powder bonded to a circular weld disk and also to a circular cover disk. There is a 0.125 in. diameter hole in the weld disk that acts as an exit plenum for the helium diffusing through the frit. The circular periphery of the frit provides a relatively large area through which the helium can enter.

The Graphite Impact Shell (GIS) is designed to provide impact protection to the fuel sphere and to the Post Impact Containment Shell under impact conditions associated with Heat Source terminal velocity. The GIS consists of a body and a cap which are produced by resin impregnating randomly wound spheres of Thornel-50 yarn and then pyrolyzing at 2500°F. The cap and body are threaded to provide a means of retention of the cap. The impact shell thickness is nominally 0.460 in. A flat surface is machined on the impact shell for alignment with the retaining ring. However, the graphite retaining ring used to assemble groups of eight (8) FSAs provides the added thickness needed to compensate for the thinner flat spot.

The Heat Source is designed to be protected from the severe aerothermodynamic heating environment that may be encountered during re-entry by the graphite aeroshell; the aeroshell also acts as the primary heat source structural member. The aeroshell is comprised of a cylindrical section and two end caps which are attached to the cylinder during the heat source assembly procedure. A purified poly crystalline graphite, POCO AXF-5Q1, is used for the aeroshell material.

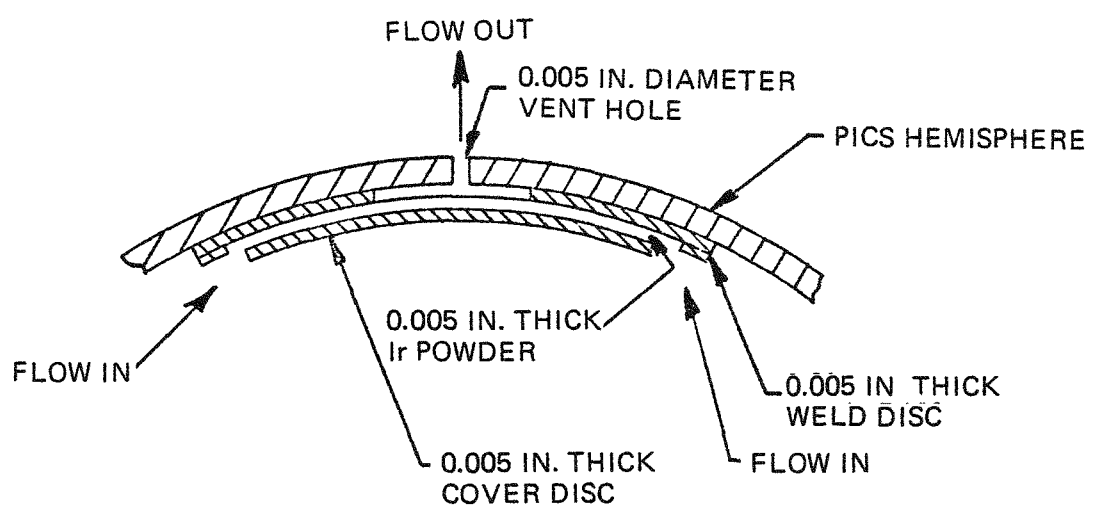


Figure 3-7 MHW Vent Design

The ablation sleeve is a cylindrical shell made of Pyrocarb-406 graphite with a wall thickness of 0.130 in. The sleeve enhances radiative heat transfer to the heat exchanger during normal operation and provides additional strength and protection for the aeroshell against excessive thermal stress during steep angle superorbital re-entries.

During the initial assembly of the MHW heat source by the Fueling Agency, a preload of approximately 800 pounds is placed upon one end of the heat source, while each heat source end plug is locked to the aeroshell by means of a graphite snap ring. Since the mating snap ring grooves in the aeroshell and end plug are made oversize in height because of the possible accumulation of tolerances during manufacturing and assembly operations, the initial 800 pound preload relaxes slightly. Because an 800 pound (minimum) preload is required to preclude excessive movement of the fuel sphere assemblies during the launch environment, it must be reapplied by the mounting of the heat source into its individual HSA.

The MHW heat source is supported by a compressive load applied to both ends of the heat source through Min-K TE-1400 support discs. Loads from the heat source are ultimately transmitted to the housing through each end cover. Preloading of the heat source takes place after it has been installed into the individual HSA.

**3.2.1.1.2 RADIATION BARRIER:** The radiation barrier, which is located in the annular space between the MHW heat source and heat exchanger, is required in order to raise the temperature of the MHW heat source during normal operation to keep the PICS in the required ductility range. It is attached to each end of the heat exchanger with sheet metal screws.

The radiation barrier is a formed, thin wall, hollow, right circular cylinder which measures 7.57 in. outside diameter by 0.010 in. thick by 16.53 in. long and is made from nickel 201 sheet. After forming, the two edges of the sheet, which are butted together, are seam welded along their entire length, to form a continuous cylinder. Each side of the cylinder is grit blasted with aluminum oxide grit to provide the desired emissivity characteristics. Nickel 201 was selected as the material primarily because in a vacuum environment it does not form an oxide thereby enabling stable emissivity characteristics to be achieved and it has a low carbon content which precludes embrittlement at operational temperatures.

**3.2.1.1.3 FSCD HEAT SOURCE HEAT EXCHANGER:** The KIPS boiler is a once-through design, comprising three, series connected, stainless steel, helically wound tube coils attached to the outside of a cylindrical copper fin. They are radiantly heated by MHW isotope heat sources. The tubes are wound in a double spiral fashion, with a reverse "U" bend at the middle of the tube length, in order that the inlet and outlet can be at the same end of the HSA.

Another tube, used for auxiliary cooling in the absence of Dowtherm flow, is attached to the fin adjacent to the boiler tube in a similar manner.

The heat source heat exchanger consists of a 0.020 in. thick copper shell that is formed around the primary and auxiliary cooling tubes. The primary cooling tube is 0.500 in. outside diameter by 0.035 in. wall stainless steel and the auxiliary cooling tube is 0.250 in. outside diameter by 0.035 in. wall stainless steel. Each tube is in a reverse spiral shape to enable the inlet and outlet portions of

the tubes to exit at the same end of the shell as shown in Figure 3-8. The tubes and shell are joined together by welding. The entire assembly is coated on the inside and outside diameter with an iron titanate coating which is intended to assist in controlling the isotope heat source temperature.

The three flight system heat exchangers are connected in series to form three fluid flow zones: the subcooled, two phase, and superheat sections. The lengths of the different heat transfer sections are: subcooled - 14.7 feet, two phase - 11.6 feet, and superheat - 1.35 feet. The subcooled and two phase sections contain a 0.3 in. diameter centerbody with a helically wound wire between centerbody and tube wall. The centerbody is discontinued after the point of critical quality (approximately 80%), but the helical wire is continued to the end of the two phase region and into the superheater. The centerbody is discontinued to ensure breakup of any rivulet type flow which may occur along the centerbody. The helical wire is wound to specified pitches to assure adequate induced acceleration levels on the fluid, ensuring that the liquid, when present, is centrifuged to the boiler walls.

The centerbody and helical wire increases the heat transfer coefficient, delays the onset of two phase flow and increases hydraulic stability by preventing plug-slug flow.

The minimum inside diameter of the heat exchanger shell is 7.63 in. and the maximum outside diameter, at the cooling tubes, is 8.81 in. The shell flange-to-flange length is 16.53 in. The heat exchanger fits in the annular space between the radiation barrier and the emergency cooling system and is supported at each end by clamping flanges between Min-K insulation rings. The shell flanges are hand formed at assembly, by making a series of cuts through the shell wall, and bent to rest upon the insulation.

**3.2.1.1.4 EMERGENCY COOLING SYSTEM (ECS):** An aluminum multifoil insulation system is used in the flight system to assure that isotope heat source temperatures are maintained within tolerable limits, should Dowtherm cease to flow through the heat exchanger, by acting as an emergency heat dumping system. In such an accident situation, the heat source temperature would rise, resulting in the melting of the multifoil insulation, thereby allowing the heat source to radiate heat through the heat exchanger walls to the housing thereby maintaining tolerable heat source temperatures. In addition to its ECS function, the multifoil system (because of its excellent insulation properties) limits radial heat losses to the housing walls. The multifoil insulation system is located in the annular space between the outside of the heat exchanger and the inside of the housing.

The multifoil insulation system is a hollow right circular cylinder measuring 8.895 in. inside diameter by approximately 0.42 in. thick by 15.00 in. long. It consists of one continuous length of 0.001 in. thick type 1100 aluminum alloy foil loosely wrapped sixty times around an 0.010 in. thick type 1100 aluminum alloy foil can. Spacing between wraps is intended to be approximately 0.007 in. The foil material is lightly coated on one side with zirconium oxide ( $ZrO_2$ ). The primary purpose of the coating is to insure a separation between wraps of the foil. Aluminum was selected as the foil system material because of its compatibility with the heat exchanger operating temperature and its low density.

**3.2.1.1.5 FIBROUS INSULATION:** Most of the insulation in the HSA is Min-K TE-1400, and serves three purposes: to minimize longitudinal and radial heat losses to the housing/end covers, to

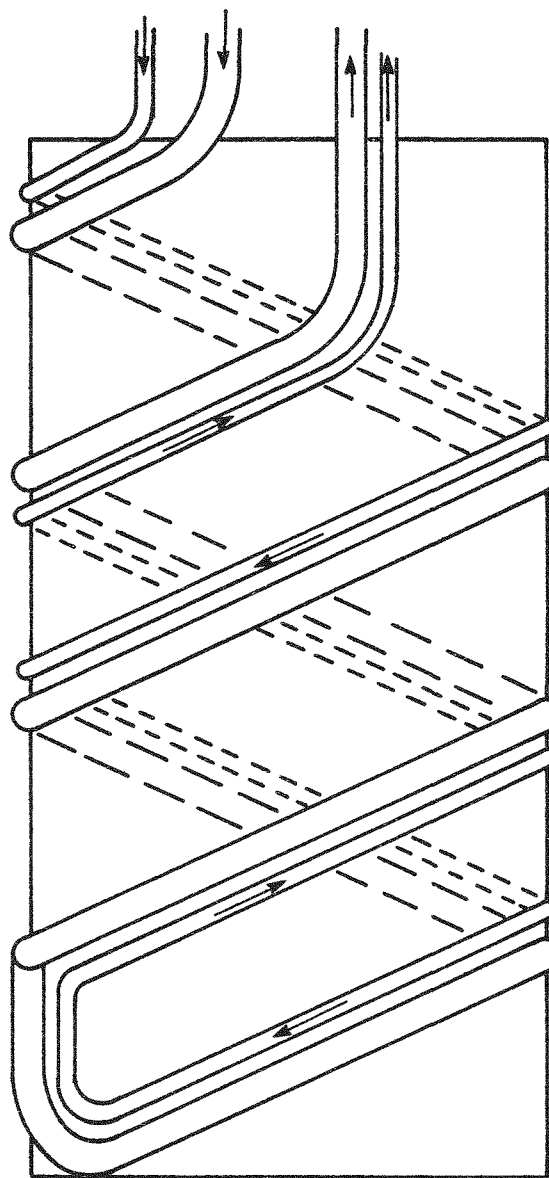


Figure 3-8 Boiler Tube Configuration

provide sufficient end preload for the isotope heat source and to support the heat exchanger and emergency cooling system. Min-K- TE-1400 was selected because of its temperature, thermal conductivity, and compressive strength properties.

**3.2.1.1.6 HEAT EXCHANGER TUBE PENETRATION ASSEMBLIES:** The penetration assembly fittings have two functions: to minimize the heat losses from the heat exchanger tubes to the end cover (where the tubes penetrate the cover) and to form a vacuum tight closure between these tubes and the end cover. The penetration assembly consists of a type 321 stainless steel formed bellows welded to a type 304 stainless steel flange. Stainless steel was selected because of its compatibility with the type 304 stainless steel heat exchanger tube material and for its relatively low thermal conductivity properties. There are four penetration assemblies in each HSA, two for the primary cooling tubes and two for the auxiliary cooling tubes.

The lower end of the bellows is pre-welded to the flange and is sized to allow the heat exchanger tube to pass through the bellows at assembly with approximately 0.06 in. radial clearance. The upper end of the bellows contains a reducing collar which is sized so the tube can be easily welded to the collar. This weld joint is made prior to outgassing the entire HSA.

There is a recess in each cover which is slightly larger than the outside diameter of the penetration assembly flange. The flange is isolated from the cover by a Viton rubber gasket and the radial clearance between the cover recess and the flange body. The only metal-to-metal contact in the penetration assembly/cover connection is through the four machine screws which attach the penetration assembly flange to the cover.

**3.2.1.1.7 END COVERS:** Each of the end covers is machined from a disc of 6061-T6 aluminum alloy plate. Based upon structural analysis, aluminum was chosen for the cover material because of its strength to weight characteristics. Each end cover is circular shaped, with a flat, smooth underside to assist in the sealing and insulation preload process and has ribs for added stiffness, machined as an integral part of the outside surface.

A single piece cover closes the upper end of the HSA and contains the inlet and outlet connection fittings for the heat exchanger. This cover is joined to the housing, at assembly, by welding. The lower end of the HSA is also closed with a single piece cover which is joined to the housing by means of a specially machined lock ring. This feature provides access to the inside of the HSA thereby enabling the electrical heat source to be removed and the isotope heat source to be installed.

**3.2.1.1.8 HOUSING:** The housing is machined from a hollow tube, 6061-T6 aluminum alloy forging which initially measures 14.00 in. outside diameter by 2.50 in. wall thickness by 23.00 in. long. Based upon structural analysis aluminum was chosen for the housing material because of its strength to weight characteristics. Because the physical properties of such a large diameter billet of material are not covered in existing commercial specifications, room temperature tests will be performed in accordance with ASTM E8-69 on test rings taken from the billet, in each of three directions, to verify that ultimate and yield strengths as well as elongation characteristics of the basic forged material will meet the properties which were used in the structural analysis to determine various wall thicknesses in the housing.

One end of the housing has an Acme thread which allows an end cover to be attached using a specially machined lock ring, the other end has a weld flange for attachment of the other end cover. The system attachment fittings are machined as an integral part of the housing. The upper end of the housing has two attachment fittings: one for attaching the PCS, the other for the radiator. The lower end has three attachment fittings: two for attaching the PCS (using struts), the third for attaching (through a shockmount) to the spacecraft structure.

**3.2.1.1.9 PRESSURE RELIEF DEVICE (PRD):** The pressure relief device (PRD) is a device used to vent the internal pressure of the HSA. It is attached to the lower cover during the pre-launch preparation cycle by means of a Swagelok-type fitting. The PRD has two primary functions: (1) maintain a hermetic seal, isolating the internal HSA from the air environment during handling and launch pad operations, (2) vent the HSA to space during the ascent period of launch and thereafter provide an orifice adequately large enough to maintain the HSA internal vacuum environment. The seal prior to launch is maintained by a puncture diaphragm which is welded into the PRD penetration assembly. The HSA is vented after launch by the action of a lance piercing the puncture diaphragm. This is caused by the expansion of an evacuated bellows/spring system which is activated by the reduction of atmospheric pressure subsequent to launch.

### **3.2.2 RADIATOR**

The flight system radiator assembly is an aluminum, welded/riveted assembly in the shape of a hollow right circular cylinder measuring 48.00 in. outside skin diameter by 96.00 in. header to header length and weighs 77.0 pounds. It has three mounting points which extend approximately 3.25 in. toward the inside to enable attachment to the Isotope Heat Source Assembly (IHSA). The radiator is spaced approximately 2.9 inches above the spacecraft mount structure to provide clearance for header connections, etc. (see Figure 3-9). Table 3-8 summarizes the radiator design criteria.

The radiator employs a forced convection heat transfer loop. The organic fluid passes through eighteen (18) vertical tube extrusions which are connected, at each end, through an adapter fitting, to a common header. Each extrusion serves three purposes: as a passageway for the organic fluid, as the required frontside and backside meteoroid armor protection, and as vertical stiffening for the radiator shell. Each header is made from a 0.500 in. outside diameter by 0.062 in. wall tube which is formed to a circular shape. They are protected from meteoroid puncture by a shadow shield which is riveted to the radiator structure.

The 0.025 in. thick radiator skin is spliced together by means of splice plates which are riveted in place. The extruded radiator tubes are seam welded to the skin prior to the sections being spliced together. Nine circumferential channel frames are riveted to the skin for structural support.

After the radiator has been fabricated and inspected, the exterior surfaces are coated with IITRI (Illinois Institute of Technology Research Institute) Z-93 thermal control coating. Z-93 is an inorganic type coating developed by IITRI which is based on a zinc oxide (ZnO) pigment with a potassium silicate ( $K_2SiO_4$ ) binder and offers acceptable beginning of life performance related material properties coupled with good reproducibility. However, future work will enable determination of radiation hardness requirements and a different coating may be required for some flight applications.

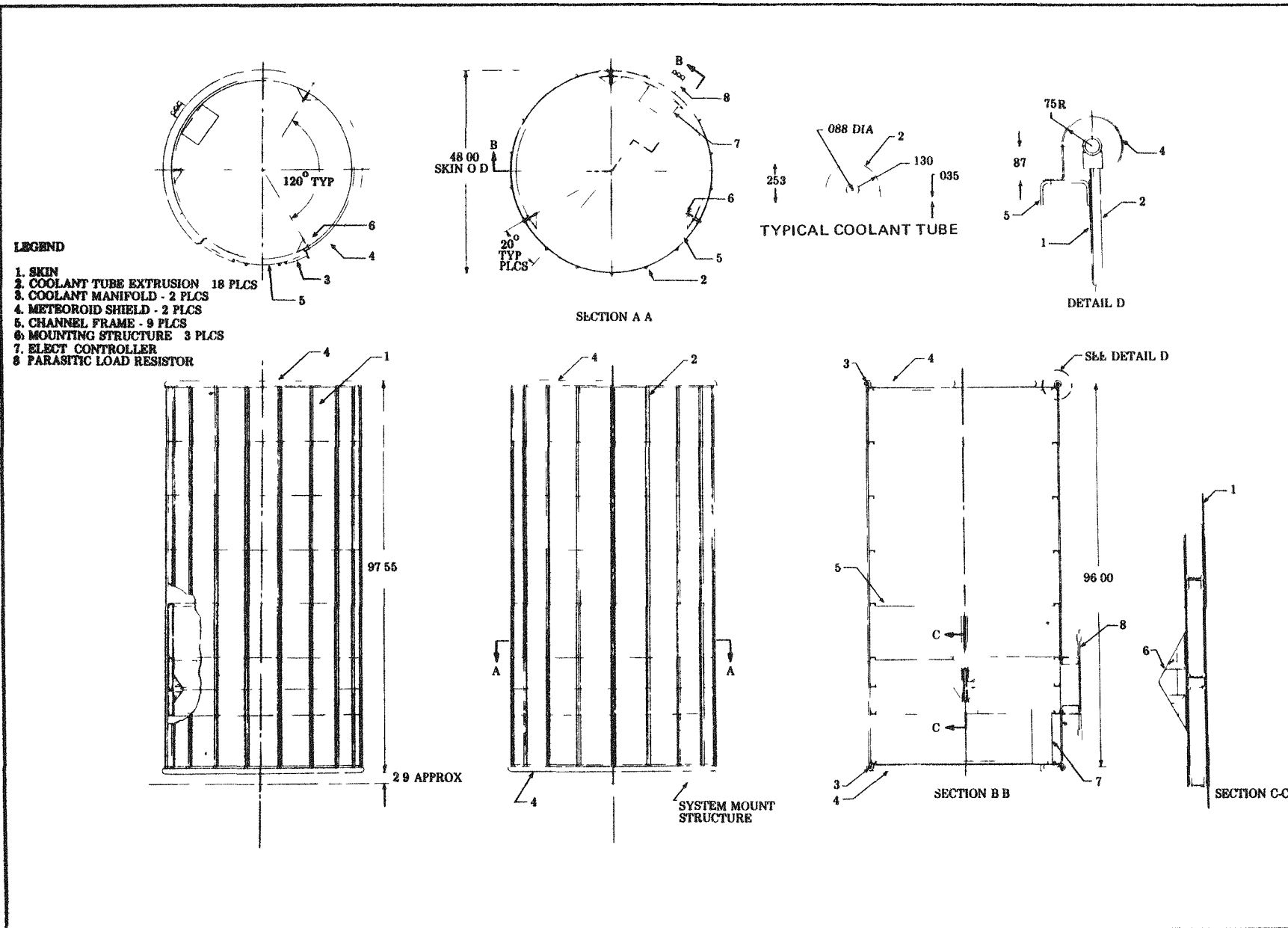


Figure 3-9 KIPS Radiator

Table 3-B Flight System Radiator Design Performance Criteria and Design Constraints

<u>Item</u>	<u>Design Value</u>
Waste Heat Load	20027 Btu/hr
Dowtherm Flow Rates	Maximum – 0.418 lbs/sec Nominal 0.268 lbs/sec Minimum – 0.107 lbs/sec
Radiator Coating Properties (IITRI Z-93)	Emissivity 0.925 Solar Absorptivity 0.25
Solar Heat Load	Geosynchronous Orbit Average Solar Load 35.25 Btu/hr-ft <sup>2</sup>
Dowtherm Inlet Temperature	212°F (Nominal)
Desired Overall Pressure Drop	≤ 10 psi (Nominal)
Reynolds Number at Exit of Flow Tubes	≥ 3000
Meteoroid Penetration Criterion (Total Radiator)	$P_{(o)} = 0.99$
Operational Lifetime	7 Years
Radiator Length Limit	8 Feet
Acoustic Noise/Spectrum	145 db Overall
Vibration/Shock	See Table 3-C

Table 3-C Expected Load Environments

<u>Environment</u>		
Acceleration	9g axial and 5g lateral simultaneous	
Vibration	Spectral Density	Frequency (Hz)
	Increasing 3 db/oct	10-900
	0.1875 g <sup>2</sup> /Hz	900-1400
	Decreasing 15 db/oct	1400-2000
	Overall level of 15.1 grms, test duration: 3 minutes along each of the three orthogonal axis	
Shock	3 pulses in each direction along 3 orthogonal axis (18 shocks total). Pulse as follows: 775 G's peak half cycle sine, 0.2 ± .1 msec pulse width	
Pressure	Sea level to 10 <sup>-10</sup> torr.	

The radiator also serves as the mounting structure for several other components. The electronic controller and auxiliary cooling tube are both attached to the inside of the radiator support structure and the parasitic load resistor is attached through the skin to the support structure as shown in Figure 3-9.

The FSCD radiator makes use of radiative heat transfer from the inside of the fin through the open end. This results in an effective radiator area increase of more than 10%. However, the use of the inside surface of the radiator to reject heat results in greater vulnerability of the flow tube backsides to puncture by meteoroids. In the present design the backside of the tubes are protected by only 60 mils of aluminum armor against direct strikes through the open end of the cylinder. The tube backsides are protected against micro meteoroids striking the outer surface of the cylinder because of the "bumper effect" of the radiator skin. The most vulnerable portion of the tube backside area to meteoroids streaming through the open end is the tube area near the top of the cylinder. For the portion of the tube area on the lower half of the radiator (nearer the base), the present 60 mils of armor is adequate protection because the "view factor" for direct strikes is small. Therefore, based on the present meteoroid environmental criteria, the upper portions of the tubes would require the addition of thin bumpers to insure complete protection if the cylinder end is open. The weight penalty would be minimal for these thin bumpers.

One radiator design characteristic which is possibly critical to overall performance objectives is the radiator coating properties at the end-of-mission (EOM). A number of coating systems are capable of providing the desired beginning of mission properties, but insufficient data exist to predict EOM (7 years) properties for most coatings. The selected coating for the KIPS program must resist not only the potential degradation mechanisms of ultraviolet exposure and space particle impacts, but also must satisfy the additional criteria that it be a nuclearly hardened coating. The IITRI Z-93 coating used for the GDS radiator, and assumed presently for the flight system radiator is expected to be as resistant to U.V. degradation as any coating which might be selected, but it is not a "radiation hardened" coating. Data for the so called "hardened coatings" are classified, and, therefore, if the "hardening" requirement remains as a criteria for KIPS missions, these coatings will have to be evaluated in Phase II for possible application.

**Radiator Auxiliary Heat Exchanger** — In order to reject the system waste heat both on the ground and in the Space Shuttle bay, an auxiliary waste heat rejection system will be incorporated. This system performs the function of the radiator. The heat exchanger is a simple, all aluminum, coaxial tube, counterflow device which is plumbed upstream and in series with the radiator. The system fluid passes through the center tube and the coolant passes through the outer tube. Placing the heat exchanger upstream of the radiator minimizes radiator temperature and, hence, minimizes heat rejection from the radiator to the Space Shuttle walls.

The heat exchanger is sized to reject the complete power conversion system (PCS) heat input of 7200 watts thermal since the unit could be operating in the Space Shuttle in an overspeed with no requirements for any power output.

### **3.2.3 FSCD POWER CONVERSION SYSTEM (PCS)**

The power conversion system comprises those components used to extract work from the superheated vapor and condense it to subcooled liquid. These components are the regenerator, jet condenser-accumulator, combined rotating unit (CRU), controls, associated hardware and plumbing.

### 3.2.3.1 Regenerator

The regenerator is an overall counterflow, spirally wound, finned tube configuration, mounted coaxially around the CRU. It consists of fourteen coils stacked one upon the other with liquid transfer to adjacent coils occurring at the ID and OD of the coil via a 180° return bend. This configuration results in a serpentine crossflow of the liquid from coil to coil, and gives compact system arrangement.

The coils are spaced and supported by baffles inserted between each coil. These baffles also ensure correct vapor flow through the regenerator. The entire assembly is held together with six tie bolts, as shown in Figure 3-10.

In order to prevent condensation of vapor on the first cold row of the regenerator core, a regenerator preheater has been incorporated to raise the liquid temperature above the local saturation conditions. This requires approximately a 2°F increase in liquid inlet temperature and a heat transfer of 100 BTU/hr. The heat input is obtained by routing the inlet and outlet plumbing tubes side by side and thermally shunting them together with a stainless steel block brazed to both tubes.

The regenerator coils are made from 6061 aluminum tubing extruded to form an integral fin/tube construction. The coils of the regenerator are separated from and supported by each other by means of 0.018 in. stainless steel (304L) baffle plates. The baffle plate assemblies are made by stamping the inner and outer plates and then joining the plates together using six equally spaced channels and welding them to the inner and outer plates. Each baffle is fabricated to ensure correct vapor flow through the regenerator. Six grooves 0.125 in. wide are machined in each coil on each side to match the baffle plate spokes and, thus, the plates nest between fins. This ensures that at least six fins are contacting coil to coil through the assembly. Nesting of the baffle plate struts into the fins gives a keying effect that allows the coils to expand radially but eliminates torsional motion. To constrain the regenerator, stiffer plates are needed at each end, and the coils are attached to the housings for axial constraint with preload on the coils.

A stiffer plate was made at the turbine end by adding six "T" sections to the baffle plate. Stiffness on the opposite end was obtained by utilizing the existing support structure frame and adding three smaller struts. The total coil assembly is mounted to the transition housing by means of six tie bolts which preload the assembly. Excessive torsional distortion is prevented by keying the turbine end baffle plate to the outer housing. Radial support is maintained by making the baffle plates a close conforming slip fit to the inner diameter of the outer regenerator housing.

The transition section between the regenerator and the jet condenser resulted from an aerodynamic design study. This study optimized the vapor flow for minimum pressure losses and to provide for uniform mixing prior to introduction to the jet condenser.

### 3.2.3.2 Condensing Heat Exchanger

The jet condenser consists of three major sections: the liquid injector, the vapor funnel, and the throat/diffuser.

The liquid injector is comprised of three hollow concentric rings supported by three equi-spaced elliptical hollow radial struts (see Figures 3-11 through 3-13). These form the liquid supply header

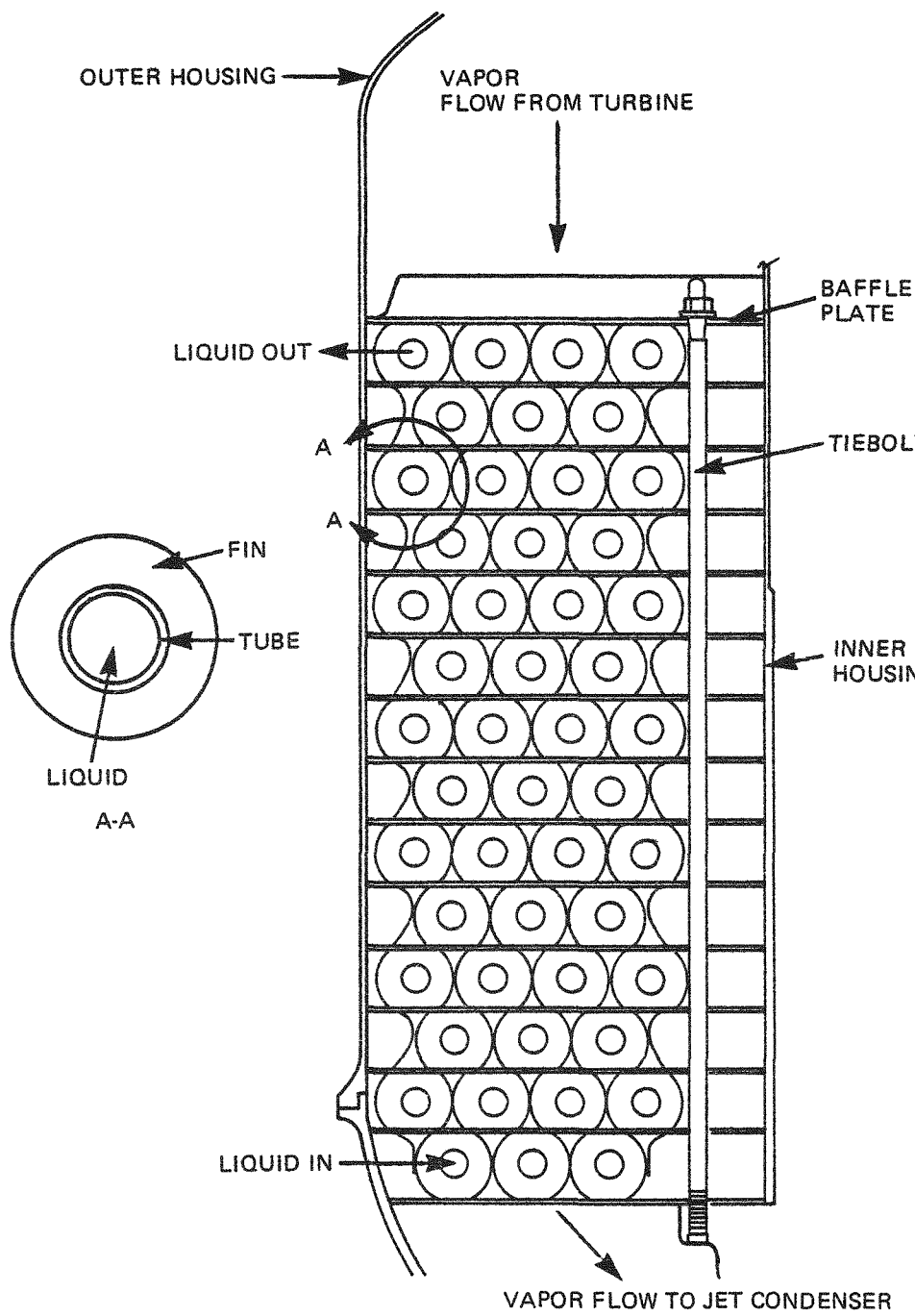


Figure 3-10 FSCD Regenerator Configuration

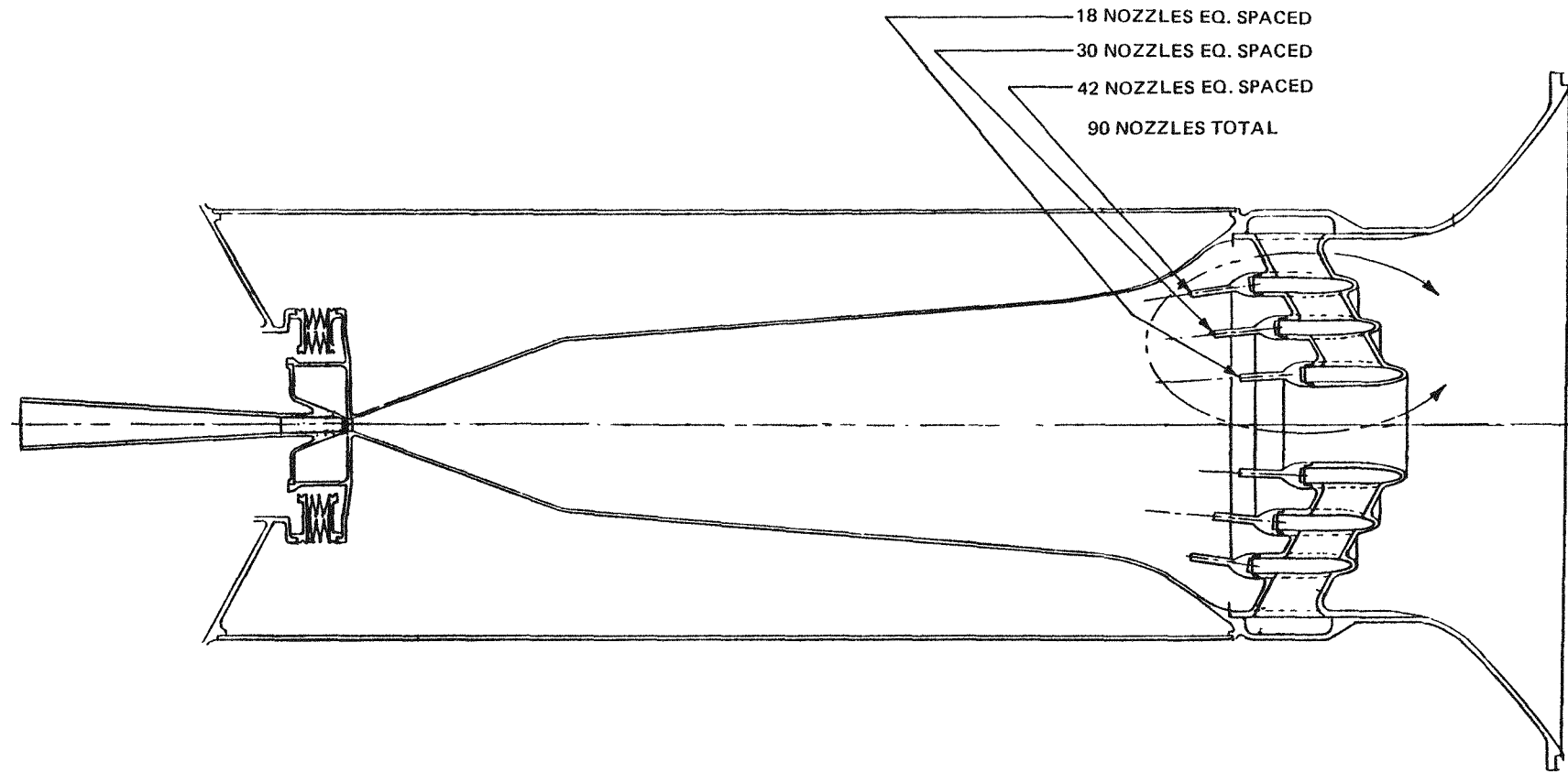


Figure 3-11 Jet Condenser

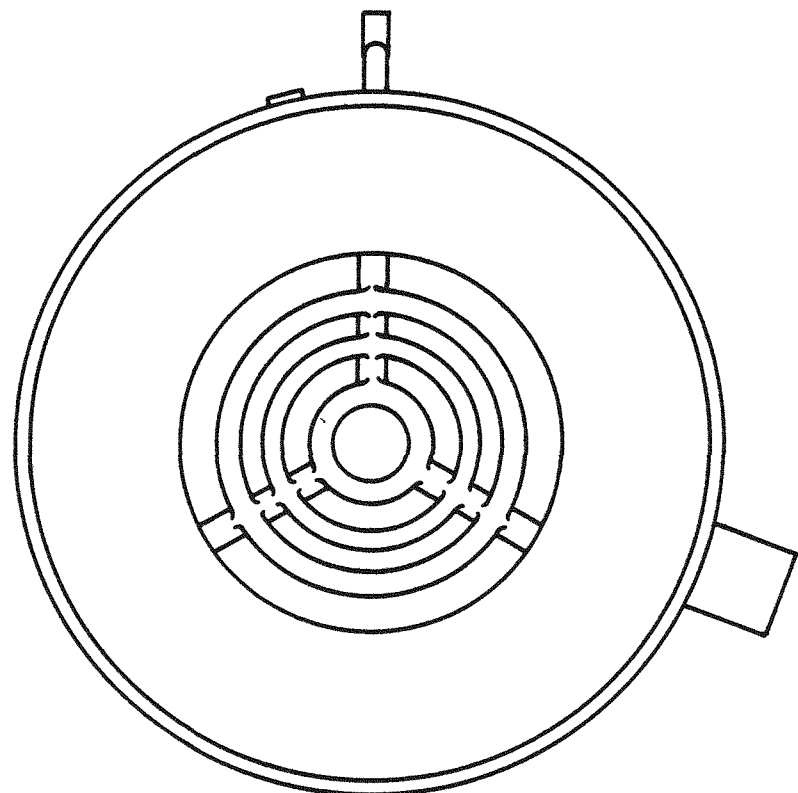


Figure 3-12 Internal View of Jet Condenser Injector Passages

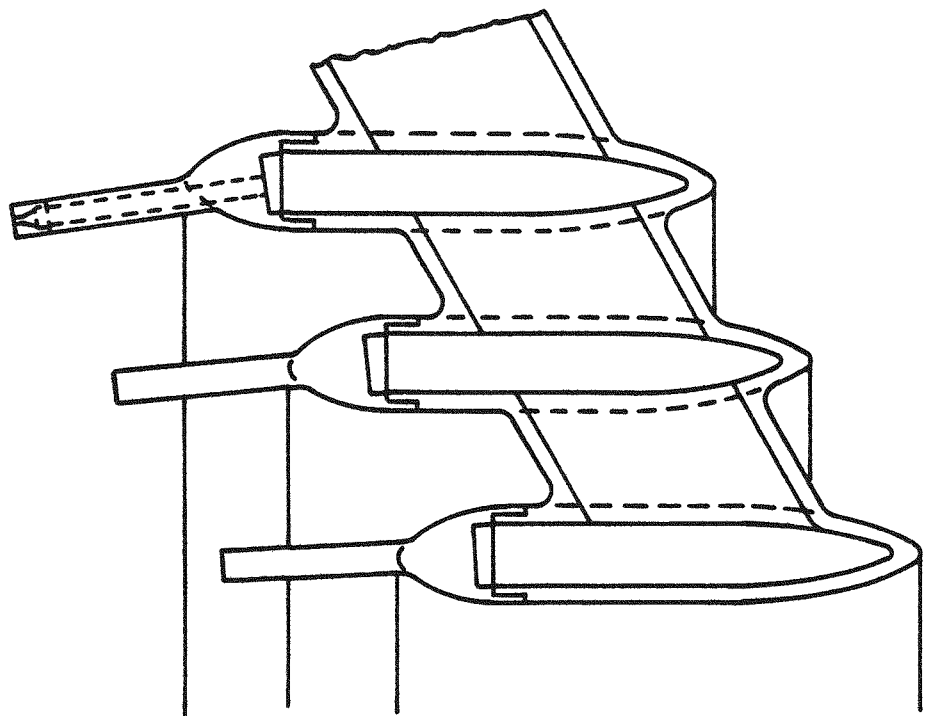


Figure 3-13 Jet Condenser Orifice Tubes

system. Arranged upon the concentric rings are ninety orifice elements, forty-two in the outer ring, thirty in the middle ring, and eighteen in the inner ring. The orifice elements and ring header end cap form a single piece part for each ring. Each orifice element is of 0.010 in. inside diameter with an L/D of five. The orifice inlet has a one diameter lead-in radius.

The vapor funnel provides a boundary for the mixing/condensation process. The first section provides a rounded, smooth transition channelling vapor from the injector to the subsequent converging sections. The second and third sections are simple conical funnels.

The throat/diffuser has a constant diameter throat with a 0.035 in. gap in the middle through which bearing scavenge flow is ported. This is followed by a compound diffuser: the primary diffuser 0.700 in. long with a 2° included angle and the secondary diffuser 2.900 in. long with a 6° included angle.

Jet condenser state points and mechanical configuration are described in Table 3-D.

All parts are machined from 304 stainless steel.

The liquid injector body is EDM'd on both internal and external surfaces. This allows maximum cross section liquid sections with rounded intersections for minimum liquid pressure drop while facilitating aerodynamic shaping and fairing of the external surfaces to minimize vapor side pressure drop.

The orifices are made an integral part of the ring header end caps to enhance the reliability. This eliminates 90 joints, which would be present if the orifices were made individually. It also allows aerodynamic shaping between the orifices and fairing of the header-to-orifice interface, which aids in minimizing vapor pressure drop. The orifices are machined into the three rings such that they are nominally focused at the throat. They are machined into tubes of 0.125 in. diameter and 0.500 in. length to facilitate fine tune focusing of the injector by slightly bending individual tubes to focus on a common focal point at the center of the throat. This fine tuning of the focus allows maximum hydraulic performance, minimum feedback to the bearing scavenge system, and minimum effect from the launch dynamic environment.

The orifice end rings are fluxless furnace brazed to the injector body to minimize distortion and eliminate contamination of the injector body. The joint was designed to provide ample safety margins on stress in all operating modes (including overspeed pressure superimposed on the launch dynamics) and to be fully inspectable after completion of the brazing. The completed injector assembly is brazed to the vapor funnel.

The vapor funnel is penetrated in one location midway through the shallow funnel to allow porting of the noncondensable gas separator vapor return. The upstream half of the throat and the outer shell of the bearing scavenge annuli form an integral part of the vapor funnel. The throat/diffuser section is a single part and also encompasses the inner shell and dividers for the bearing scavenge annuli. This configuration minimizes the number of joints and eliminates external joints with the exception of tubing connecting the liquid inlet, bearing scavenges and noncondensable gas separator vapor return.

Table 3-D Jet Condenser Geometry and Performance

State Points:			
Location	Mass Flow (lbm/sec)	Temperature (°F)	Pressure (psia)
Liquid In	0.275	169	80.0
Vapor In	0.030	239	0.1
Bearing In	0.009	211	2.75
Liquid Out	0.314	211	32.0
Length		$L = 10$ in.	
Mixture chamber pressure		$P_{mix} = 0.083$ psia	
Number of nozzles		$N = 90$	
Orifice diameter		$D_o = .0100$ in.	
Effective vapor diameter at the liquid injector		$D_{mix} = 3.14$ in.	
Diameter at liquid injector		$D_l = 4.00$ in.	
Number of rings		$n = 3$	
Distribution	No. of Nozzles	Diameter (In.)	Angle to Axis (degrees)
Outer	42	2.808	8° 12'
Middle	30	1.932	5° 31'
Inner	18	1.014	2° 49'
Vapor velocity at liquid injector		$V_v = 278.3$ ft/sec (M=.6)	
Liquid velocity		$V_l = 103.0$ ft/sec ( $Re_D = 8140$ )	
Throat diameter		$d_t = 0.133$ in.	
Diffuser	Length (In.)	Half Angle (degrees)	
Primary	0.700	1	
Secondary	2.900	3	
Pressure recovery		= 40%	
Liquid side pressure drop		= 1.9 psid	

### 3.2.3.3 System Accumulator

The system accumulator is located between the jet condenser and system pump. It provides a reference back pressure for the jet condenser and, hence, establishes the dynamic head recovery. It also provides adequate inlet head to the system pump.

During overspeed operation, the amount of fluid in the regenerator, radiator, vaporizer, and lines will be different than in steady state normal speed operation of the system. The accumulator accommodates this fluid inventory transfer among the system components by acting as an expansion compensator.

The accumulator is a redundant bellows type and is shown in Figure 3-14. In this configuration two identical bellows are used. A partition is welded between the bellows to isolate the system fluid from the precharged gas. The space between the bellows OD and the housing ID is partially filled with system fluid. A small ullage space is left in this space to allow for thermal expansion of fluid. The ullage space is evacuated and sealed. The gas side is charged with a proper amount of nitrogen so that when the system attains steady state operation, the accumulator will set the required reference pressure at the jet condenser outlet and also hold the required amount of inventory. With this design, if the bottom bellows develops a crack, only a small amount of  $N_2$  ends up in the ullage space, but the system continues operation without noticeable change in performance. If the top bellows develops a leak, a small amount of working fluid ends up in the ullage space, but the system continues operation without noticeable change in performance. All other welds in this configuration are static joints.

Since the FSCD has a noncondensable gas removal device, the amount of fluid in the accumulator has to be just enough to provide a reference to the jet condenser at all times and is not required to serve as a liquid reservoir to minimize the concentration of noncondensable gases. In the event that the bellows between the system fluid and ullage space failed, approximately 2.2 cubic inches of system fluid will enter the ullage space. The accumulator displaceable fluid at normal operating condition is 7.2 cubic inches and thus provides a safety margin of greater than 2.

An inventory summary of the system fluid in various parts of the loop during normal speed and overspeed has been calculated. Based on this calculation, the system fluid will require 5 cubic inches of additional space during overspeed which will be provided by compression of the bellows inside the accumulator. In the design of the accumulator, provision has been made to accept 15 cubic inches volumetric displacement and thus provide a safety factor of 2.

In order to minimize system weight, the system filter element is located in the accumulator, thereby eliminating a separate filter housing.

### 3.2.3.4 Combined Rotating Unit

The Combined Rotating Unit (CRU) extracts useful work from the Dowtherm fluid and converts it into electric power from the alternator and hydraulic power from the system pump.

The CRU comprises three major components, the turbine, the alternator, and the pump, mounted on a common shaft and supported on working fluid lubricated bearings.

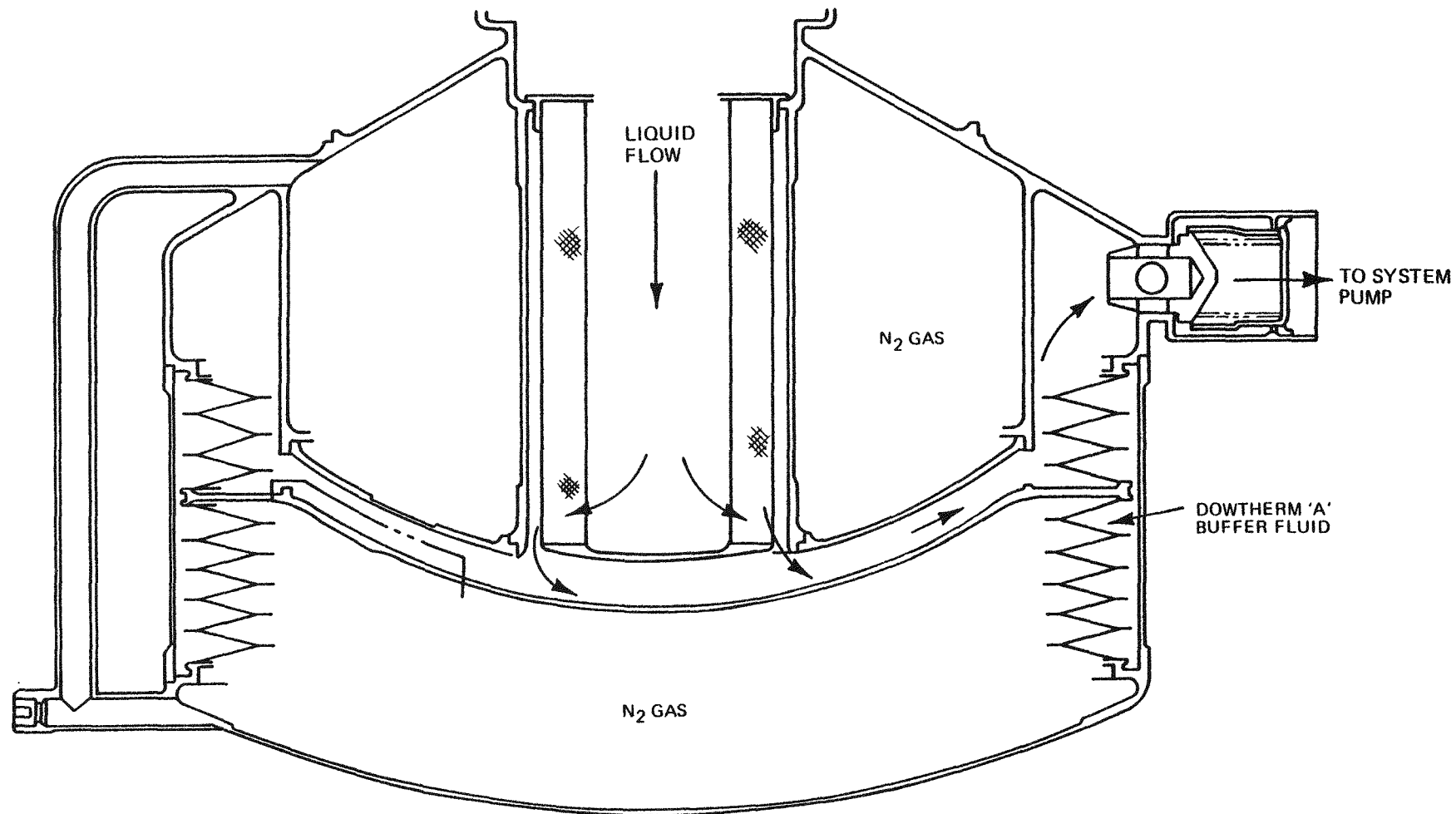


Figure 3-14 Redundant Bellows Configuration

The turbine extracts work from the high temperature, high pressure fluid leaving the boiler and converts it to useful shaft power. The KIPS turbine is a single stage, axial flow supersonic impulse type with a constant channel type shrouded blading. It uses multiple shock cancellation type nozzles.

The turbine directly drives the alternator rotor. The alternator is a homopolar induction type with four laminated poles on the shaft rotating within the stator windings. High efficiency is achieved by minimizing current density. The alternator waste heat is extracted by the working fluid flowing through a cooling coil. Thermal input from the turbine is minimized by thermal dams in the shaft and the turbine housings.

The system pump is at the end of the shaft away from the turbine. It is a six vaned, centrifugal type employing backward swept vanes and shrouds at both front and back. The flow exits from the impeller into a volute and is discharged through a diffuser for recovery of dynamic pressure. A floating close-clearance seal minimizes leakage into the bearing cavity. Sufficient inlet pressurization to prevent cavitation is provided by the jet condenser.

The rotating shaft is supported radially by two sets of tilting pad bearings, each comprised of four pads. Axial load, which is unidirectional, is supported by a set of tilting pad thrust bearings utilizing six pads with load equalizers. All bearings are lubricated by the liquid working fluid.

**3.2.3.4.1 TURBINE:** The turbine selected for the flight system has the blade passage shape, blade height, and nozzle ring design experimentally determined to be most efficient of those tested during turbine rig testing. With the addition of a shroud on the turbine blades to reduce leakage losses and rim friction, a diffuser and close fitting side shrouds on the disc to reduce disc friction, it is predicted that the flight configuration will yield 69% efficiency at design conditions.

A cross section showing the turbine arrangement for the flight system is shown in Figure 3-15. The turbine drives the alternator and feed pump and provides power for the mechanical, electrical, and friction power losses in the CRU.

The turbine speed selected was 33,680 rpm for nominal total inlet conditions of 57.0 psia and 650°F for superheated Dowtherm A vapor and an exhaust pressure of 0.100 psia. The speed selection was based on an optimization of CRU design. The large pressure ratio results in supersonic Mach numbers at the nozzle exit and supersonic relative Mach numbers at the inlet to the rotor blading. A single stage, partial admission, axial impulse turbine is used to satisfy the power requirements of the KIPS.

The convergent-divergent axisymmetric nozzles were designed using the real gas properties of Dowtherm A vapor. The nozzles are arranged to provide full admission when using 9 nozzles at the 2 KW power level. The number of nozzles is reduced for other design power levels. Figure 3-16 shows the nozzle geometry and number of nozzles used for the reference power levels of 0.5, 1.3, and 2.0 kilowatts.

The vapor discharged from the exit of the turbine is diffused to a low Mach number by an annular diffuser. The diffuser exit then discharges the gas vapor into a larger annulus which is the inlet to the regenerator.

The turbine wheel consists of an Inconel 718 disc with integral impulse blading and a Hastelloy X shroud which is brazed to the blade tips. The disc is first rough machined and then blades are cut by

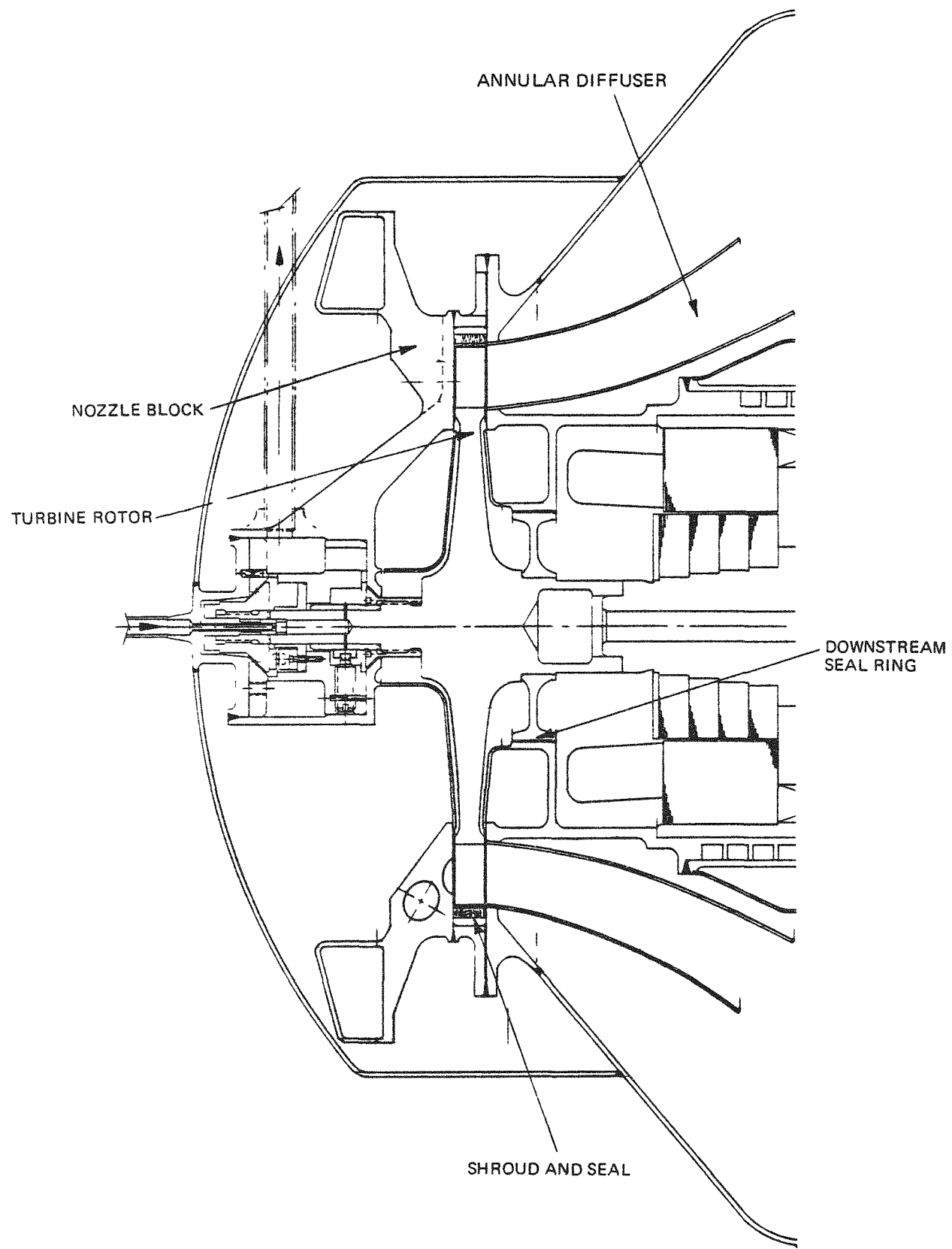
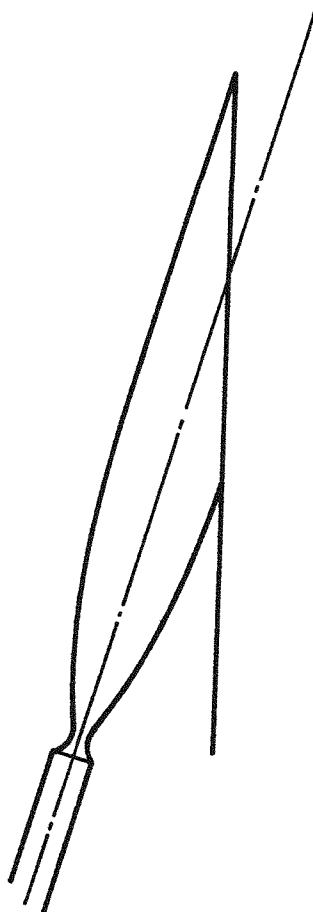


Figure 3-15 Flight System Turbine



<u>QUANTITY</u>	<u>0.5 KW</u>	<u>1.3 KW</u>	<u>2.0 KW</u>
Nozzle Throat Area (Sq. In.)	.007547	.015093	.02264
Throat Diameter (In.)	.056594	.056594	.056594
Nozzle Exit Area (Sq. In.)	0.69197	1.38394	2.07590
Nozzle Exit Dia. (In.)	0.54192	0.54192	0.54192
Number of Nozzles	3	6	9
Nozzle Angle (Deg.)	15.0	15.0	15.0
Nozzle Total Pressure (psia)	53.2	57.0	61.0
Mass Flow (lbm/sec)	.0140	.030	.048
Arc of Admission	.320	.640	.960

Figure 3-16 Turbine Nozzle Configuration

an ECM process. The ECM process is controlled to obtain a smooth surface finish. The wheel OD is then machined and the shroud installed and brazed. Constant channel width blading geometry is employed with a chord length of 0.36 in. The blade geometry is shown in Figure 3-17 and described in detail in Table 3-E.

**3.2.3.4.2 SYSTEM PUMP:** The system pump is located on the turbine shaft at the opposite end from the turbine wheel. Its function is to provide high pressure fluid through the regenerator and vaporizer to the turbine nozzles and through the radiator to the jet condenser. The pump is shown in Figure 3-18.

The pump impeller is made from 17-4 PH steel with a brazed front shroud. Carbon floating seals are used on both the frontside and the backside of the impeller.

The pump is designed to deliver 2.28 gpm at 65 psid and 33,680 rpm. The critical dimensions are:

Impeller OD	:	0.686 in.
Impeller port width at OD	:	0.0455 in.
Volute throat size	:	0.107 x 0.175 in.
Recirculation flow	:	0.004 gpm
Leakage flow	:	0.002 gpm
Axial thrust	:	1.1 pound

**3.2.3.4.3 ALTERNATOR:** The KIPS flight system alternator is a four pole homopolar inductor device. Selection of this type of alternator was dictated by the high operating speed and long service life of this application. A homopolar inductor alternator contains no rotating electrical windings, slip rings, cages, magnets, etc. All electrical components are contained in the stator and are not subjected to rotational stresses and vibrations. This eliminates winding failures commonly associated with rotational loads.

The rotor of the flight system alternator is an integral part of the combined rotating unit (CRU), as shown in Figure 3-19. The rotor configuration is a typical four pole, homopolar, inductor design with two poles of like polarity at each end, the ends displaced 90° (180 electrical degrees) from each other and connected by means of a magnetic shaft. To control pole face losses, the rotor is designed with laminated pole structures. Rotor laminations are made from fully processed AISI grade M-19 electrical sheet steel, 0.014 in. thick. They are electron beam welded to a shaft made from AISI 8620 steel.

The stator assembly consists of a magnetic yoke containing the field coil sandwiched between two cores, which contain the armature windings. The yoke is a cylindrical piece of low carbon steel (AISI 1008) fully annealed to obtain maximum permeability. Each stator core is a stack of laminations containing 24 slots on its inner periphery. The laminations are made from 3% silicon sheet steel (Magnesil-N) and are 0.005 in. thick. This material was chosen for its high permeability, its low core loss characteristics, and its ability to produce a high resistance oxide surface coating which is essential to control eddy current iron losses and maintain high efficiency.

The stator winding is a conventional three phase, WYE connected, 60° phase belt winding. Because of the stringent efficiency requirements, the winding was designed for minimum losses. Current density was kept below 1620 amps/in<sup>2</sup> at rated load and measures were taken to minimize eddy losses. These can be considerable when the stator slot is relatively deep and the alternator output

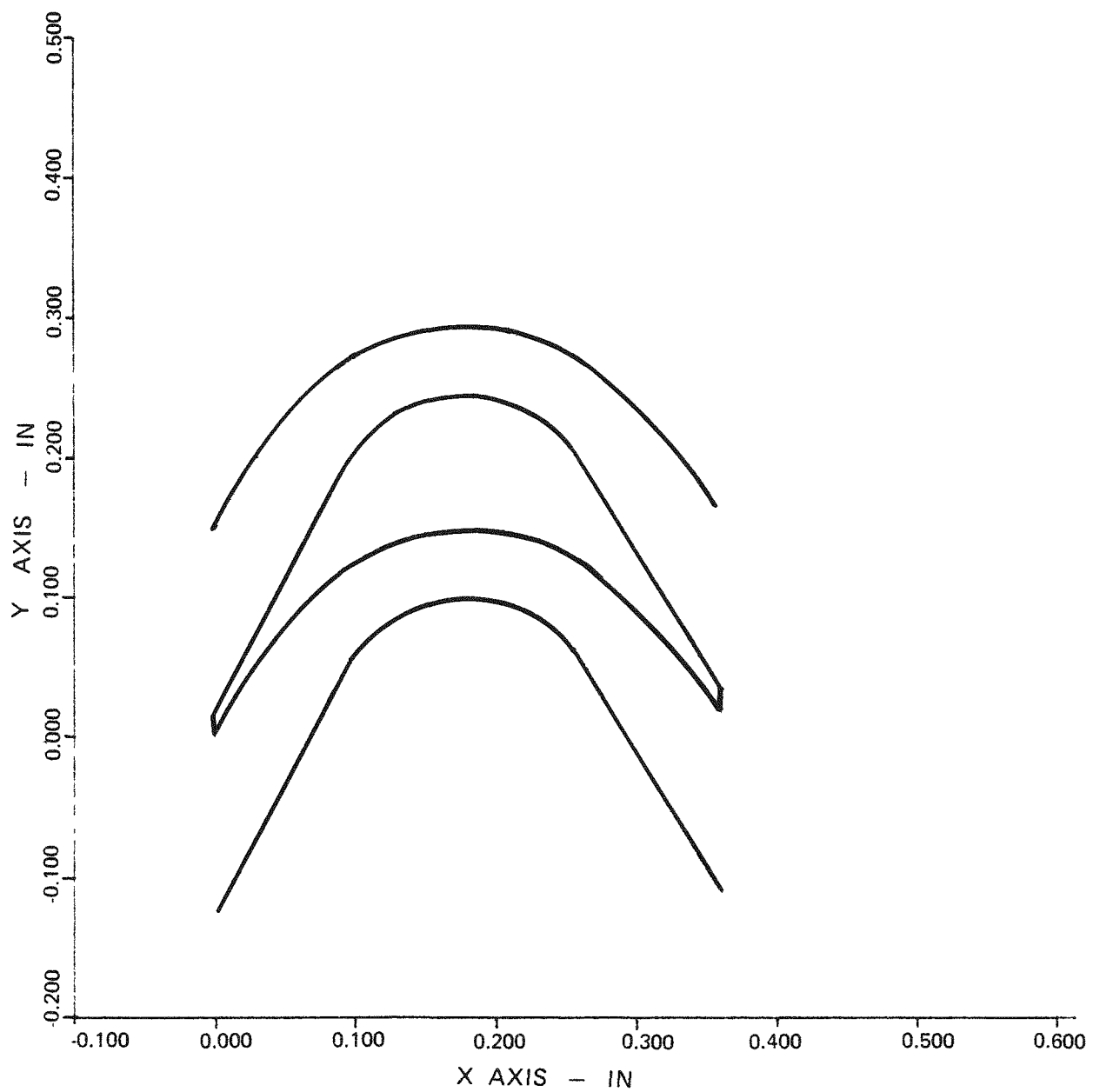


Figure 3-17 KIPS Turbine Blade Profile

Table 3-E Blade Geometry at Pitch Line

Channel Width	Constant
Axial Chord (In)	0.36
Aspect Ratio	1.806
Minimum Blade Thickness (In)	0.0080
Minimum Blade Thickness to Chord Ratio	0.0222
Maximum Blade Thickness to Chord Ratio	0.275
Leading Edge Blockage	0.103
Trailing Edge Blockage	0.103
Inlet Area to Minimum Area Ratio	1.00
Minimum Rotor Area to Nozzle Throat Area	212
Blade Area (In <sup>2</sup> )	Ratio 0.0258
Blade Perimeter (In)	1.038
Number of Blades	111
Solidity (Chord/Pitch)	2.14
Blade Inlet Angle (DEG)	27.35
Blade Exit Angle (DEG)	27.35
Blade Turning Angle (DEG)	125.3
Blade Reynolds Number at Exit (Length)	$0.83 \times 10^4$
Hydraulic Reynolds Number at Inlet	2687

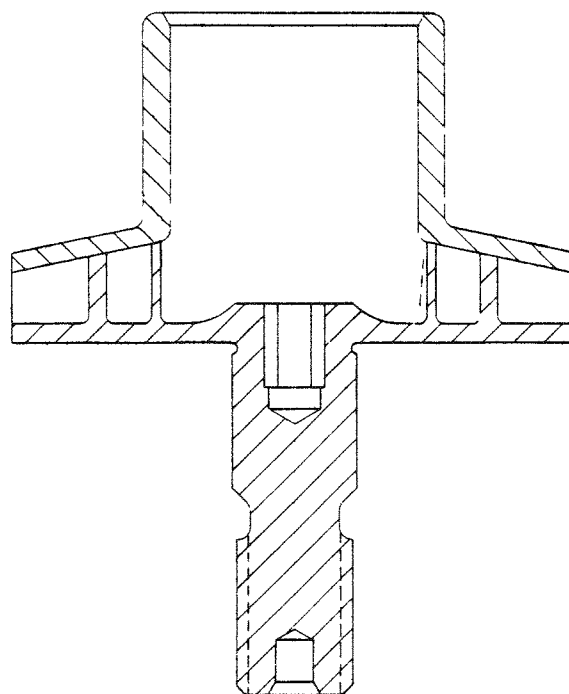
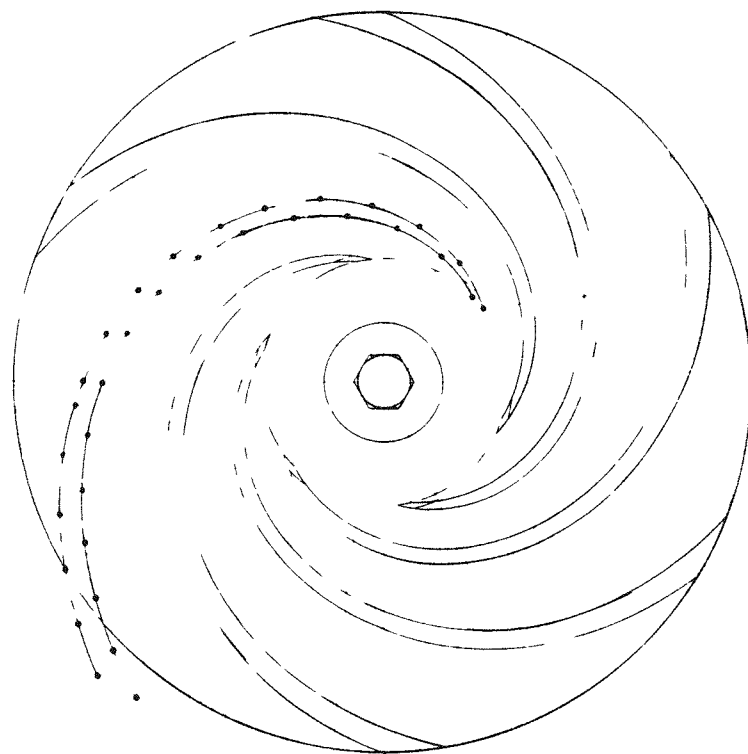


Figure 3-18 Swept Vane Pump Impeller

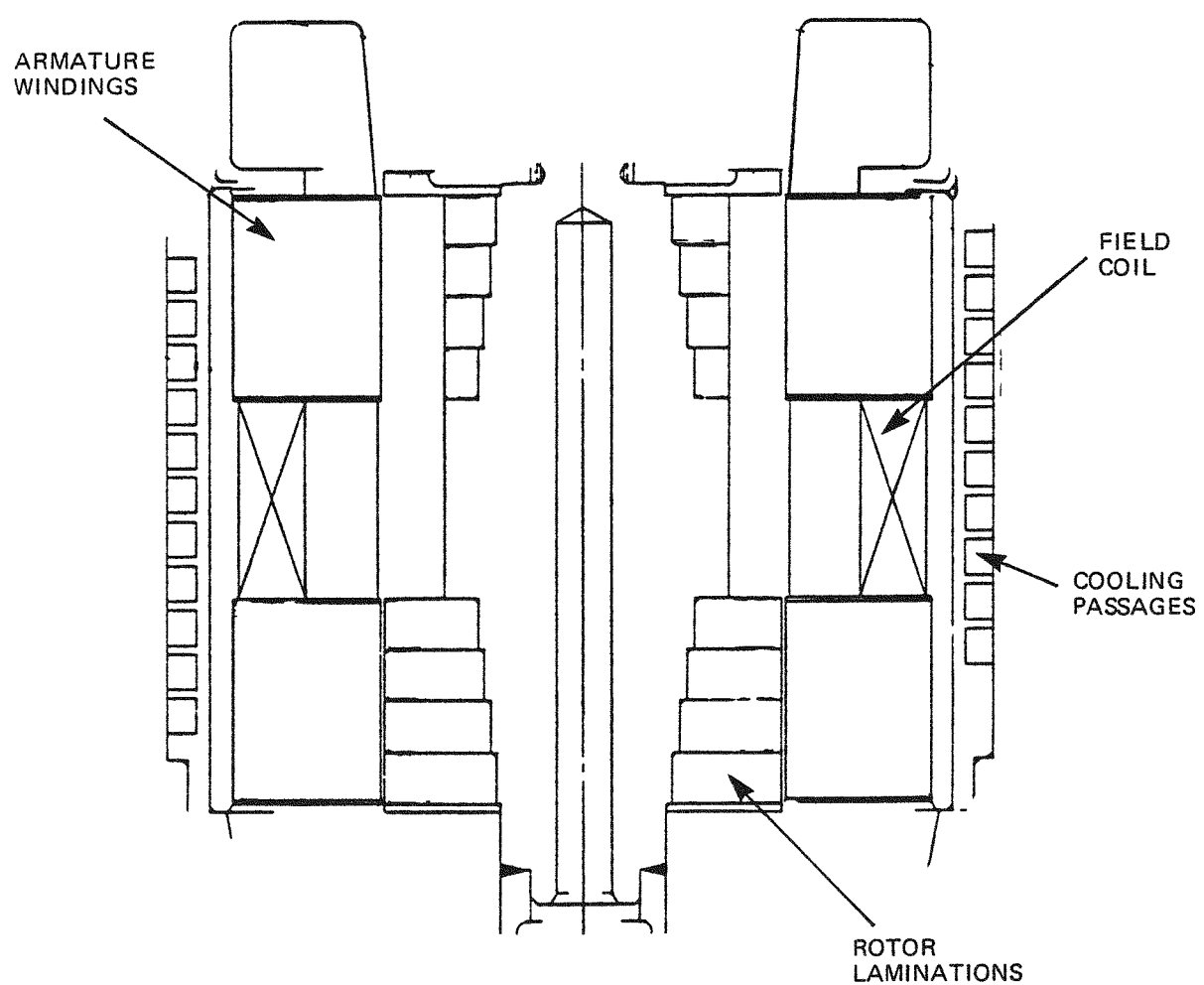


Figure 3-19 Alternator

frequency is high. To reduce eddy losses, the stator conductors are made up of 31 strands of AWG No. 20 insulated wire each, and the strands are transposed (twisted) in the end turn area such that those located at the bottom of one slot will be at the top of the next slot. In this fashion, all strands have nearly equal reactances and the eddy current producing voltages are minimized. Because specific output voltage waveform requirements were not defined, the stator winding was designed with a full pitch and minimum distribution to obtain maximum possible output with minimum field excitation.

The field coil of the alternator is a simple toroid of 375 turns of DuPont HML Insulated AWG No. 19 wire wound on an aluminum bobbin. As the coil is wound, DuPont ML varnish per MIL-L-24092B is brushed on each layer of wire and then is cured to hold the winding together during handling, prior to insertion into the magnetic yoke. The coil is insulated with double layers of 0.005" thick Kapton sheet. Once installed in the stator assembly, the coil is snugly held on both sides by the stator cores, the yoke on the OD, and the aluminum bobbin on the ID.

The materials for the alternator insulation system were selected on the basis of dielectric strength, long term compatibility with Dowtherm A, and best life versus temperature characteristics.

With the exception of teflon sleeving and fiberglass tie cord, the entire KIPS alternator insulation system consists of polyimides in various forms (see Table 3-F). Polyimides possess the greatest dielectric strength and best life versus temperature rating of all known organic insulation materials.

The alternator is nominally rated at 1.56 KVA, 22.5 volts line-to-line, 40 amps, 0.93 to 1.0 power factor. It has a continuous thermal overload capability of 2.5 KVA; with added cooling, the electromagnetic capacity is well over 3 KVA.

In the alternator, both the armature and field windings contain sufficient copper to maintain low current densities and, therefore, low copper losses. At rated load, the current densities are 1620 amps per square inch in the armature and 1980 amps per square inch in the field windings.

The alternator rotor is assembled by welding and becomes an inseparable one piece assembly. The stator limitations are assembled into cores using Scotchcast 265 epoxy adhesive, and the cores are fitted into the yoke with a 0.001 in. diametral interference fit. The armature windings are held within the cores by the semiclosed slot design. The alternator stator is held in its housing by means of a shrink fit. No mechanical fasteners are used in the alternator assembly.

**3.2.3.4.4 BEARINGS:** The bearings for the combined rotating unit (CRU) support both axial and radial loads under a variety of different operating conditions. The baseline operating point for which losses need to be minimized and, hence, performance maximized is the zero g condition when bearing loads are at a minimum and comprise only turbine, pump, alternator, and imbalance loads. The most stringent operating conditions will be during launch when either: (1) accelerations in the axial and radial directions reach nine and five g's respectively with superimposed vibration loads or (2) the short term shock loads are applied independently of the acceleration load. In addition, ground operation in the vertical direction will have one g axial load while horizontal operation would have one g radial load. The bearing geometries are shown in Figures 3-20 and 3-21.

The radial bearings consist of working fluid lubricated tilting pad bearings. Each set of bearings comprises four tilting pads of 80 degrees of arc pivoted at 44 degrees from the leading edge. The

Table 3-F KIPS GDS Alternator Insulation System

<u>Component</u>	<u>Trade Name</u>	<u>Material</u>
Magnet Wire	DuPont Heavy ML Film	Double Coat Polyimide Varnish
Slot Cells	DuPont Kapton Sheet .005 inches Thick	Polyimide Sheet (Flexible)
Field Coil Ins.	DuPont Kapton Sheet .005 inches Thick	Polyimide Sheet (Flexible)
Tie Cord	Varglas Non-Fray Sleeving	Braided Fiberglass Sleeving
Slot Wedges	Dixon Corp. Meldin Polyimide 0.025 inches Thick	Polyimide Sheet (Rigid)
Impregnating Varnish	DuPont Pyre ML Varnish	Polyimide Varnish
End Leads	Teflon	

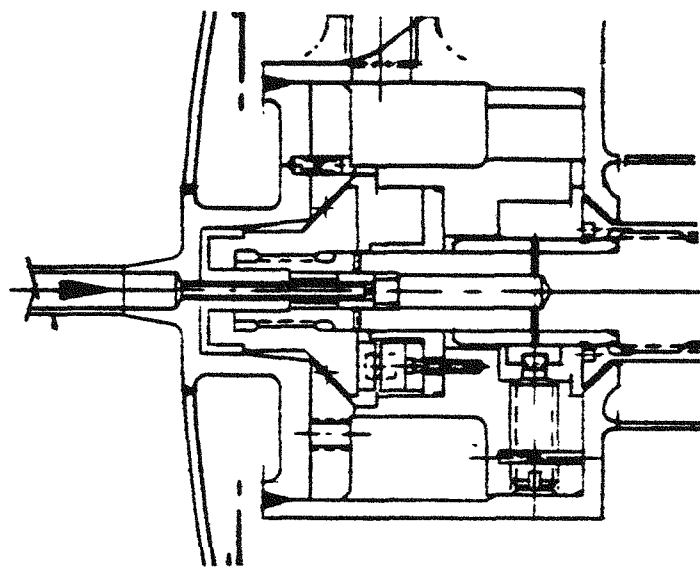


Figure 3-20 Turbine Bearing

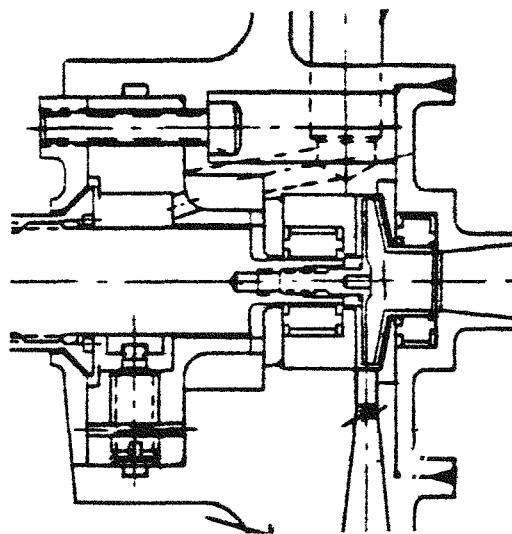


Figure 3-21 Pump Bearing

bearing pads are hardened M-50 tool steel with a thin electroplated silver coating. The coating enhances start-stop characteristics.

The tilting pad radial bearing is inherently stable due to the fact that the shaft movement is essentially colinear with the applied loads. The tilting pad bearing comprises a series of equally spaced shoes arranged circumferentially around the shaft. A pivot in the backside of the shoe allows it to tilt in the pitch direction in order to form a converging wedge for hydrodynamic pressure generation. Typically, instability only arises when pad pitch inertia is high enough to prevent adequate shaft tracking. This potential instability can be precluded by "preloading" the bearing and minimizing pad inertia. Preloading sets the bearing pads closer to the shaft than would be dictated by the machined clearance and thus has the same effect as applying an external load. An additional advantage of the tilting pad bearing is the self-aligning characteristic which eliminates alignment problems common with rigid bearings.

The radial bearings operate in the laminar flow regime throughout the operating range with Reynold's numbers of 544 and 920 at design point and maximum runaway speeds, respectively. The radial bearing geometry is summarized in Table 3-G.

The maintenance of bearing radial clearances is important to prevent excessive whirl orbit amplitudes and prevent the possibility of other components with close radial clearances from contacting. For this reason, special attention has been given to restraining the radial movement of the bearing pads. The bearings are preassembled into steel support modules. The bearing clearance is set using an oversized mandrel by tightening a threaded pivot pin which, in turn, is locked in place by drilling and inserting a roll pin.

The materials selected for the radial bearings comprise a hard-hard combination of M-50 pads versus either an M-50 sleeve at the turbine end or carburized AISI 8620 shaft at the pump end. A flash of silver plate is added to the pad inner surface to give additional bearing protection in the event of a high speed rub, and to enhance start-stop capability. The pivot pin is silver plated M-2 and is screwed into an AISI 8620 housing.

The thrust bearing is designed for unidirectional thrust loading only, though short term reverse thrust loads resulting, for instance, from rocket staging, can be accommodated.

The thrust bearing configuration employs six M-50 pads with two rows of six leveling pads. A hemispherical pivot engages into a hemispherical socket in the pad. The pivot pin is mounted to the first leveler which, in turn, pivots on two of the second levelers by contact along radial lines. The bottom leveler pivots on an M-50 insert which doubles as a shim to set the turbine wheel clearance. The pin through the bottom leveler prevents circumferential motion while relatively tight radial clearances act as restraints in that direction. Similarly, a tight clearance at the inner diameter of the thrust pads prevents windmilling of the pads about the pivots. The pad surface and the pivot surfaces have a flash of silver plate (0.0004 in.). The thrust runner is also made of M-50. The geometry is summarized in Table 3-H.

Although the preferred orientation of the power system axis precludes reverse thrust during normal operation and through launch, it is feasible that momentary reverse thrust loading could occur during orbit transfer or within the Space Shuttle bay. This can be accommodated by a bronze

Table 3-G Radial Bearing Geometry

Number of pads:	4
Pad length:	0.275 $\pm$ 0.005 (inches)
Shaft diameter:	0.5500 + .0000 (inches) - .0002
Pad I.D.:	0.5525 + 0.0002 (inches) - .0000
Machined clearance:	0.0025 $\pm$ 0.0002 (inches)
Assembled clearance:	0.00175 (inches)
Preload coefficient:	0.3
Pad thickness at pivot: (tapered towards leading and trailing edges)	0.150 (inches)
Pad arc:	80 (degree)
Pivot point location	44 (degrees from leading edge)
Leading edge radius:	0.05 (inches)
Pad material:	M-50 with silver flash
Shaft material:	M-50 at turbine end AISI 8620 at pump end
Pivot spherical diameter:	0.666 (inches)
Socket spherical diameter:	1.00 (inches)
Design point power loss:	7.5 (watts/bearing)

Table 3-H Thrust Bearing Geometry

Number of pads:	6
Active pad circumferential length:	0.25 inch
Active pad radial width:	0.25 inch
Pad thickness:	0.10 inch
Pivot location from leading edge:	0.15 inch
Pad material:	M-50 with silver flash
Thrust runner material:	M-50
Pivot spherical diameter:	0.666 inch
Socket spherical diameter:	1.00 inch
Number of upper load levelers:	6
Cylindrical pivot diameter:	0.125 inch
Cylindrical pivot length:	0.125 inch
Number of lower load levelers:	6
Cylindrical pivot diameter:	1.00 inch
Cylindrical pivot length:	0.175 inch
Total axial clearance:	0.007 inch
Design point power loss:	25 watts

snubber which can withstand the surface speeds at which this occurs without lubrication and damage. This snubber also serves as a protection for the turbine wheel during handling and accommodates the initial reverse thrust load at start resulting from pump inlet pressurization by the start pump.

In order to maintain the design point operating characteristics of the bearings throughout the operating life, it is necessary to preclude any possibility of pivot fretting type wear. The results of such wear are a decrease in the pad stability due to an increase in the pivot friction and an increase in the bearing clearance leading to a change in minimum film thickness. For this reason, maximum Hertz stresses were limited to 220,000 psi and a radius ratio of 1.5 was selected. A summary of the pivot geometry is given in Table 3-1.

### 3.2.3.5 Control System

The KIPS control system is designed to accommodate a wide variety of requirements. Some of these are fundamental control functions required on any organic Rankine cycle system, some are necessitated by the particular requirements of the changing thermal output of the isotope heat source used in the KIPS system, and additional functions are necessitated by spacecraft requirements.

The basic control functions include turbine loop flow control, turbine inlet temperature control, combined rotating unit (CRU) speed control, electrical overload protection, output voltage regulation, and system heat rejection control.

The control functions are performed by two separate modules: a valve pack and an electronic controller. The "valve pack" contains the turbine loop flow and temperature controls as well as the radiator bypass valve. The electronic controller provides voltage regulation, overload protection, and speed control.

The fluid loop controls are powered directly by mechanical and hydraulic forces and require no internal or external electrical power for operation. Because of this, the KIPS system can continue to operate safely under conditions of electrical overload.

The KIPS CRU is structurally designed to withstand continuous operation in a frequency wild (no speed control) mode which allows disabling the speed control system when desired. This capability provides the ability to run the CRU at higher speed during launch and orbital maneuvers resulting in added bearing load capability and jet condenser jet stiffness during periods of high shock and vibration.

A block diagram showing the location of the control components in the system is shown in Figure 3-22.

**3.2.3.5.1 TURBINE FLOW CONTROL:** A Rankine cycle system utilizes a control system to maintain turbine inlet conditions at the selected design point. Keeping turbine inlet conditions relatively close to the design point ensures that the system will be able to produce the required power and that the turbine will always be supplied with superheated vapor. This will avoid erosion damage from partially vaporized working fluid. The flow control method employed in KIPS adjusts the boiler flow rate to maintain constant turbine inlet temperature.

Table 3-I Pivot Design

<u>Pivot Location</u>	<u>Pivot Type</u>	<u>Pivot Diameter (inch)</u>	<u>Socket Diameter (inch)</u>	<u>Pivot Length (inch)</u>
Thrust Pad	1	0.666	1.00	---
Upper Load Leveler	2	0.125	---	0.25
Lower Load Leveler	2	1.00	---	0.175
Radial Pad	1	0.666	1.00	---

(1) Spherical pivot in spherical socket.  
(2) Cylinder on flat.

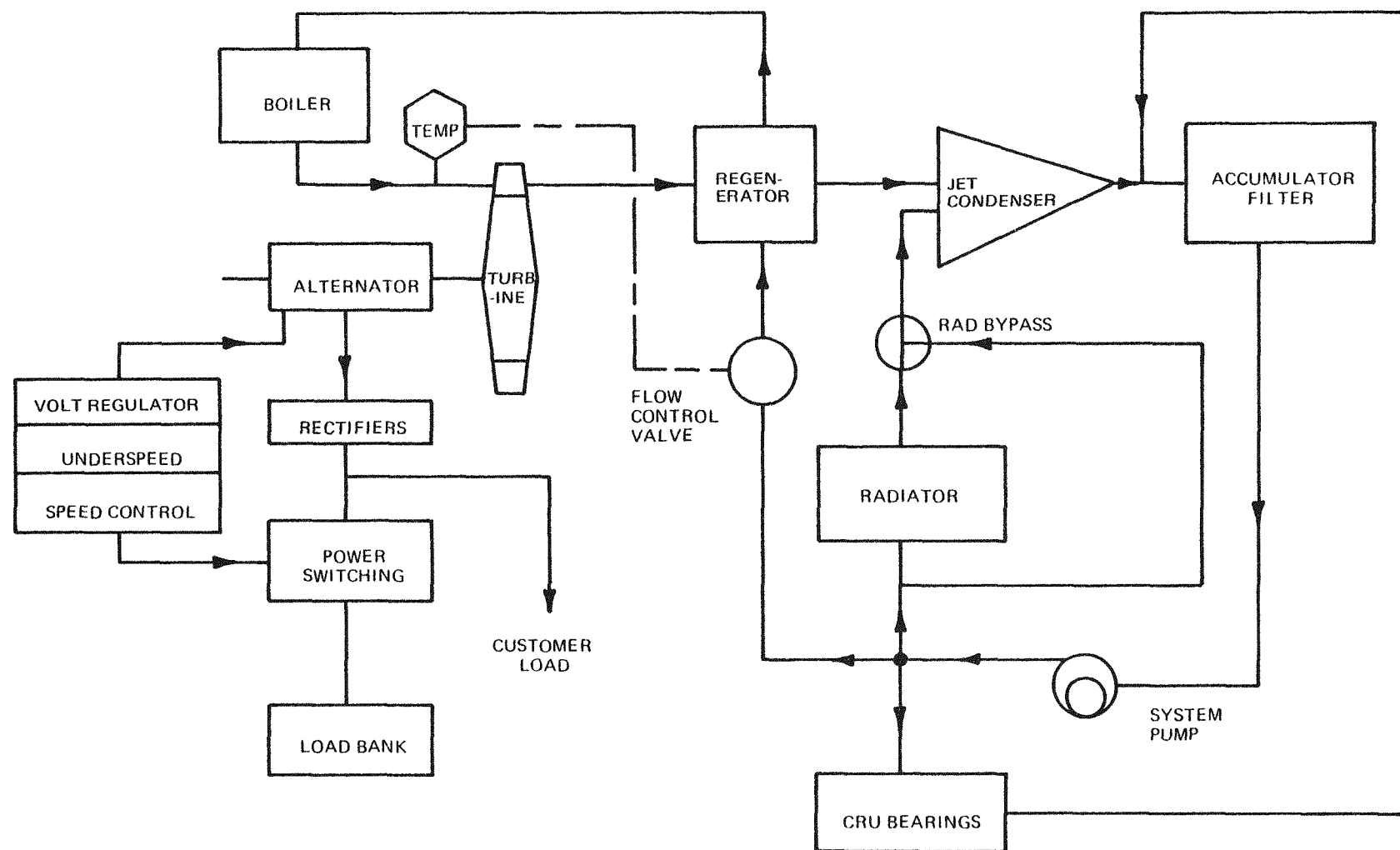


Figure 3-22 KIPS Block Diagram

A cross section of the integrated valve pack including the turbine loop flow control valve is shown in Figure 3-23. The inlet receives flow from the system pump and the regulated outlet flow enters the turbine loop. The pressure regulator bellows assembly senses valve chamber pressure on the side facing the valve chamber. The back of the bellows is connected via internal porting to the valve outlet. The bellows therefore moves in response to pressure drop across the temperature control orifice. When turbine inlet temperature is constant, the temperature control flapper remains in a fixed position and the effective orifice area of the temperature control orifice is constant. With the pressure regulator controlling the delta P across the orifice, system flow is kept constant regardless of inlet pressure. The pressure regulator performs this function by actuating the pressure regulator flapper which throttles inlet flow as required to keep the temperature control orifice delta P constant. Changes in valve inlet pressure are therefore prevented from affecting the flow rate through the valve.

The resulting valve performance characteristic curves are shown on Figure 3-24, where it can be noted that flow remains essentially constant (for constant turbine inlet temperature) as overall valve delta P varies from 20 to 160 psi.

As turbine inlet temperature increases, expansion of the NaK in the thermal sensor moves the temperature control flapper away from the temperature control orifice, thus increasing the area and the system flow rate. This effect is shown for several steady state temperatures on Figure 3-24. Superimposed on the figure is a map of required KIPS flows and pressure drops for frequency wild operation. It can be noted that the control valve keeps turbine inlet temperature between 645 and 658°F under all operating conditions. When the speed control circuit is actuated and the system running at constant speed, variations in system pressure are very small and the system operates along the full load line. Under this condition, where the KIPS operates most of its life, the turbine inlet temperature range is 647 - 653°F.

The flow control valve was designed with redundant bellows in the pressure regulator assembly. These were sized such that a failure of either bellows would have only a minor effect on system operation. The effect of a cracked or failed bellows is a shift of turbine inlet temperature of less than 2°F. Dual thermal sensor assemblies are utilized to provide complete redundancy in the temperature sensing portion of the valve.

The flight system flow control valve pack is integrated into the valve pack and utilizes an all welded assembly of stainless steel components to preclude internal or external leaks.

**3.2.3.5.2 RADIATOR BYPASS FLOW CONTROL:** The primary means of PCS heat rejection is via the system radiator. The radiator must be large enough to reject beginning of life waste heat at full load and the highest heat sink temperature. At other operating conditions, the radiator is oversized and it is desirable to limit the heat rejected to maximize PCS efficiency; this capability is particularly desirable at end of life when the PCS output power is lowest. It is also very desirable to have some means of controlling radiator outlet temperature when the radiator auxiliary cooling loop is used for system heat rejection when the PCS is installed in the Shuttle bay. PCS control of the radiator temperature eliminates the need for active Shuttle control of the cooling temperature. Another function of the radiator heat rejection control is to permit subcooling of the radiator metal to act as a heat sink if the KIPS system is launched using a Titan vehicle. This heat sink permits the KIPS system to continue running during the critical launch period when the radiator is shrouded.

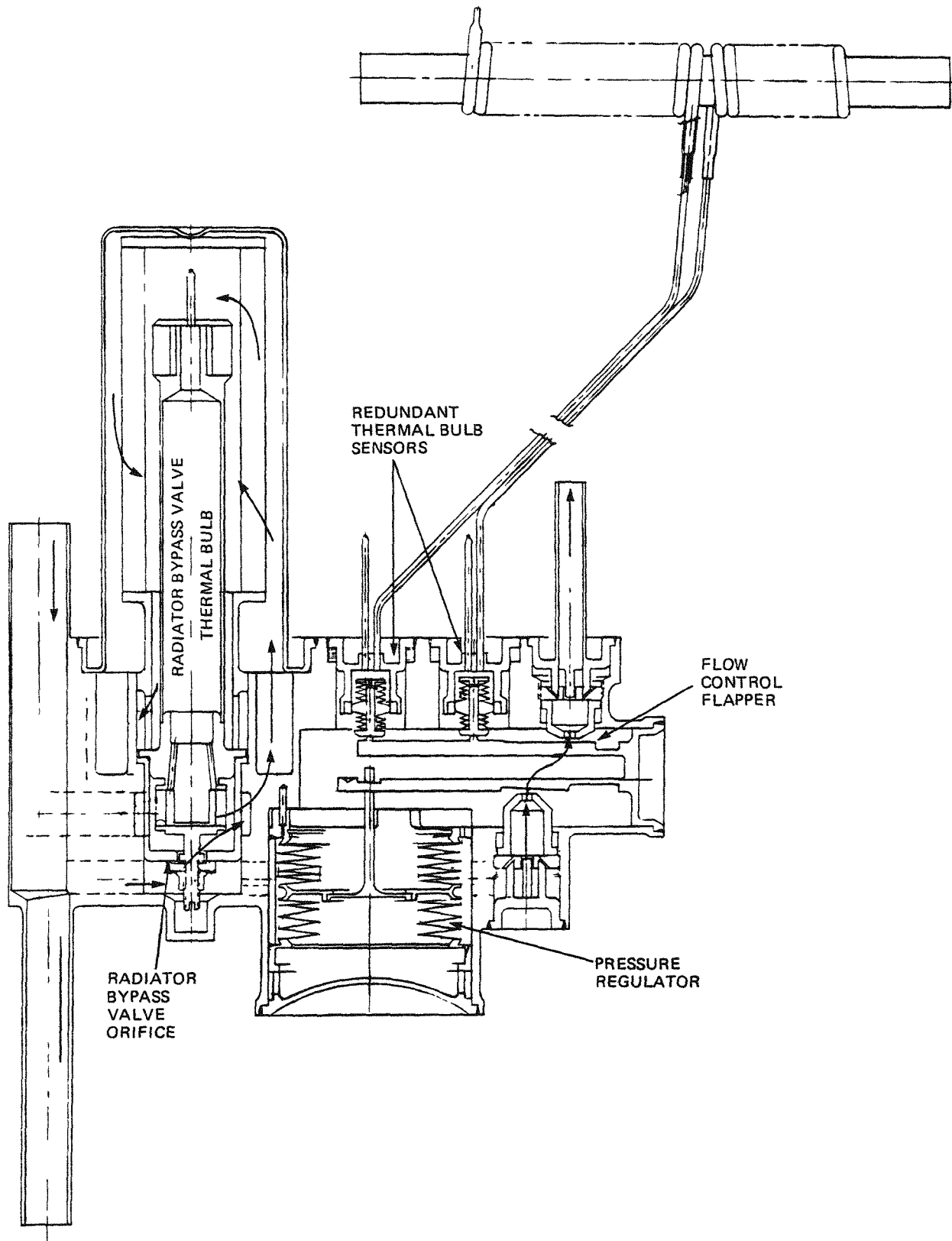


Figure 3-23 FSCD Fluid Loop Controls

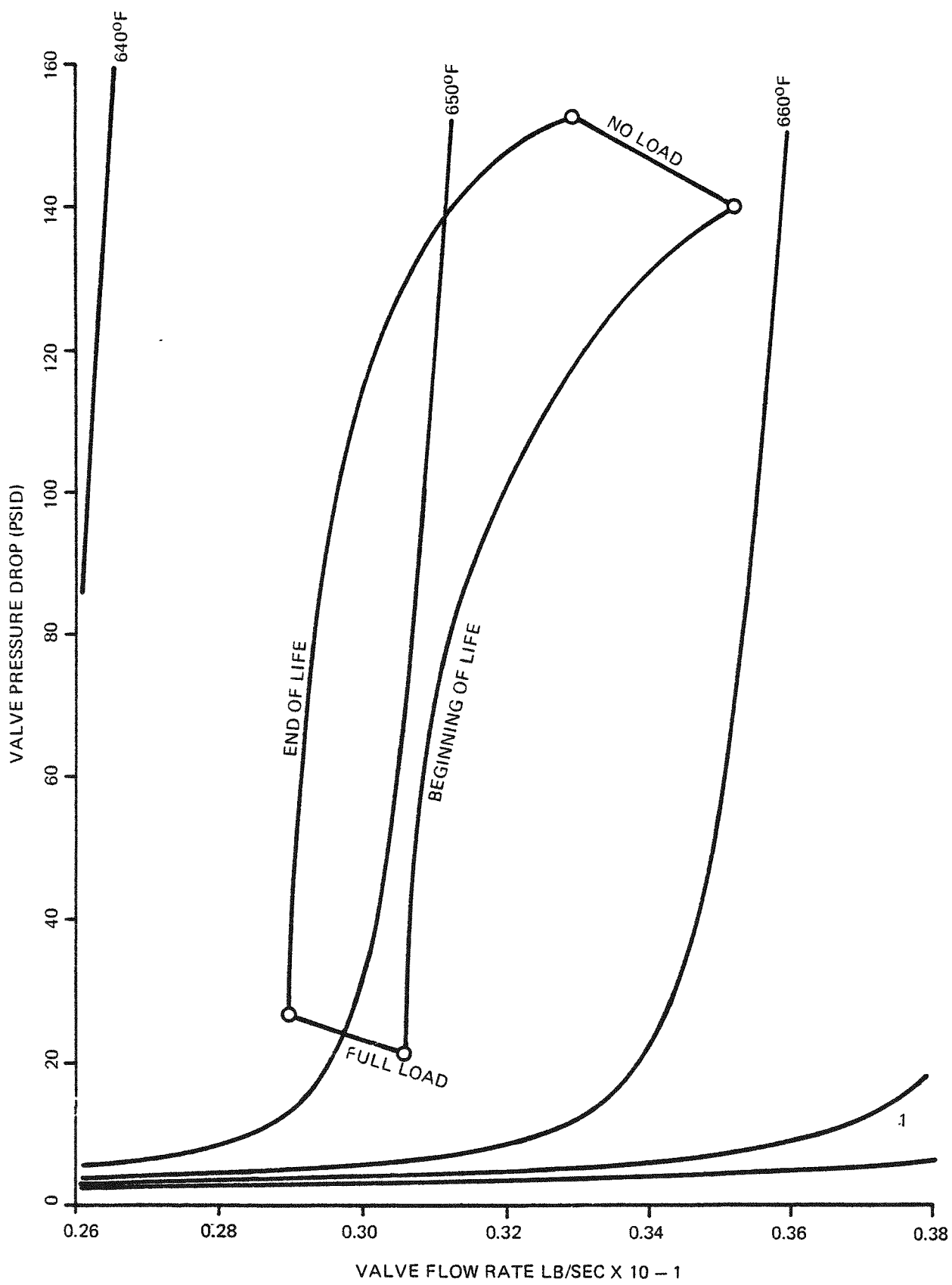


Figure 3-24 KIPS Turbine Loop Flow Control Valve

A thermal bulb type valve is used for the radiator bypass valve. A cross section of the valve is shown in Figure 3-23, integrated into the valve block and filter assembly. Warm fluid from the pump passes through an orifice and mixes with cooler radiator outlet fluid. The mixed fluid is circulated around the thermal bulb and then exits to the jet condenser. When the mixed fluid temperature is excessive, expansion of the fluid in the thermal bulb moves the valve seat closer to the orifice restricting the influx of warm fluid to reduce the mixed fluid temperature. The actuation bellows free length is shorter than its operating length so that a leak in the thermal bulb or bellows will cause the bellows to fully contract, thus pulling the auxiliary seat against the orifice to completely shut off the bypass flow.

The radiator bypass valve has only one flexing part, the fluid containment bellows assembly. This bellows was designed such that cyclic fatigue would not occur, although a failure here is not critical to continued system operation. The working fluid in the thermal bulb is Dowtherm A, identical to the system working fluid, so there is no ill effect on the system of a leaking bellows. Redundancy was therefore not provided on the radiator bypass valve bellows.

**3.2.3.5.3 ELECTRICAL CONTROLS:** The controller provides output power conditioning, voltage regulation, speed control, and electrical overload protection. The controller is powered by the alternator. No external electrical power is required. Power conditioning includes rectifiers and an appropriate filter to achieve 0.1% rms voltage ripple. The voltage regulator provides 28 VDC  $\pm$  2% voltage control through control of the alternator field. Speed control is achieved by applying a parasitic electrical load as required to keep the speed within  $\pm$  2% of the design speed. Electrical overload protection is provided by an underspeed detection circuit which removes alternator field current whenever the speed is less than 95% of rated speed.

Figure 3-25 shows a block diagram of the baseline control system.

Speed control is accomplished by a frequency discriminator which monitors the alternator output frequency (which is proportional to speed), a comparator (pulse width modulator), and the parasitic load resistor.

The parasitic load is comprised of three parasitic load resistors (PLRs), each capable of drawing 50% of the load. Thus, two PLRs are capable of providing full load. Having three PLRs with any two capable of handling full load greatly increases the reliability of the system.

The frequency discriminator consists of a passive tuned circuit which produces a DC output voltage proportional to system frequency near the resonant frequency of the tuned circuit.

The Pulse Width Modulator (PWM) comparator is set at a 50% duty cycle at a voltage proportional to 1122 Hz (33,700 rpm). The PWM rate is controlled by the carrier frequency which is the ripple frequency of the three phase, full wave bridge rectifier. The PWM comparator turns the power switches on or off, applying or removing power to the PLRs. Since the carrier frequency is high ( $6 \times 1122 = 6732$  Hz), the time averaged effect is a steady load determined by the PLR duty cycle. The duty cycle will change in response to system capability and customer loading.

The voltage regulator is pulse width modulated to minimize the regulating losses. The switching point of the PWM regulator is set at the 50% duty cycle of the carrier frequency. When the output voltage is low, the PWM duty cycle goes toward 100% causing maximum field current to flow in the

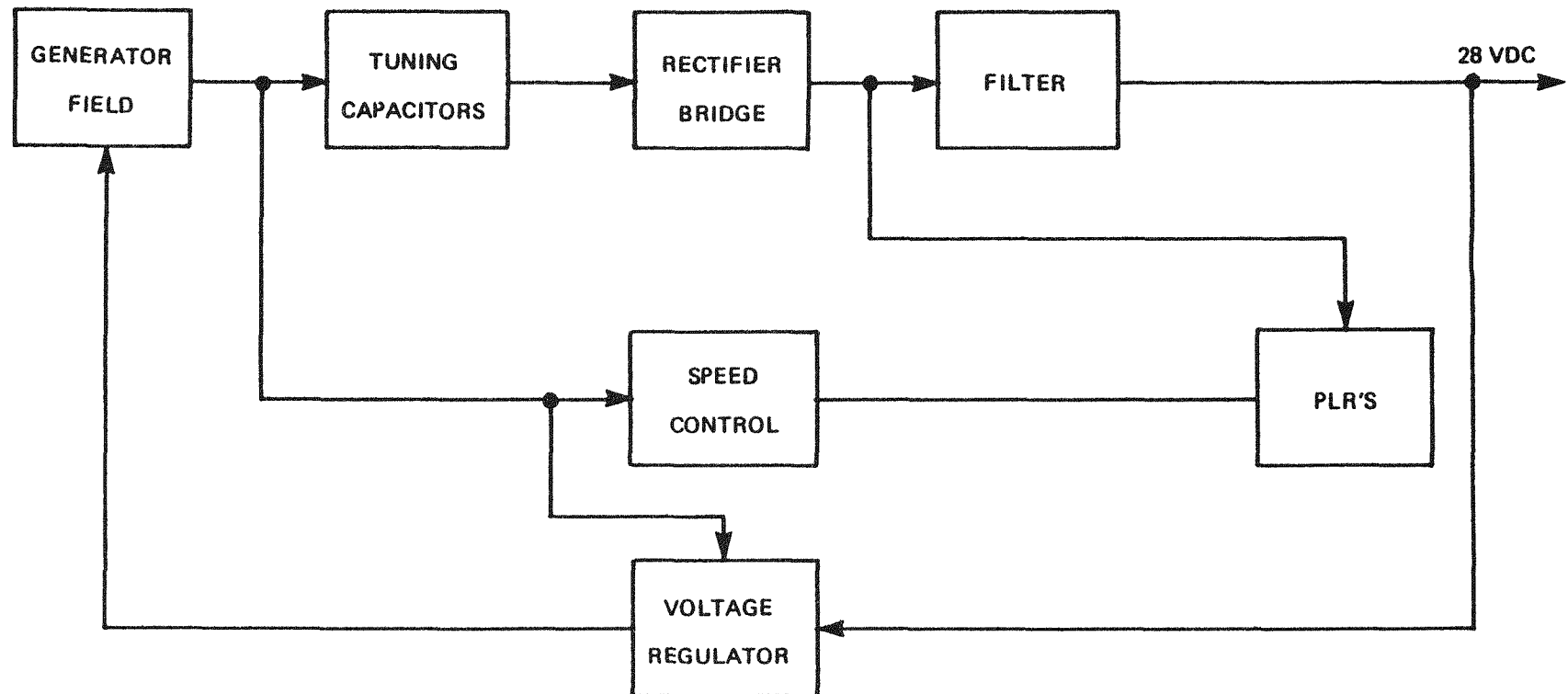


Figure 3-25 Control System Block Diagram

field winding, increasing the generator voltage. When the output is high, the PWM duty cycle tends toward zero, allowing the field current and generator output voltage to decay.

The overload protection circuit uses a frequency discriminator similar to the speed control frequency discriminator and a comparator to detect when turbine speed falls below 95%. When this is detected, the switching amplifier is turned off, decreasing the generator output voltage and lowering the generator load. The generator output voltage will not decrease below a small residual voltage which is sufficient to operate the frequency discriminator, comparator and switching amplifier.

The alternating current (AC) output of the alternator is converted to a DC voltage by a three phase full wave bridge rectifier assembly.

A low pass filter, consisting of an inductance and a capacitance, conditions the output voltage to a DC level having a 0.1% rms ripple content.

Alternator tuning capacitors are used to improve the power factor of the alternator, thus reducing the diode commutation overlap time of the full wave bridge rectifiers. Calculations indicate that the overall efficiency is improved by one percent using tuning capacitors. The tuning capacitors are sized to the load requirements for the particular mission.

When the turbine and alternator are operated in the frequency wild mode, the tuning capacitors can cause the alternator to operate self-excited. Self-excitation of the alternator results in excessive output voltage. To maintain proper voltage regulation, the signal which commands the frequency wild operation is also used to switch out the tuning capacitors from the alternator.

The allocated controller reliability for seven years was 0.986. The PLRs are sized such that two PLRs are capable of full load. With this configuration, the baseline controller has a reliability of 0.982. Any additional changes that would significantly increase controller reliability would also significantly increase system weight. The achieved controller reliability is adequate to meet the overall KIPS reliability goal.

A functional schematic of the controller is given in Figure 3-26. The main circuit groups, labeled on the schematic, are:

Main Power Rectification, including tuning capacitors, rectifier diodes, and a power line filter

Voltage Regulation, including a 95% speed detector, a voltage sensing network, a comparator, and a field switch

Speed Control, including a 100% speed detector, comparator, and PLR driver stages

Synchronization, including a ripple amplifier, phase detector, and a voltage controlled oscillator (VCO)

Key features of the design are the simplicity of the circuits, the use of components of the highest available reliability level and the low operating stress levels of the components. The low power losses achieved provide a margin of compensation for parameter variations due to production tolerances and estimates of aging effects.

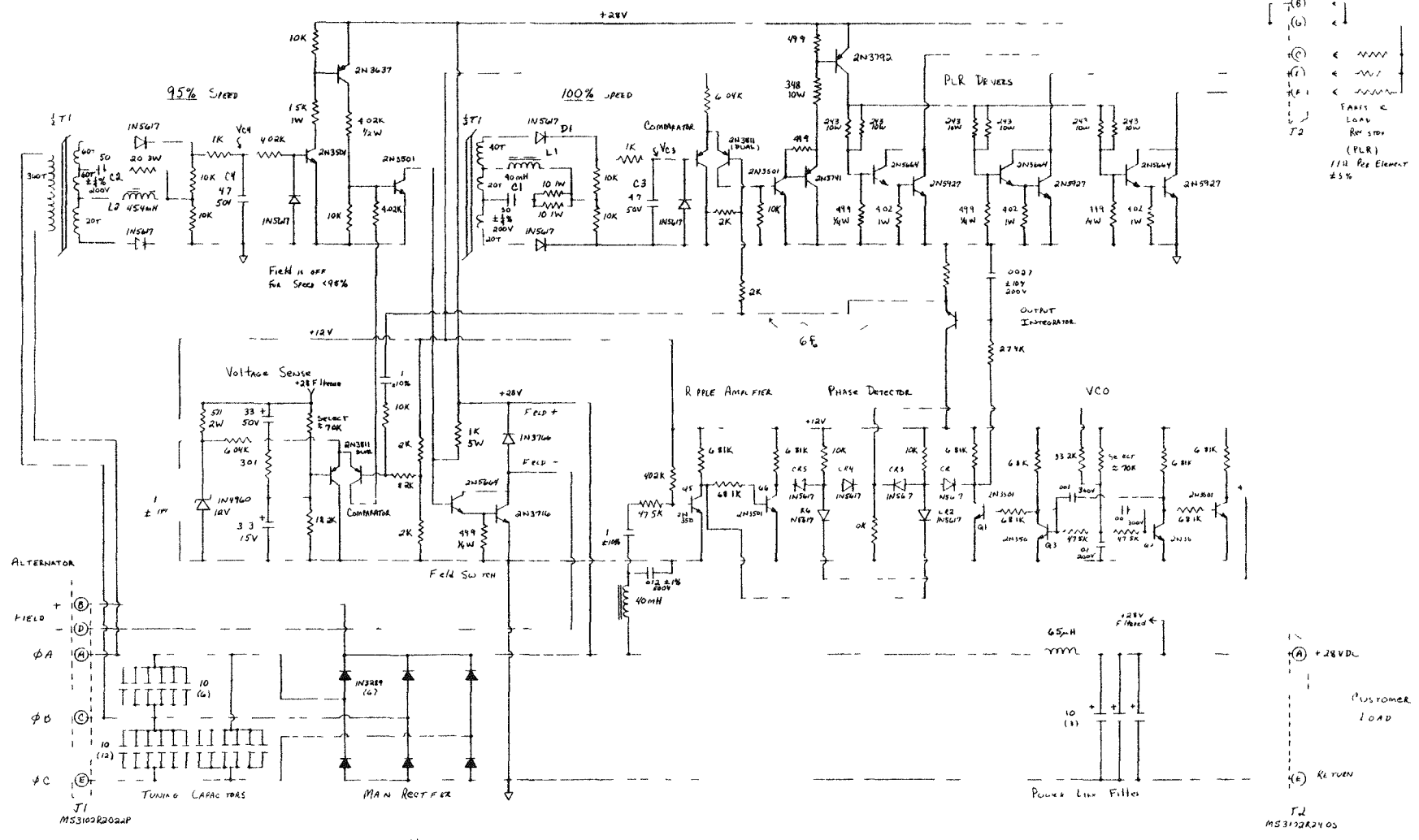


Figure 3-26 KIPS Alternator Controller

The controller is mounted by integral lugs protruding from the base casting (see Figure 3-27). All components with large power dissipation are mounted on the chassis either by threaded studs or threaded fasteners in their bases. Insulation is used in these mountings where electrical isolation is required.

Heavy wound core components employ threaded fasteners cast into their encapsulation. Printed wiring boards provide mounting and interconnection of the small electronic components. The board assemblies are mounted by threaded fasteners to brackets attached to chassis side and end plates. Auxiliary support is provided by standoffs mounted to the chassis by threaded fasteners.

Wiring and bus bars are supported by standoffs and by clamps and the devices which they terminate. Electrical connectors are chassis supported by their shell flanges with threaded fasteners. To assure good thermal contact and reliability, while minimizing chassis weight, the cooling tube will be cleaned and sealed and then cast into the aluminum chassis.

The controller is protected against corrosion and malfunction in humidity and salt atmospheres as required by MIL-E-5400. Metals are protected by plating where required and the printed wiring boards protected by conformal coating.

The coldest fluid in the power conversion system, radiator outlet flow, is used as the heat sink for the waste heat from the electronic control package. In order to keep thermal contact resistance between the component base and the plate to a minimum, an elastomeric interface material is employed, namely, Choetherm 1661. Special mounting nuts are employed for the rectification diodes and power switching transistors, both of which were high dissipative losses, to reduce the thermal resistance into the coolant fluid. The tube is sized to give a good liquid heat transfer coefficient with a low liquid side pressure drop.

### 3.2.3.6 Miscellaneous Components

In addition to the major subsystems discussed previously, several equally important, but less complex, components are utilized in the KIPS.

**3.2.3.6.1 NONCONDENSABLE GAS REMOVAL SYSTEM:** The Dowtherm A organic working fluid undergoes a slight pyrolytic decomposition under long term thermal cycling at high temperatures, forming gases and high molecular weight substances (liquid droplets) at the boiler outlet conditions. In addition, other system components may evolve gases at a low rate during operation. To assure continued reliable system performance over the mission duration in the presence of these factors, a noncondensable gas separator and a palladium window are utilized to remove the gaseous degradation products.

Any noncondensables present in the working fluid will tend to be concentrated in the jet condenser by means of natural separation at that location. Tests at Sundstrand have demonstrated that free stream noncondensable gas (air) concentrations in excess of 30 ppm will degrade performance and that concentrations in excess of 90 ppm can cause condenser failure. Performance degradation occurs because of the occlusion of the subcooled liquid jets by the noncondensable gas. At higher concentrations of gas in the liquid, the jet condenser floods out due to "brooming" of the liquid jets; i.e., the jets become unfocused due to the gas coming out of solution when the Dowtherm A is accelerated by the pressure drop through the jet condenser liquid nozzles.

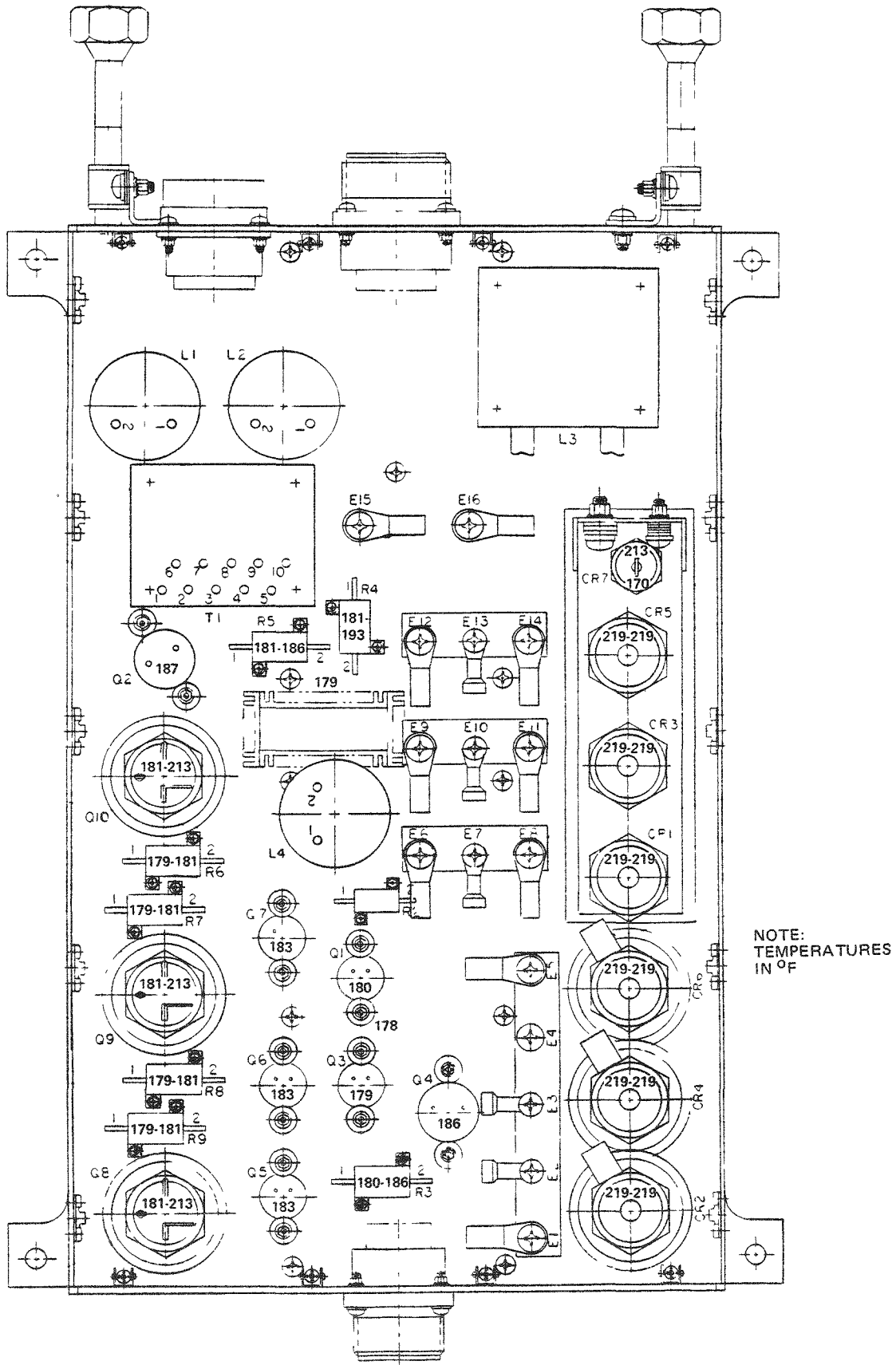


Figure 3-27 KIPS FSCD Controller

The noncondensable gas removal system is comprised of a hydrogen diffusion cell made of palladium and a noncondensable gas separator (NCGS).

The tolerance to any noncondensable gas is a function of its solubility in the working fluid. Since hydrogen is the most insoluble of the expected constituents and comprises the largest mole fraction of the pyrolytic degradation source term (which is the largest source term), it is of special concern.

It was noted in the AEC Organic Working Fluid Stability Program that the initial hydrogen generation rate for the first 2500 hours was approximately 50 times the asymptotic rate which prevailed after 2500 hours. In order to cope with this initial high generation rate, a palladium diffusion cell has been incorporated.

A palladium diffusion cell is a widely accepted method of removing hydrogen from process loops in industry. The diffusion cell consists of a palladium-silver diffusion material in the form of a tube, 0.062 in. OD x 0.003 in. wall thickness. The tube is 26 in. long with one end sealed and the other brazed to a nickel tube. The diffusion tube is coiled into a helix 1.125 in. diameter by 1.75 in. long and is supported by a "bird cage" constraint system. This constraint protects the diffusion tube from damage by handling or dynamic environment. The palladium diffusion cell assembly is placed at the regenerator vapor exit with the constraint welded to the wall interior and the nickel extension tube brazed through the wall. Model analysis indicates that with one cell, a maximum concentration of only 3% of the maximum tolerable level would occur. This would be reached at approximately 200 hours.

To remove potential noncondensable gases other than hydrogen, a heat pipe noncondensable gas separator (NCGS) is used. The internal characteristics of the NCGS and its system integration are illustrated in Figure 3-28.

The noncondensable gas separator is based on the gas controlled heat pipe principal (see Figure 3-29). Its two major sections are the condenser and the evaporator. The heart of the device is a 14 in. section of extruded ID grooved aluminum tube upon which the vapor condenses and is collected. It is then wicked through the grooves to the evaporator where the fluid is vaporized and returned to the flight system. At the aft end of the condenser the inlet to a capillary passage is located which collects and removes the noncondensable gases concentrated there.

The capillary passage is a 15 in. long section of tube 0.010 in. OD x 0.005 in. ID. The cooling fluid for the NCGS condenser is the jet condenser inlet flow. The heating fluid for the NCGS evaporator is the regenerator liquid outlet fluid (see Figure 3-28). The NCGS is integrated with the valve pack to minimize tube lengths, weight and number of joints, and, thus, assure high reliability.

A small portion of the vapor from the regenerator outlet is circulated into the NCGS where the undesirable gases are removed and the vapor outlet is discharged to the jet condenser mixing chamber. This configuration provides a net "driving potential" of 0.017 psi through the separator to ensure continuous, steady flow. There is always a positive pressure gradient from the condenser to the evaporator sections. Thus, shunting or recirculation of the vapor is eliminated, even though no positive seal is incorporated between the condenser and evaporator.

The heat pipe consists of a 14 in. long section of grooved tubing extruded from AISI 6063 aluminum. This heat pipe material has been the workhorse of many NASA heat pipe applications, is well characterized and has been space qualified. Its main advantage is the high film coefficient achievable.

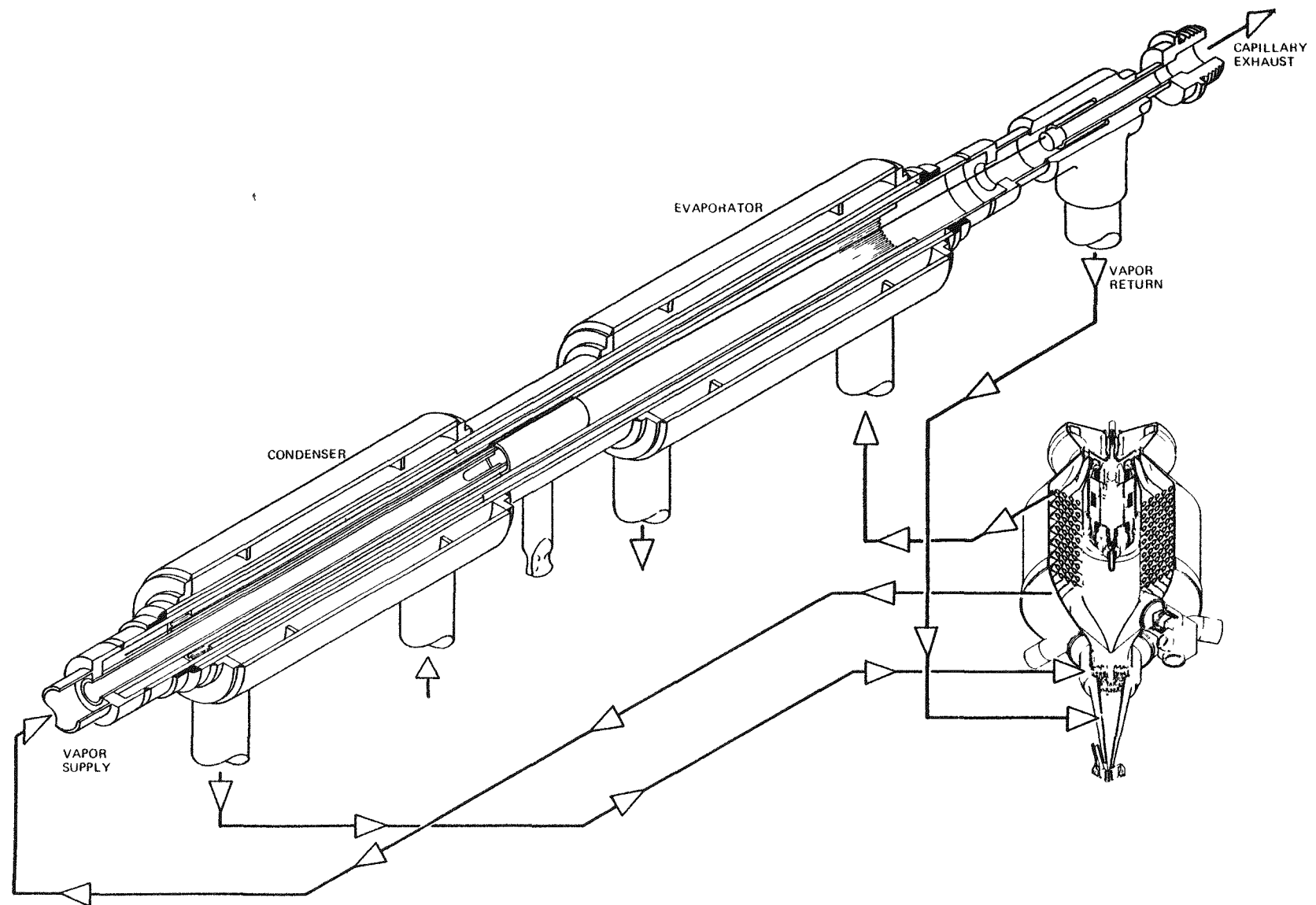


Figure 3-28 Noncondensable Gas Separator

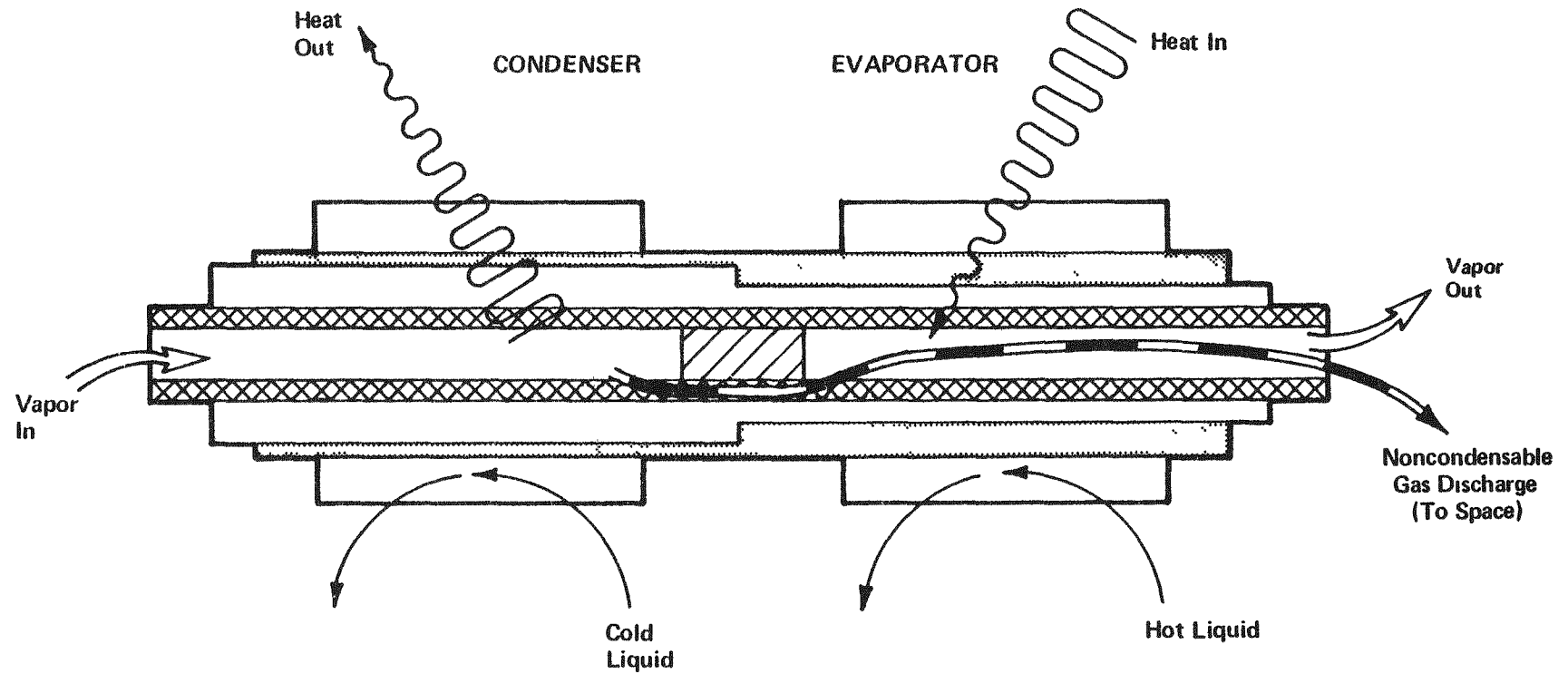


Figure 3-29 Noncondensable Gas Separator

with low conductivity fluids. Evaporator and condenser lengths were chosen to be six inches each, with a two inch adiabatic section separating them. The six inch lengths were selected to yield adequate separation of noncondensable gas.

At the evaporator end, the heat pipe will be closed by a stainless steel end plug which is penetrated by the capillary. The latter consists of a 15 in. long tube with an inside diameter of 0.005 in. This capillary will reject a volume flow rate of  $6 \times 10^{-8} \text{ ft}^3/\text{sec}$  at the system pressure of 0.1 psia. This corresponds to a noncondensable gas flow rate of  $3 \times 10^{-12} \text{ lbm/sec}$  and a Dowtherm flow rate of  $1 \times 10^{-10} \text{ lbs/sec}$  passing through the capillary. The condenser end closure is wicked with a single layer of wire mesh in order to return any liquid which condenses there to the grooves.

The seal between condenser and evaporator consists of a 1 in. long stainless steel plug which is interference fitted into the grooved aluminum tube. A 0.250 in. OD x 0.020 in. wall stainless tube will connect the condenser to the vapor source. The flow resistance of the tube (assuming a 6 inch length) is 0.023 psi-hr/lbm. Thus, for the nominal flow rate of 0.16 lbm/hr, the pressure loss in this tube will be 0.004 psi and the pressure drop across the seal between the condenser and evaporator will be  $0.017 - 0.004 = 0.013$  psi. The maximum delta P which the wick can sustain without blow-through is 0.015 psi which exceeds the existing pressure. Thus, in zero g, no vapor will bypass from the condenser to the evaporator. However, during vertical operation on the ground, the grooves will partially drain and some vapor can bypass the seal. The flow resistance of the seal is 0.288 psi hr/lbm. This will result in a bypass flow of approximately 15% of the nominal vapor flow rate. It should be noted that this bypass flow occurs in addition to the useful flow and does not detract from it.

**3.2.3.6.2 CENTRIFUGAL SEPARATOR:** The Dowtherm A organic working fluid undergoes a slight pyrolytic decomposition under long term thermal cycling at high temperatures, forming high molecular weight substances (liquid droplets) at the boiler outlet conditions. It is desirable to separate these droplets from the vapor stream to prevent their deposit and subsequent buildup on the low pressure turbine nozzle surfaces. A centrifugal separator is located between the boiler and the turbine nozzle plenum. Its function is to prevent the buildup of any substance on the nozzle surfaces by swirling the vapor, causing foreign material to accumulate inside the swirl chamber.

A cross-sectional view of the flight system centrifugal separator is presented in Figure 3-30. The separator consists of a rectangular-tangential inlet nozzle which accelerates the stream to a velocity of 50 ft/sec. The main body is comprised of three sections: an annular inlet and transition funnel, particle trap, and vapor exit nozzle.

The vapor enters the separator tangentially in the annular section and is forced in upon itself resulting in an axial acceleration toward the particle trap. This swirling axial motion continues through the straight section of the body and into the tapered section where the axial velocity is again accelerated to the throat. At the throat, a small carry-over of the vortex occurs, sweeping with it the separated particles and forcing them to the outer walls of the separator trap. At the throat, the primary vapor flow undergoes a reversal in axial direction and begins to swirl toward the vapor exit nozzle.

**3.2.3.6.3 QUICK DISCONNECTS:** There are five locations in the FSCD where quick disconnects will be used. Their locations are as follows:

Accumulator outlet line — This allows one of two connections to be made to the start module to start the system.

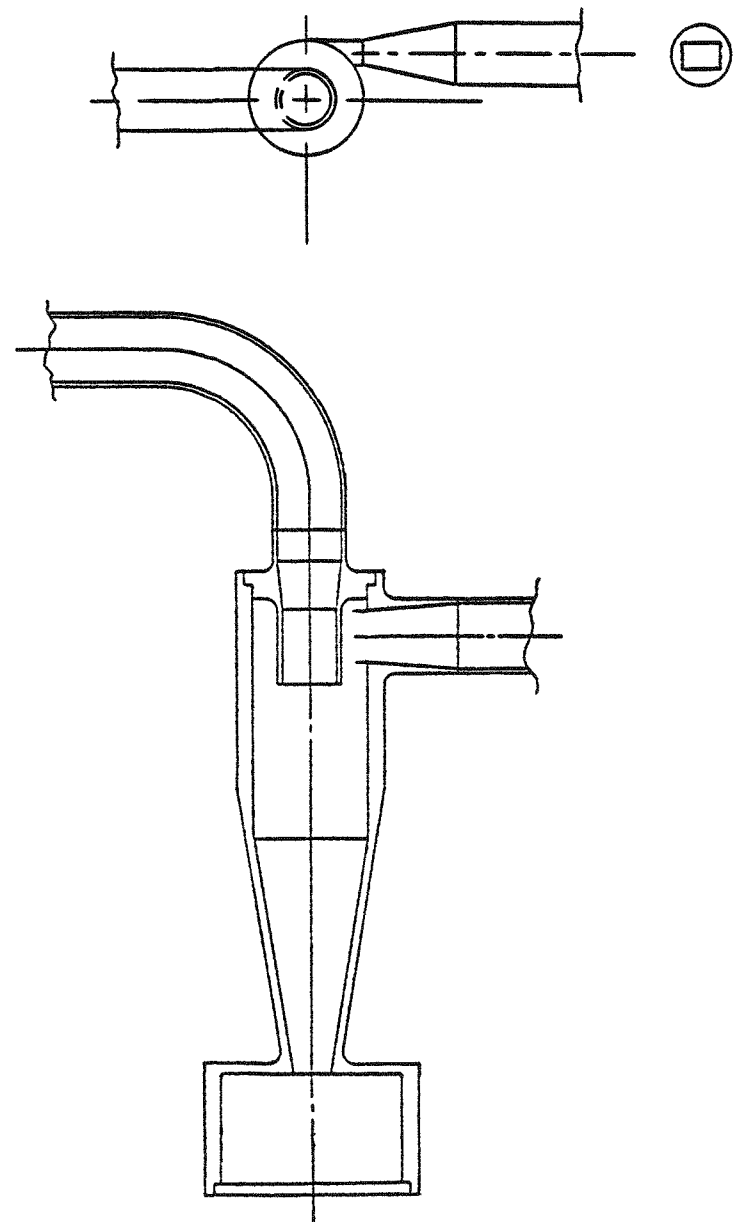


Figure 3-30 FSCD Centrifugal Separator

System pump outlet line — This allows the second connection required to be made to the start module.

System evacuation line — This allows the connection required to pump down the system prior to startup.

Auxiliary cooler coolant lines (2) — These allow connection of auxiliary cooler coolant lines to the system to allow the system to operate while on the launch pad or in the shuttle bay.

The functions of the quick disconnects are to: 1) allow hookup with a minimum amount of air inclusion (0.002 cubic inch maximum), 2) allow disconnect with a minimum amount of fluid spillage (0.003 cubic inch maximum), and 3) where system connections are made, to keep the system hermetically sealed (leak rate less than  $1 \times 10^{-8}$  standard cc/sec).

Final configuration selection has not been determined at this time.

**3.2.3.6.4 FILTRATION:** The KIPS FSCD has two filters in its loop. The jet condenser inlet filter is located between the radiator and the jet condenser. Its function is to prevent the jets of the condenser from being plugged should spallation products, by some chance, be generated from micrometeoroid strikes. The system filter is located in the accumulator. Its function is to remove particles that may score the bearings. Both filter elements are of a conventional type made similar to AN 6235 configuration with 304 stainless steel construction. The end is modified so that an O ring is not required.

In space, due to potential micrometeoroid impact, some spallation at the inside diameter of radiator tubes may occur. A filter is therefore placed at the radiator outlet to preclude any spallation products from plugging nozzles in the jet condenser. Since the nozzles are approximately 0.010 in. in diameter, a 60 micron absolute filter was selected. The filter element selected has a nominal 6 gpm rating. The maximum radiator flow is 3.2 gpm. Therefore, the delta P is very low even if a substantial buildup of particulates occurs.

The system filter element is located in the accumulator to save the weight required for a filter housing. During launch conditions, the minimum bearing film thickness is calculated to be approximately 0.00017 in. The inner diameter of bearing pads are plated with 0.0004 minimum silver plating thickness, hence, the absolute filtration level of retaining all particles larger than 0.00057 in. (14 micron) is desirable. The filter selected has a nominal rating of 2 microns and absolute rating of 10 microns. The filter area is equivalent to an AN 6235-3A element so, at normal operating conditions, the pressure drop through the filter will be low.

**3.2.3.6.5 RADIATOR AUXILIARY HEAT EXCHANGER:** In order to reject the system waste heat both on the ground and in the Space Shuttle bay, an auxiliary waste heat rejection system will be incorporated. This system performs the function of the radiator.

The heat exchanger is a simple, all aluminum, coaxial tube, counterflow device which is plumbed upstream and in series with the radiator. The system fluid passes through the center tube and the coolant passes through the outer tube. Placing the heat exchanger upstream of the radiator minimizes radiator temperature and, hence, minimizes heat rejection from the radiator to the Space Shuttle walls.

The heat exchanger is sized to reject the complete power conversion system (PCS) heat input of 7200 watts thermal since the unit could be operating in the Space Shuttle in an overspeed with no requirements for any power output. The coolant for Space Shuttle operation is Freon 21, while water would probably be used on the ground.

The heat exchanger configuration is given below:

Tube length = 7.46 ft  
Outer tube OD = 0.750 in  
Outer tube ID = 0.652 in  
Inner tube OD = 0.500 in  
Inner tube ID = 0.402 in  
Freon side  $\Delta P$  = 3.37 psid  
Dowtherm side  $\Delta P$  @ overspeed = 2.43 psid  
Dowtherm side  $\Delta P$  @ design speed = 1.25 psid

For system operation at different power levels, the heat exchanger length will vary in the same proportion as the radiator size.

### 3.2.4 FSCD GROUND SUPPORT EQUIPMENT

The KIPS will utilize ground support equipment (GSE) to enable it to be started and operated during installation and prelaunch operations. This GSE will provide the capability for (1) rejecting the heat from the electric or isotope heat sources prior to PCS starting and for emergency cooling, (2) starting, draining, and restarting the PCS, and (3) rejecting the radiator heat load when the KIPS is operating on the ground and in the launch vehicle prior to and during launch.

#### 3.2.4.1 Start Module

The start module is used to provide liquid flow to the jet condenser, to the bearings, and to the boiler during startup. When turbine output shaft power is sufficient for the unit to be self-sustaining, the start module can be disconnected.

The flight system start module will be an all welded, hermetic, hydraulic loop comprising a 28 VAC electrically driven start pump, an inverter, a spring loaded, nitrogen pressurized bellows accumulator and a 28 VDC solenoid valve. The Dowtherm loop will be connected to the power conversion system (PCS) through quick disconnects (QDs) with another quick disconnect being connected for accumulator charging. The loop schematic is shown in Figure 3-31.

The fill quick-disconnect allows the start accumulator to be evacuated and then filled with deaerated fluid. Filling will be accomplished by connecting a deaerated Dowtherm supply to the QD and relieving the  $N_2$  pressure on the bellows, allowing the spring to force the bellows to the fully compressed condition; gravity will then fill the accumulator. The start system does not require a deaeration system since both the start system and PCS are hermetic and no leakage of air into the hydraulic circuit can occur.

Pressure transducers are provided on the nitrogen side of the accumulator, the pump inlet, and pump outlet. The nitrogen pressure transducer allows the system accumulator pressure to be set at

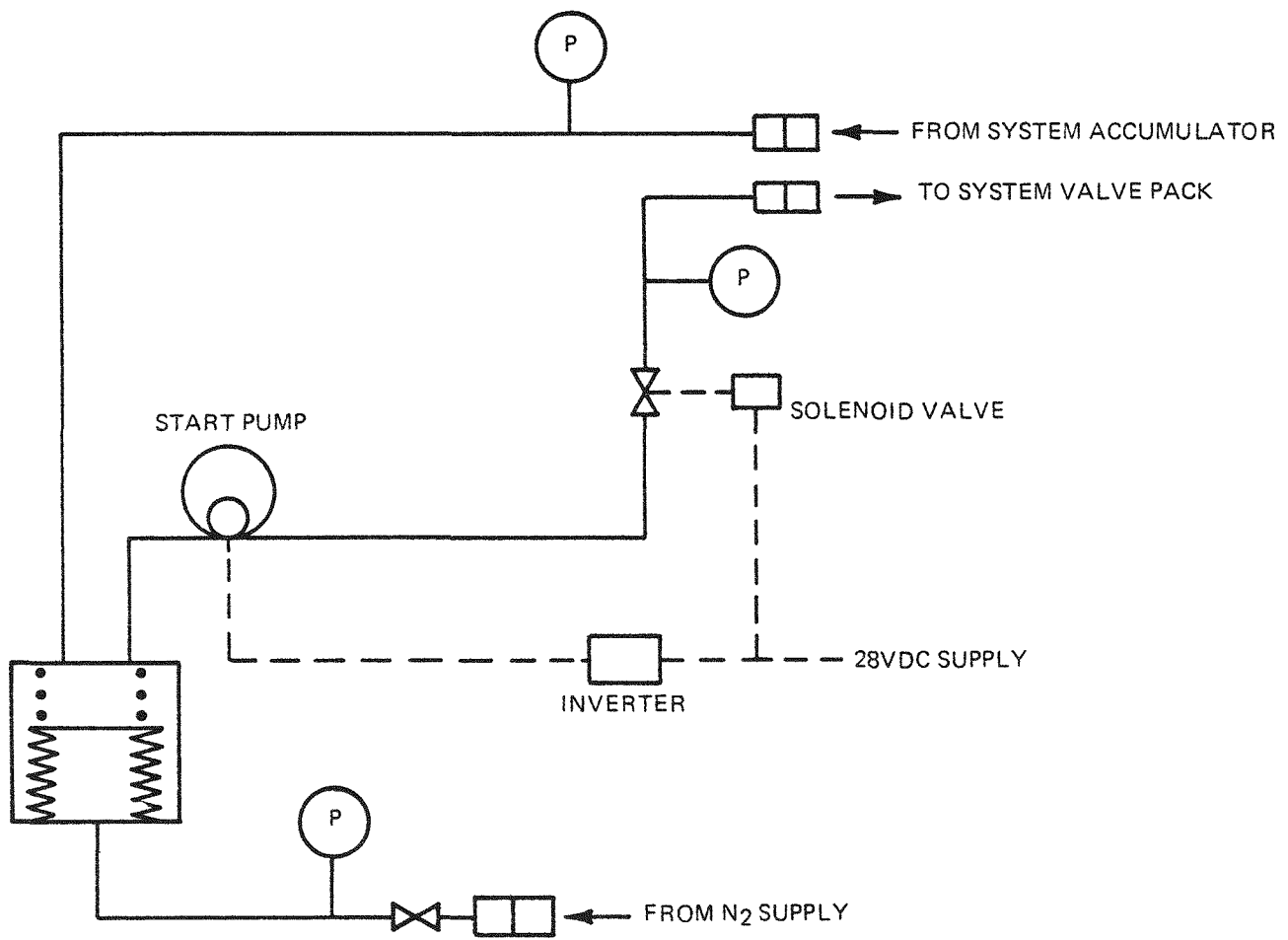


Figure 3-31 Flight System Start Module

the proper value for starting the system and then at the required value for transferring the fluid inventory from the start accumulator to the system accumulator prior to disconnecting the start module. The transducers on the start pump inlet and outlet provide an indication of system pump operation.

### **3.2.4.2 Heat Source Auxiliary Cooling**

The auxiliary cooling system provides isotope heat rejection capability between isotope loading and system startup. The cooling loop is also available during the launch mode to prevent activation of the emergency heat dump system in the event of a fault requiring shutdown of the KIPS. The cooling system would also be used for ground checkout with electric heat sources before installation of the isotope heat sources.

The baseline start procedure provides for startup on the ground, prior to launch. Nitrogen coolant will be used for system checkout and for startup with the isotope heat sources. For emergency cooling capability in the Space Shuttle, flash evaporation cooling, using water, will be employed since the temperature will be too high for the Freon system and a controlled temperature would not be required. If a space start of the KIPS system were to become a requirement, then temperature control would be necessary and a secondary loop employing Dowtherm with a Dowtherm-to-Freon heat exchanger would be used.

Individual heat source assemblies incorporate a 0.25 in. diameter coolant tube welded to the fin adjacent to the Dowtherm tube. Each HSA is connected in series with interconnecting tubes. The coolant inlet connection is made to the inlet end of HSA No. 1 and the outlet exits from HSA No. 3. Coolant passes in the same direction as the Dowtherm. By flowing in a series fashion, the resultant fin temperatures are close to actual operating temperatures, thus minimizing temperature changes during startup. Activation and control of the coolant loop is accomplished by a thermocouple sensing the outlet boiler tube/fin temperature on HSA No. 3. After the isotope is loaded, the fin temperature will rise and command coolant flow. HSA No. 3 will be the first to be loaded to ensure coolant flow while loading the other two.

During Shuttle launch, the cooling loop will be connected to the emergency water supply using quick disconnects. Just prior to deployment, these will be disconnected.

When the isotopes are loaded, or the electric power of the electric heat sources activated, the boiler fin temperatures will increase. The temperature controller maintains the fin temperature at the design point by modulating the coolant flow. As working fluid flow increases, the coolant flow decreases preventing the fin temperature from exceeding the set point.

### **3.2.4.3 Radiator Auxiliary Cooling**

This item of ground support equipment provides system heat rejection capability on the ground during checkout with electric heat sources and after startup with isotope heat sources. It also provides heat rejection in the Space Shuttle bay when the radiator is shrouded.

For shuttle operation, the auxiliary heat exchanger described in section 3.2.3.6.5 is connected into the Space Shuttle closed loop freon coolant supply loop. For ground operation, water will be used as the coolant; this is obtained by connecting to an external, softened supply of city water and flowing in an open loop mode. For ground operation where water is the coolant, the total system heat input can be rejected with 1 gpm water flow. The heat rejection coolant loop requires no temperature control, since the radiator bypass valve will compensate for coolant flow fluctuations.

### 3.3 FLIGHT SYSTEM PERFORMANCE

---

#### 3.3.1 FLIGHT SYSTEM SIZE

The flight system envelope dimensions are shown on Figure 3-32. Less than half of the space inside the radiator is occupied by the KIPS components, leaving space available for other spacecraft components in integrating the KIPS with a spacecraft.

The flight system radiator may easily be reconfigured to match specific spacecraft requirements. Radiator length and diameter can be varied as desired with radiator surface area being the only requirement for a given maximum power level.

For the baseline FSCD, the radiator diameter is 4.3 ft and the height is 8 ft.

The flight system weight breakdown showing major component weights is shown in Table 3-J.

#### 3.3.2 FLIGHT SYSTEM EFFICIENCY

A summary of the flight system design point efficiency is presented in Table 3-K. Performance benefits can be accrued by operation at turbine inlet temperatures slightly higher than the 650°F design. The slight increase in degradation at these temperatures can be accommodated by the noncondensable gas separator. The result of increasing turbine inlet temperature is given in Table 3-L.

#### 3.3.3 PERFORMANCE CHARACTERISTICS

##### 3.3.3.1 Startup

On start initiation, the start valve will be opened and the system will start to fill. The start pump will be designed to have only a slight change in head capacity in the flow range expected between filling the system and flowing through the jet condenser. This ensures a high pressure jet will be maintained for proper operation of the jet condenser at all times. Therefore, as soon as the liquid reaches the jet condenser, the jet condenser will start and flow will be established through the radiator loop. Startup of the jet condenser will be performed with the system accumulator bellows at their operating pressure, so that the jet condenser recovery pressure will be determined by the start module accumulator pressure. The system will fill the radiator, within about 10 seconds from start initiation, and slowly fill the regenerator, at a low rate determined by the turbine flow control valve which will be at its minimum flow value, since the turbine inlet line will be cold. After approximately 5 minutes, hot vapor, at approximately 630°F, will start leaving the boiler and, as the boiler fills, the turbine inlet pressure will reach a value sufficient to start rotation.

The turbine exhaust will simultaneously heat the regenerator so that boiler inlet temperature will begin rising and the flow control valve will start increasing the flow to keep the turbine inlet temperature at the set point.

As the turbine accelerates, the system pump outlet pressure will reach a value which matches the start pump outlet pressure and the system pump outlet check valve will open, allowing the system pump to start sharing the flow with the start pump. By the time rated speed is reached, the system pump is supplying most of the flow.

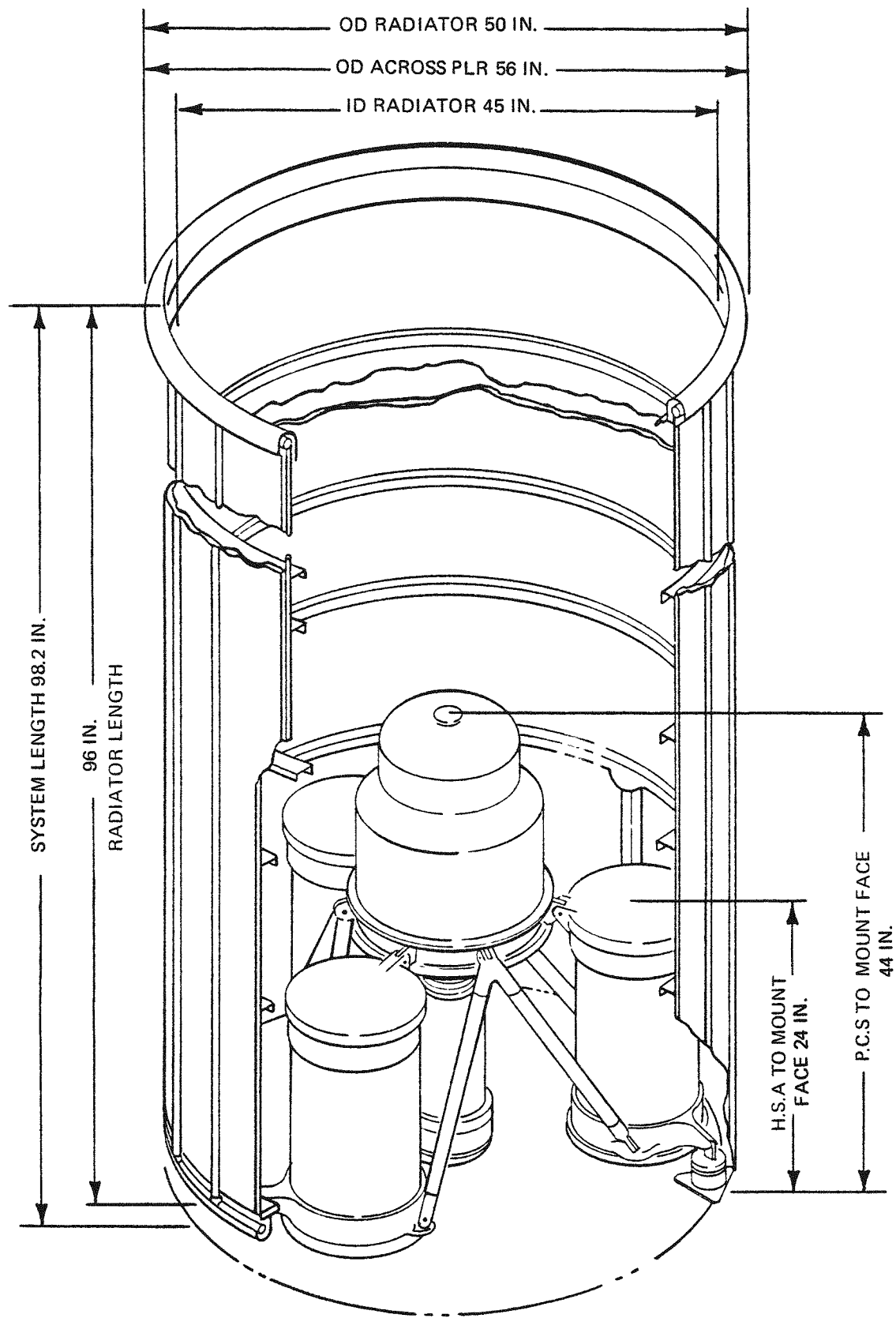


Figure 3-32 Flight System Envelope

Table 3-J Flight System Weight Breakdown

<u>Component</u>	<u>F.C.D. Lbs.</u>
Fluid Radiator	80.0
P.L.R.	8.6
H.S.A. (3 Loaded)	222.0
C.R.U.	56
P.C.S.	52
Valve Pack	6.5
Jet Condenser	5.1
Accumulator	5.0
Centrifugal Separator	0.4
Support Struts	3.1
Shock Mounts	2.5
Tubing	5.6
Controller	13.0
Electrical Harness	1.30
Insulation	3.0
Auxiliary Cooler	1.6
Fluid Weight	8.3
<b>Total System Weight 474.0 Lb.</b>	

Table 3-K Flight System Design Point

INPUT			
TURB EFF	= 0.693	ALTERNATOR EFF	= 0.430
BEAR + SEAL LOSS	= 0.080 KW	CONDITIONING EFF	= 0.944
REGEN EFFEC	= 0.950	J COND RECOVERY	= 0.400
CRU RPM	= 33700.	PUMP FLOW RATIO	= 10.000
NET O/P POWER	= 1.300 KW	PARASITIC POWER	= 0.038 KW
DES TURB IN PRES	= 57.000 PSIA	TURB INLET TEMP	= 650.0 °F
COND PRESS	= 0.0	BOILER HEAT LOSS	= 550.0 BTU/HR
REGEN VAP P DROP	= 0.032 PSID	REGEN LIQ P DROP	= 4.40 PSID
BOILER PRES DROP	= 9.40 PSID	CENT SEP P DROP	= 2.50 PSID
RADIATOR P DROP	= 10.00 PSID	CVN VALVE P DROP	= 23.10 PSID
CONTROL P DROP	= 6.40 PSID	ACCUM P DROP	= 1.30 PSID
DIFF PRES RISE	= 0.032 PSID	ALT WINDAGE	= 0.013 KW
TURB HEAT LOSS	= 167.0 BTU/HR	REGEN HEAT LOSS	= 175.0 BTU/HR
TURB IN HT LOSS	= 22.0 BTU/HR	REG HSG HT LOSS	= 12.0 BTU/HR
PLUMBING HT LOSS	= 8.0 BTU/HR	J=COND DES PIN	= 80.0 PSIA
RAD DES FLOW	= 0.0		
OUTPUT			
STATE POINT	PRESS(PSIA)	TEMP(F)	ENTHALPY(B/LB)
TURBINE PLENUM IN	57.000	650.000	396.266
TURB NOZ IN	57.000	640.464	344.550
TURB OUT	0.101	525.065	341.722
REGEN VAP IN	0.133	521.237	340.025
J COND VAP IN	0.101	239.387	229.432
J COND OUTLET	32.000	211.713	63.330
PUMP INLET	30.700	212.634	63.728
RAD+C VALVE IN	96.400	213.329	64.028
RAD OUTLET	86.400	167.333	44.603
J COND LIQ IN	80.000	167.993	44.874
REG LIQ IN	73.300	224.543	68.904
BOILER INLET	68.900	456.222	179.497
BOILER OUT	59.500	650.472	396.338
TURBINE CP	= 0.338BTU/LB°F	TURBINE GAMMA	= 1.037
PUMP SPEC SPEED	= 1160.	PUMP EFFICIENCY	= 0.650
TURBINE FLOW LB/SEC	= 0.03077 LB/SEC	RADIATOR FLOW LB/SEC	= 0.277 LB/SEC
TURBINE FLOW GPM	= 0.2226 GPM	RADIATOR FLOW GPM	= 1.960 GPM
HEAT ADDED IN BOILER	= 24018. BTU/HR	HEAT REJ BY RADIATOR	= 20131. BTU/HR
ALT HEAT ADDED	= 540.0 BTU/HR	CONTROLLER HEAT ADDED	= 270.9 BTU/HR
OUTPUT RW	= 1.300 KW	ALT INPUT KW	= 1.524 KW
BEARING+SEAL LOSS KW	= 0.080 KW	PUMP SHAFT KW	= 0.097 KW
ALTERNATOR EFF	= 0.930	PUMP FLOW RATIO	= 10.00
RECTIFIER LOSS KW	= 0.079 KW	BOILER HEAT LOSS	= 550.0 BTU/HR
HEAT SOURCE WATTS	= 7198.3 WATTS		
SYSTEM EFFICIENCY	= 18.05991%	CYCLE EFFICIENCY	= 18.47346%

Table 3-L System Performance as a Function of Turbine Inlet Temperature

<u>Input Power Watt(t)</u>	<u>Turbine Inlet Temperature (°F)</u>	<u>Output Power (Watts)</u>	<u>System Efficiency(%)</u>
7200	650	1300	18.1
7200	675	1325	18.4
7200	700	1350	18.7

As the system warms up to steady state, the parasitic load will automatically increase to keep speed constant. When the system is operating at design speed, the start accumulator pressure is increased to a value slightly above the system accumulator design value and all the liquid left in the start accumulator is forced into the system, thus charging it with its correct inventory. The start pump is now deactivated and the quick disconnects are disconnected. For the final start, prior to launch, the final hermetic seal caps on the Dowtherm lines are applied. While operating on the ground prior to launch, the power system output will be slightly less than normal due to increased heat losses from natural convection but by no more than 150 watts.

The estimated times required to start are summarized in Table 3-M.

Table 3-M Startup Times

<u>Start Phase</u>	<u>Time from Start Initiation</u>
Start Initiation	0
Jet Condenser Start	2 Seconds
Radiator Filled	10 Seconds
Hot Gas at Turbine Inlet	6 Minutes
Rotation	6.5 Minutes
100% Speed	10 Minutes
Full Power	3 Hours

### 3.3.3.2 Thermal Interchange

The KIPS system operates at relatively low temperatures, and, therefore, rejects heat to the spacecraft at low temperatures. Thermal interchange occurs by two processes only, conduction and radiation.

The conduction heat losses all pass through the three shock mounts by which the system is mounted to the spacecraft. The skin temperature at the heat source mount point is approximately 200°F which, with an assumed spacecraft temperature of 100°F and the high thermal resistance of the shock mounts, gives 11 watts due to conduction.

Heat is transferred by radiation from the bottom of the heat sources at a temperature of 200°F; from the system accumulator and cold end of the regenerator, both of which are thermally insulated and have skin temperatures of 150°F and 175°F; and finally from the inside of the radiator skin which has an average temperature of 190°F, but has a relatively low view factor to the spacecraft. A low emissivity surface, with a value of 0.04, is assumed for the spacecraft. With these assumptions, a total radiator loss of 35 watts is calculated.

### 3.3.3.3 Torque Effects

Changes in rotative speed of the CRU produce torque reactions in the KIPS which are transmitted to the spacecraft. The magnitude, duration and repetition rate of these torque effects are all of interest to the spacecraft designer.

The moment of inertia of the flight system combined rotating unit (CRU) including all of the rotating components, is  $0.00385 \text{ ft-lb-sec}^2$ . At the design speed of 33,700 rpm (3529 rad/sec), the angular momentum of the CRU is 13.59 ft-lb-sec.

On the KIPS there are four types of speed variations. These are speed shifts due to customer load change, long term speed change due to isotope decay, speed modulation at constant load caused by the interaction of the controller voltage regulator and speed control circuits, and speed changes which occur if a customer electrical overload is applied. Diurnal changes in heat sink capability are accommodated by the radiator bypass valve and have no effect on speed.

The speed shift due to customer load changes consists of a 2% drop in speed (from +1% to -1%) when customer load changes from zero to full load.

The initial torque when full load is added or dropped is 0.32 ft-lb. As the speed changes, the dissipative load is applied proportional to the speed error so that the average torque during the 1.7 second interval required to accomplish the 2% speed change is 0.16 ft-lb. For step load changes of less than 100%, the peak torque, average torque and speed change all decrease proportionally to the load change. These angular impulses occur only when load is changed and average out to zero when the load returns to the base load.

The second type of speed change occurs if input power decays due to isotope decay. This effect has been investigated on the KIPS alternator-controller test stand by changing the input power and noting the change in steady state speed. The expected speed change on the flight system based on these results is a reduction of 0.35% in CRU speed over the seven year mission. This speed change produces a minuscule but continuous torque of  $2.15 \times 10^{-10}$  ft-lb.

The third type of speed change occurs at the natural frequency of the integrated CRU-controller-load bank system. The magnitude of the speed excursions depends on the response of the voltage regulation and speed control circuits to changes in voltage and speed. For a worst case condition, speed variations of  $\pm 0.05\%$  at a frequency of 0.14 Hz have been predicted. This produces a fluctuating torque of  $\pm 0.004$  ft-lb.

Both the frequency and magnitude of this variation can be controlled by damping and tuning of the controller circuits.

The fourth type of speed variation occurs only in the event of a customer electrical overload; i.e., spacecraft demands exceed the power output capability of the KIPS. The KIPS control system will accommodate this condition without causing a PCS shutdown.

When excessive electrical load is demanded, the excess alternator torque causes the CRU to slow down. As the CRU passes through 95% speed, the KIPS controller removes all output power by shutting off the alternator field current. The CRU is then unloaded and speed increases until 95% speed is again attained, where alternator field is again applied. If the overload continues, the speed will then again fall and the cycle is repeated. In the case of a small overload (0 to 100 watts), the resulting torque pulses are  $\pm 0.032$  ft-lb at a rate of about 11 Hz. For an overload of 1300 watts (i.e., 2 x rated load), the torque pulse is  $\pm 0.47$  ft-lb at a rate of 21 Hz. The system returns to rated speed when the electrical overload is removed.

### 3.3.3.4 Orbital Transfer Power — Launch Power

The PCS has designed-in capability to withstand the high shock and vibration loads of launch and orbital transfer without affecting the normal performance of the system. The areas of concern when operating through shock and vibration are the extra bearing loads and the deflection forces on the fluid jet streams in the jet condenser. Extra capability could have been provided by oversizing the bearings to carry the extra load and by increasing the design pressure of the system feed pump to supply extra jet velocity to minimize jet deflections. These solutions waste power in the normal mode of operation and would have caused a reduction of system efficiency.

The solution adopted for the KIPS PCS is to let the CRU speed increase during periods when extra vibration loads are present. By switching off the speed control system, the CRU speed will vary inversely with electrical load, running at rated speed at maximum design load and at 175% rated speed at no load. As speed is increased, the tilting pad bearing film thickness increases and the bearing develops additional load carrying ability. The feed pump, attached to the CRU shaft, develops additional pressure as speed is increased to supply the jet condenser with additional jet velocity to resist jet deflection. The bearings and jet condenser can therefore be designed for low g operation and have capability for higher loads without reducing system design point efficiency.

The amount of spacecraft power which can be extracted during launch and orbital maneuvers depends on the vibration and shock levels which the CRU must withstand. Should the system be launched on the Titan IIIC where shock and vibration loads are high, it is desirable to keep the PCS nearly unloaded so that maximum resistance to vibration and shock are retained. For space shuttle launch and orbital transfer maneuvers where vibration and shock are less severe, the PCS can deliver more power. During portions of the launch and orbital maneuvers where the PCS experiences no vibration, the speed can be permitted to drop to rated speed, so full electrical output is available.

Figure 3-33 shows the effects of customer load on CRU speed when operating in the frequency wild mode. A speed of 53,000 rpm is expected to be adequate for all shock and vibration loads which occur during launch, including orbital maneuvering loads. This figure shows that 320 watts are available under these worst case conditions (assuming Titan III launch).

The KIPS PCS can be used on either spin stabilized spacecraft or on nonrotating spacecraft, and will function in a zero g environment as well as a one g field. The PCS is configured to withstand launch loads and orbital transfer on a spinning vehicle while operating or nonoperating. The capability of being launched while running is especially useful in that power can be produced during launch.

### 3.3.3.5 Multipower Performance

The system performance has been investigated at power levels other than design. The limits of investigation were 500 watts to 2000 watts. Component performances were investigated at these power levels and incorporated into the off-design performance analysis, with the assumption that modification to the system for power levels other than design must be performed with only minor component changes. Figure 3-34 summarizes the performance expected for the multipower operation. For power levels within the range of those defined, the system performance would fall between the limits.

### 3.3.4 PRELAUNCH HANDLING

At some time prior to launch, the spacecraft and the KIPS must be integrated into a package and functionally checked. Various procedures and locations for performing this integration have been studied. It was determined that it is desirable to ship the spacecraft, PCS and IHS modules to the launch site after each component is assembled and checked out and perform the final integration at the launch site.

The spacecraft can be checked with a ground support 28 VDC power supply and the PCS operated with electrical heat sources to ensure integrity after shipping and storage. The IHS modules in their shipping containers are natural convection cooled and can be shipped and stored without the need for active cooling.

The present flight system design assumes that the KIPS will be attached to a spacecraft at one end of the specified 4.3 ft. x 8 ft. radiator. To minimize overhung weight and resulting high structural loads under shock and vibration, the KIPS boiler assemblies, including the IHS modules, are located as close as possible to the spacecraft. Access to the boilers for IHS loading is readily available from the spacecraft interface end of the radiator but difficult from the outboard end due to the length of the radiator. Loading from the "outboard" end is further complicated by the need for boiler and IHS inerting during loading. The present baseline approach, therefore, is to fuel and start the KIPS system prior to mounting to the spacecraft. This presumes the spacecraft is configured to prevent access for fueling from the KIPS/spaceship interface end of the package.

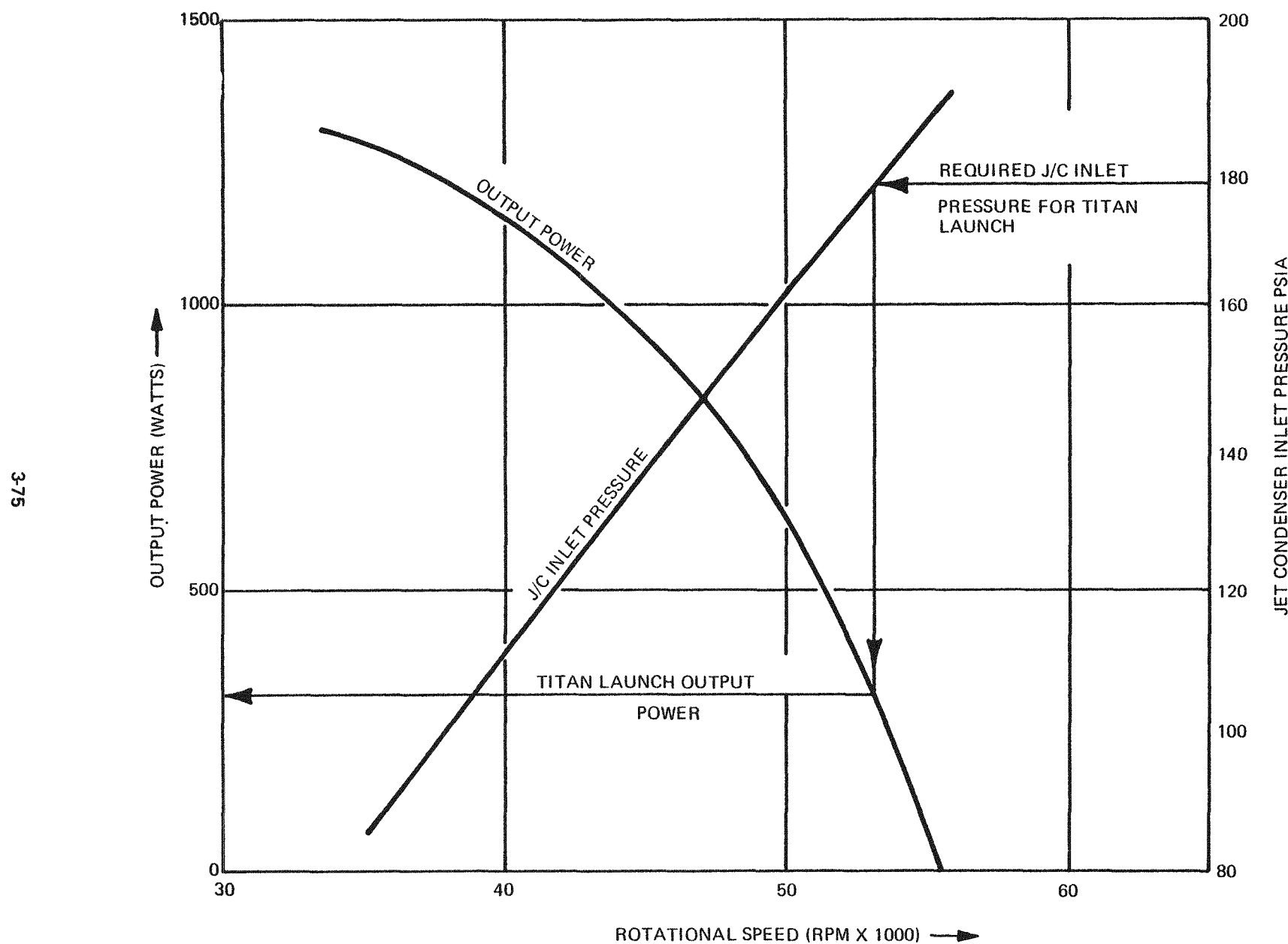


Figure 3-33 Output Power and Jet Condenser Inlet Pressure as a Function of Rotational Speed

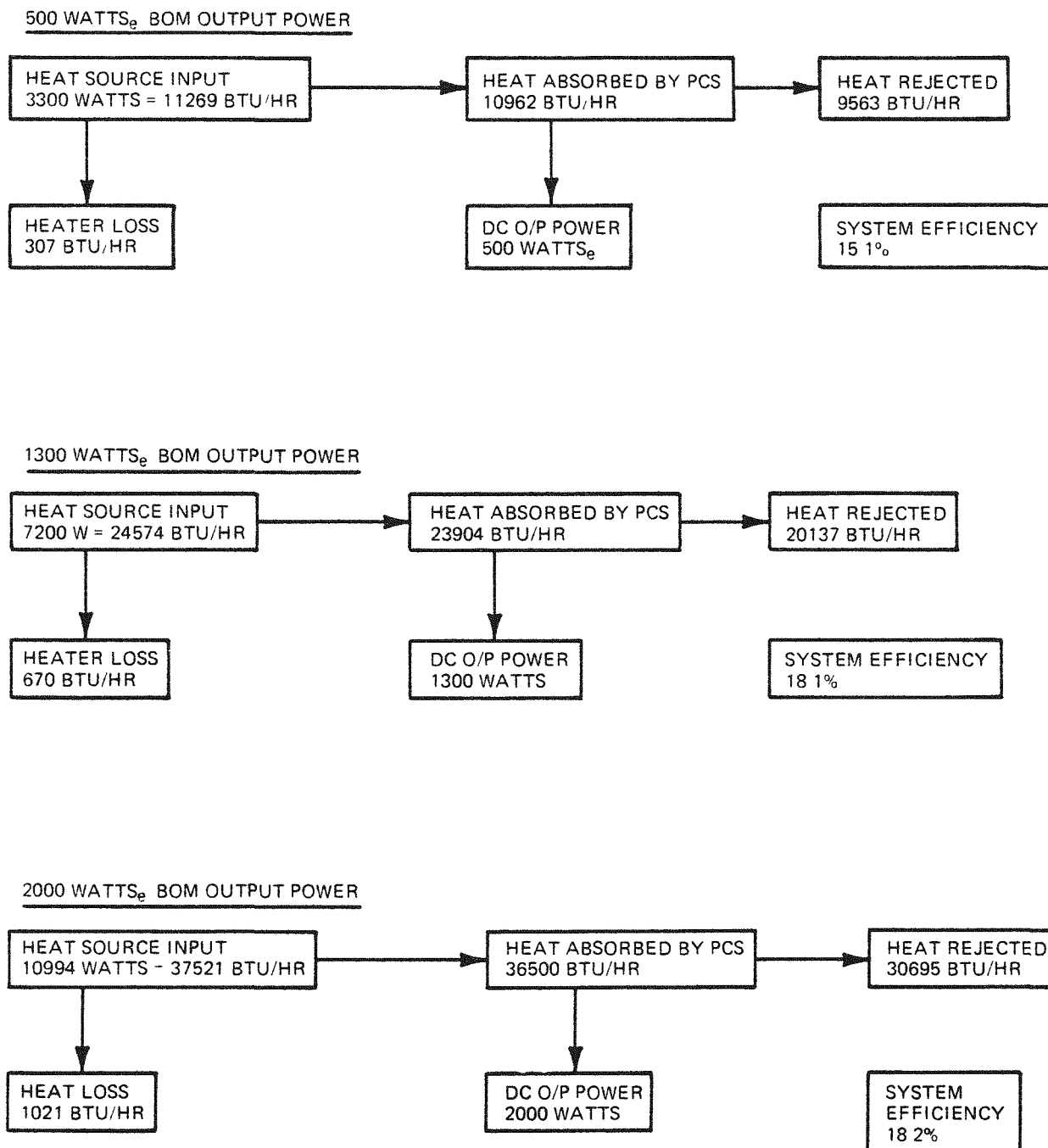


Figure 3-34 Performance Summary

The spacecraft configuration has not been defined, nor has the arrangement and location of the spacecraft and KIPS been defined with respect to the interim upper stage (IUS) and space shuttle for shuttle launched systems. For space shuttle usage, it may be desirable to reduce overall length by using a larger diameter and shorter radiator and installing both the KIPS and the spacecraft inside this envelope. In this case, fueling can easily be accomplished from either end and at any desirable point in the integration sequence.

For the baseline approach, the KIPS is tested with electrical heat sources after delivery to a fueling facility near the launch site. After checkout, the KIPS is shut down and the EHSs removed. The KIPS is then mounted to the loading and assembly station and the inerting chamber attached as shown in Figure 3-35. The KIPS boiler auxiliary cooling system and the isotope cooling coils inside the inerting chamber are attached to ground support cooling loops to maintain thermal control of the IHS during fueling. The chamber is then inerted and the boilers loaded. After the boilers are fueled and closed, the KIPS is removed from the loading and assembly station and attached to the start module. A facility nitrogen supply with nitrogen flow regulated to maintain the boiler fin at approximately 700°F is used to remove isotope heat until the start system is activated. As Dowtherm enters the boiler tubes, the boiler fin is cooled by system working fluid and the nitrogen flow can be shut off. N<sub>2</sub> lines remain attached to provide emergency IHS cooling in the event of a KIPS shutdown. After the KIPS attains operating temperature, the start module is disconnected and disconnect points capped. The KIPS radiator has adequate heat rejection capability via natural convection on the ground so auxiliary cooling is not required if the building is ventilated. The radiator has an auxiliary cooling loop which can be used if desired. Control of coolant flow rate and temperature is not required as the KIPS radiator bypass valve will bypass fluid around the auxiliary cooler as required to maintain 170°F mixed radiator outlet temperatures.

When the spacecraft checkout is complete, the operating KIPS can be attached via the three shock absorbing mounts and electrically connected to the spacecraft.

The spacecraft/KIPS assembly is then mounted to the IUS, the shuttle or other launch vehicle and emergency cooling lines transferred to the vehicle.

A prelaunch performance test may be desirable to provide final assurance that the KIPS is operating properly and that integration and handling have not affected system operation.

In addition to tests of electrical output power, voltage regulation, transient response, and other electrical parameters of interest to the user, it is also easy to check the PCS at higher stress levels, pressures and flow rates than normally occur. This test can be conducted by shutting off the speed control system and permitting the system to run to maximum unloaded speed. The speed attained is controlled largely by bearing, seal and pump losses and provides a good indication of the condition of these components.

By applying successive load steps to the system, turbine speed versus load can be determined for comparison with acceptance test results to verify that system characteristics have not changed. The system can be left running in the frequency wild mode for launch after checking that the speed control system also functions properly at various loads.

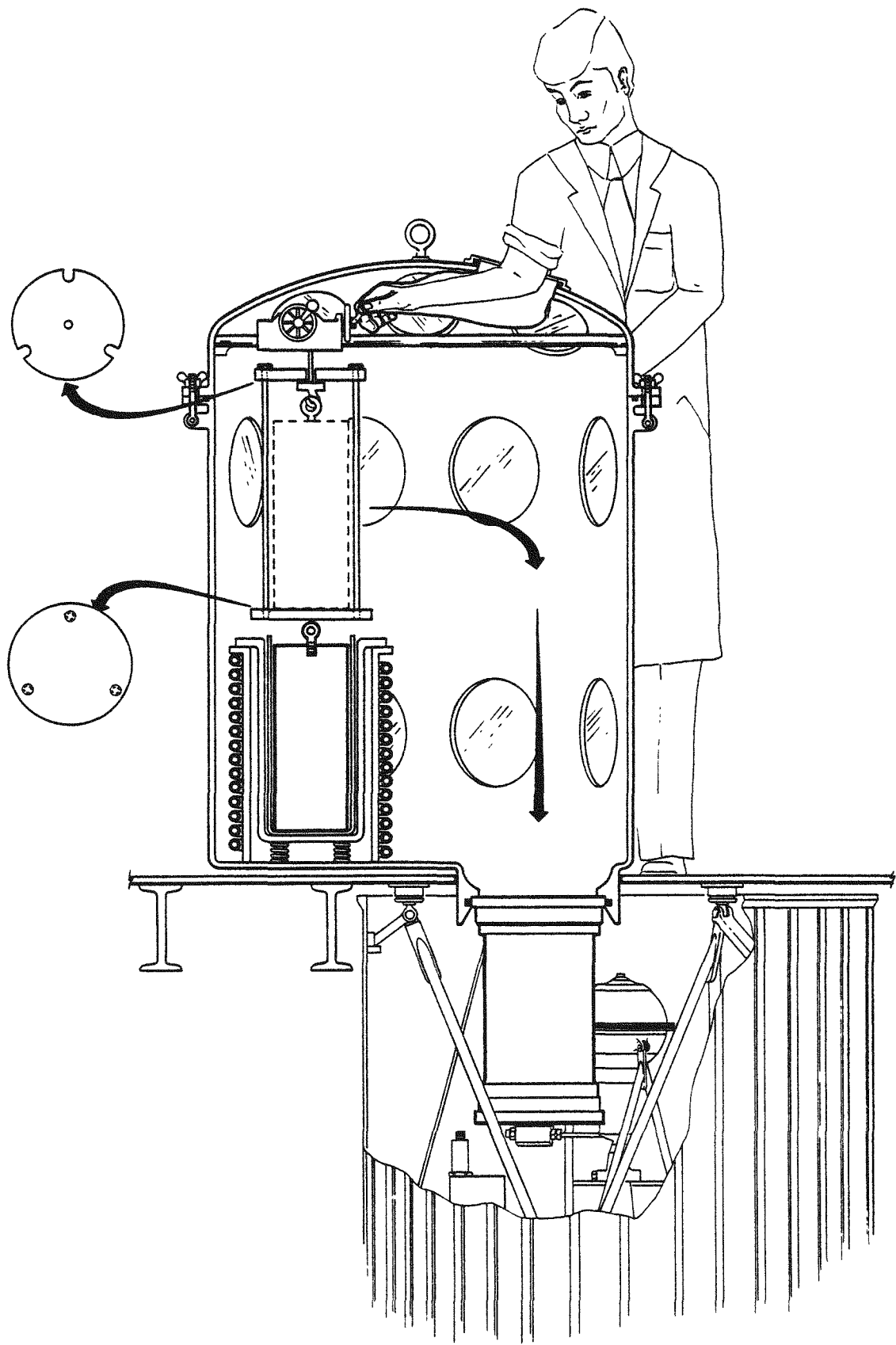


Figure 3-35 KIRS Loading and Assembly Station

**SECTION 4.0**  
**GROUND DEMONSTRATION SYSTEM (GDS)**

## SECTION 4.0

### GROUND DEMONSTRATION SYSTEM (GDS)

---

The GDS is illustrated in Figure 4-1 and shows the basic arrangement of the Power Conversion System (PCS) and Heat Source Assemblies (HSA) separately mounted on a plate. For convenience of assembly and test the electronic controller and auxiliary heat exchanger are also mounted separately from the plate.

The GDS design contains the following major subsystems:

- Heat Source Assembly
  - Heat source - electric
  - Boiler and auxiliary cooler
  - Emergency Heat Dump System
- Power Conversion System
  - Combined Rotating Unit - turbine, alternator, pump and bearings
  - Electrical and fluid controls
  - Regenerator
  - Jet condenser
- Auxiliary Cooler

Key features of the KIPS GDS design are a supersonic axial flow impulse turbine, homopolar inductor alternator, centrifugal pump, working fluid (Dowtherm A) lubricated fluid film bearings, once-through radiantly heated boiler, jet condenser, and liquid working fluid pumped cooler. The KIPS is designed for 1300 W(e), 28 VDC. The radiator is not tested as part of the total KIPS system but has been evaluated at the component level.

Figure 4-2 is a block diagram of the system illustrating typical operating conditions. The liquid outlet from the pump is split into two loops. The power loop passes liquid through the regenerator to extract energy from the turbine exhaust vapor. At the energy source, additional heat is transferred to the working fluid, which is vaporized and expanded, driving the turbo-alternator

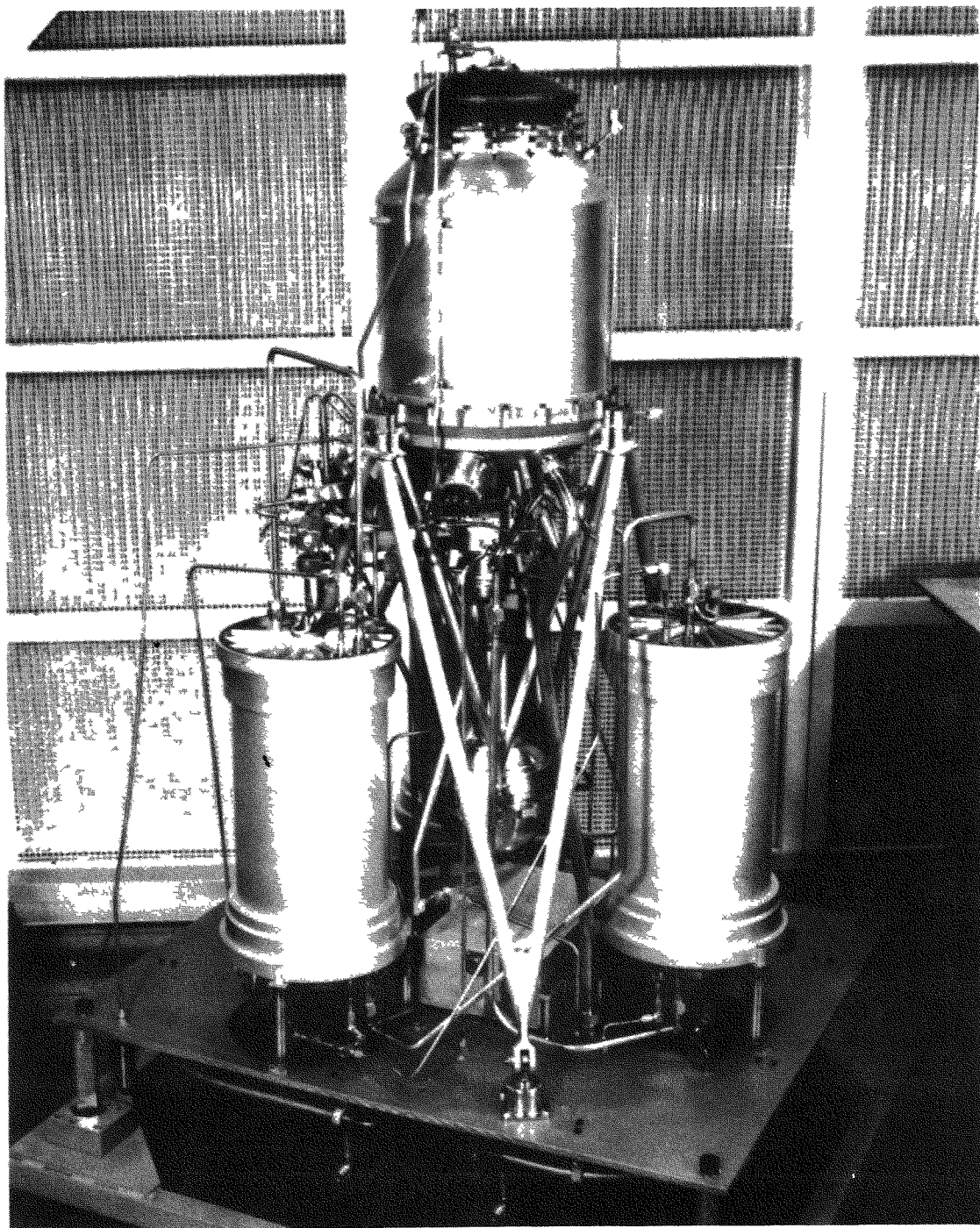


**Figure 4-1** Ground Demonstration System

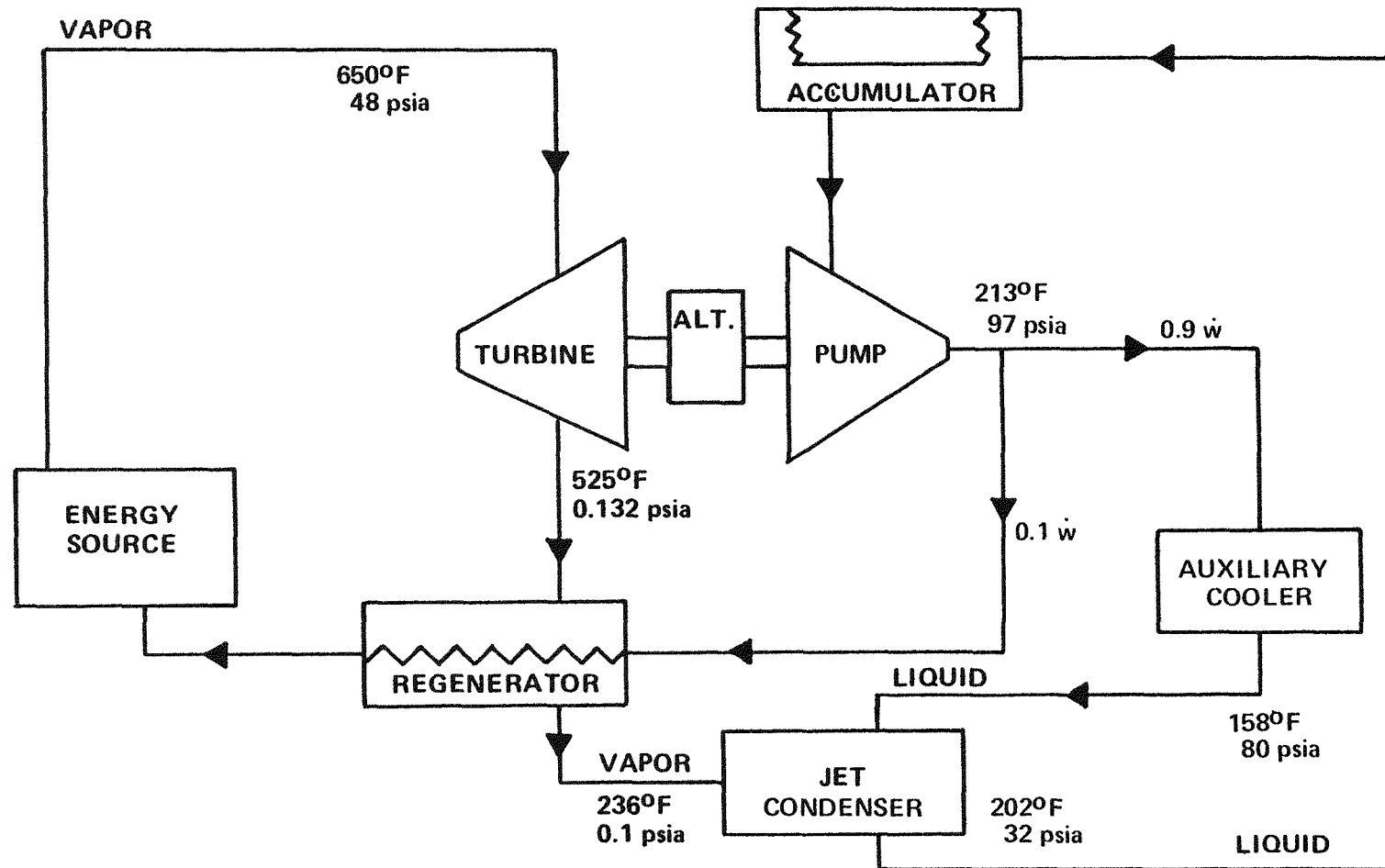


Figure 4-2 Typical GDS Operating Conditions

pump. The cooling loop passes liquid flow through the cooler to reject waste heat and then to the jet condenser to condense the turbine exhaust vapor emanating from the regenerator. The combined liquid is returned through the accumulator, which serves as an expansion compensator, to the pump.

The GDS as tested is prototypic of the FSCD in all major aspects of design and operation. The principal differences are (1) the use of O rings and flanges for ease of assembly and to permit convenient disassembly of the GDS hardware, (2) the use of electrical heat source assemblies instead of a radioisotope, and (3) the use of a conventional liquid-to-liquid heat exchanger instead of a space radiator. Any component differences in sizing, performance characteristics, or methods of fabrication are discussed later in this section.

Figure 4-3 is a schematic of the GDS. Operationally, it is nearly the same as the FSCD. Three units of ground support equipment are used: a start module for starting the system; a heater temperature control system which maintains heater block temperatures at desired values when the system is inoperative; a heat rejection module which removes system waste heat in the absence of the radiator.

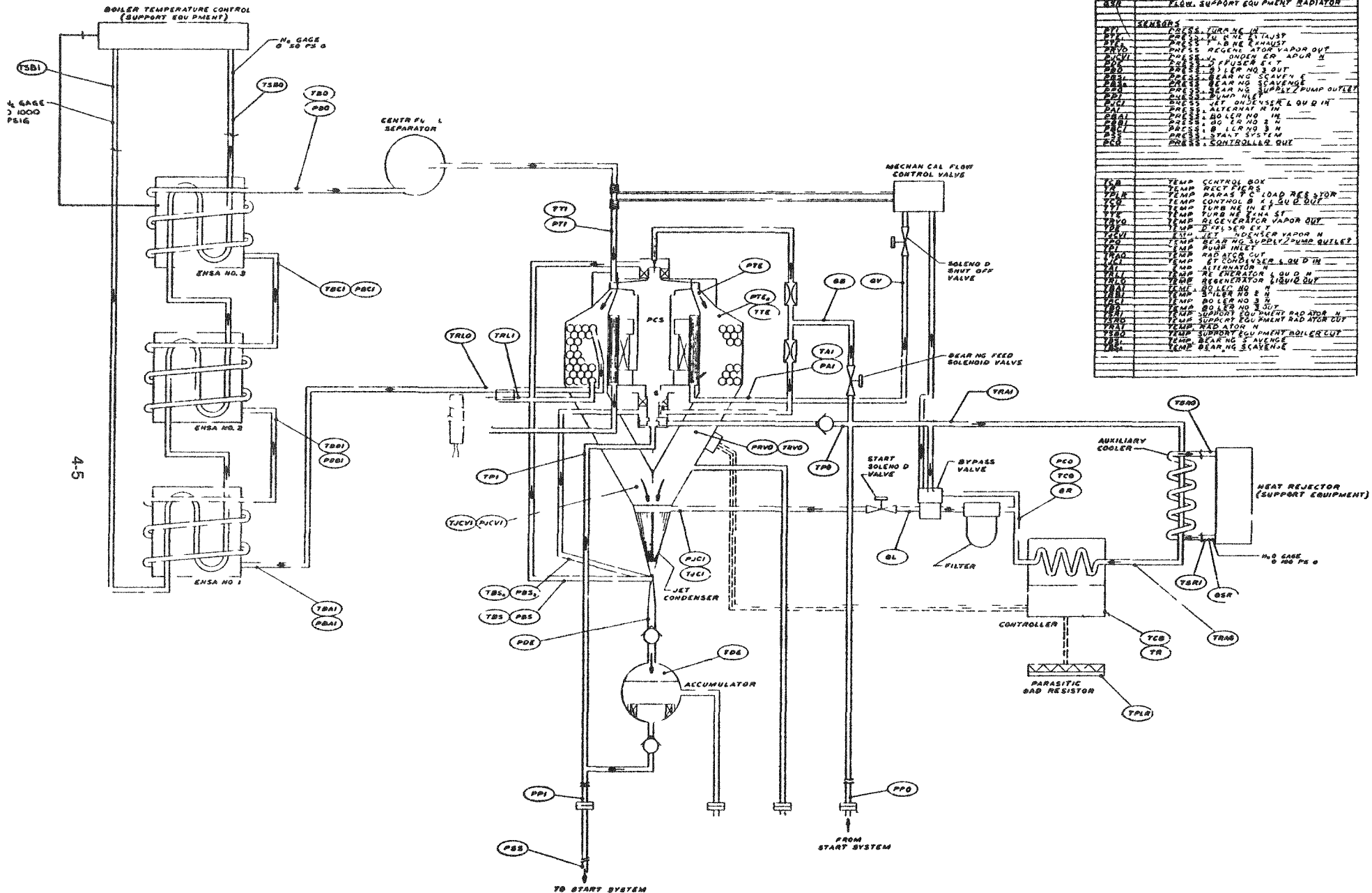


Figure 4.3 GDS Schematic

## 4.1 GDS CONFIGURATION

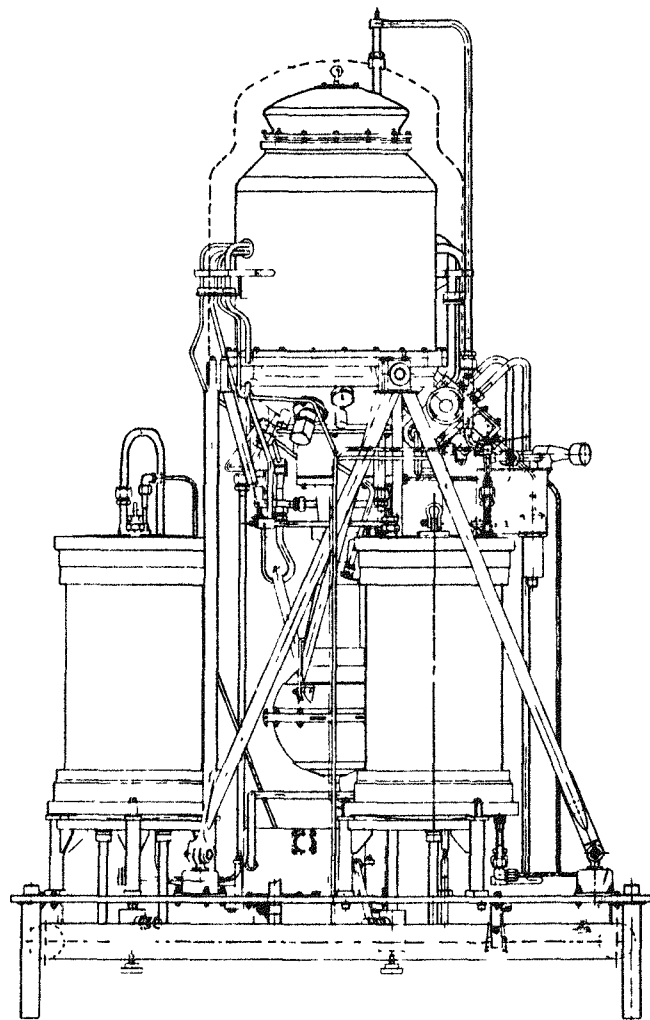
---

The GDS is comprised of the power conversion system, three heat source assemblies, an electrical controller and an auxiliary heat exchanger, all mounted from a support plate. The GDS was designed to be prototypical of a Flight Conceptual Design with the exception of demountable 'O' ring flanges and instrumentation. In addition, the various components were mounted from a support plate for ease of assembly and modification, where required. Since the system was not to be shock tested, dummy shock mounts were used. The system was also not integrated with the GDS radiator and all testing was performed with waste heat removal through the auxiliary heat exchanger.

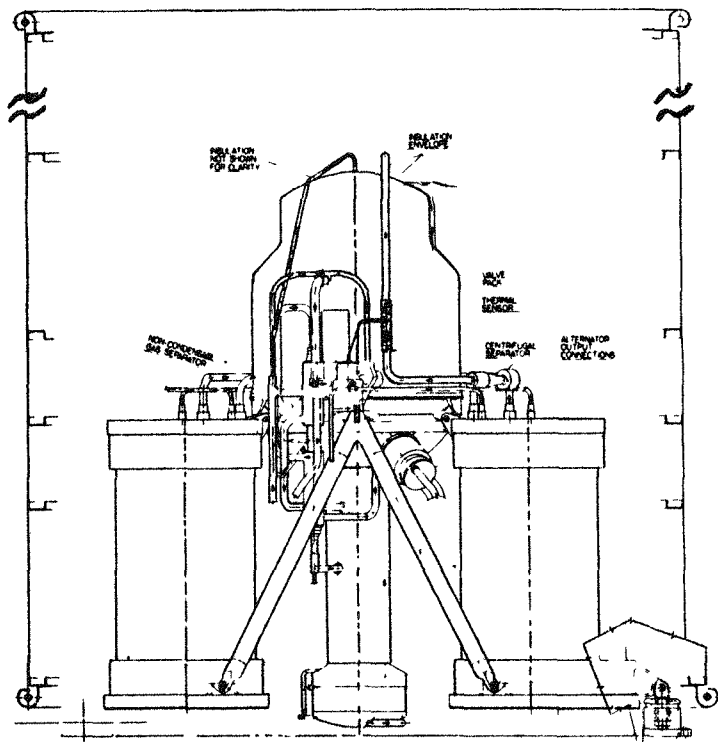
### 4.1.1 COMPARISON OF GDS WITH FSCD CONFIGURATION

The mechanical arrangement of the two systems are shown in Figure 4-4. The most obvious difference is the improved packaging of the FSCD resulting from the change in accumulator design and mounting arrangement. The major differences are listed below:

- The FSCD has three point mounts directly to spacecraft, the GDS has components mounted separately to plate.
- The FSCD controller is mounted to the radiator, the GDS controller is mounted to the plate.
- The FSCD uses parasitic radiatively cooled load resistors mounted to the radiator, the GDS uses a facility air cooled load bank.



GDS



**FSCD**

Figure 4-4 System Comparison

## 4.2 COMPONENT CONFIGURATION

---

### 4.2.1 HEAT GENERATION SYSTEM

Heat is generated electrically and transferred to the working fluid in three Electrical Heat Source Assemblies (EHSA). Each comprises an electric heater block, a fin-tube heat exchanger, radiation shield, insulation and structural support.

#### 4.2.1.1 Electrical Heat Source Assembly (EHSA)

The EHSA is a circular, stepped cylinder which measures 12.70 in. diameter at the mounting end (13.60 in. diameter at the three mounting lugs), 10.22 in. diameter at the midpoint, 12.02 in. diameter at the upper end, 28.84 in. overall length from boiler tube inlet to outlet fitting and weighs 80 pounds. See Figures 4-5 and 4-6. There are three ESHAs in the GDS each supplying 2400 W(t) input to the GDS system for conversion to output power.

Each EHSA is attached to the GDS baseplate by means of a triangular shaped, three legged support structure. Electrical power input and instrumentation receptacles, as well as the inlet connections to the boiler assembly, are located in the mounting (lower) end of the unit. The outlet connections to the boiler assembly are located in the upper end of the unit. The EHSA is designed to permit end loading/unloading of the electrical heat source without having to disturb either of the boiler assembly tube connections. The unit also has the capability of being suspended from its upper end by using a special fitting which threads into the center of the upper cover.

Each of the ESHAs in the GDS is identical except for the boiler centerbodies and the location of instrumentation on each boiler assembly. The major components of an EHSA are the housing, upper and lower end covers, penetration fitting assemblies, fibrous insulation, multifoil insulation system, radiation barrier, electrical heat source and the boiler assembly.

**4.2.1.1.1 ELECTRICAL HEATER:** Each of the three electrical heat sources is a right circular cylinder which measures 7.42 in. diameter by 16.53 in. long, weighs 42.0 lb. and has a total power capability of 7200 W(e) or three times the nominal requirement of 2400 W(e) each. It simulates, as nearly as practical, the characteristics of the isotope heat source. The electrical heat source consists of two major components: the body and the cartridge heaters, see Figure 4-7.

The heater body consists of a heater block body, which has internal Acme threads on each end and two end plugs which thread into place on each end of the body. Each component is made from EBP purified P-5710 graphite which is manufactured by Union Carbide. This grade of graphite, which is a purified grade of type ATJ graphite, was selected primarily because of its availability. After final machining, but prior to assembly, these components are vacuum outgassed at 1150°C for 6.5 hours.

The heater body serves as the housing for the twelve cartridge heaters. Initially, the body is machined oversized in length and the heater cartridge holes machined undersized. The body and end plugs are temporarily assembled and the assembly machined to the proper length. Each heater cartridge hole is reamed to match a particular heater cartridge and thereafter, they become a matched set. Cartridges cannot move during a dynamic test because their sheath is welded, on one end, to a nickel 200 anti-rotation clamp which is first threaded into the heater body.

There are twelve cartridge heaters in each electrical heat source assembly, each with a power output capability of 600 watts(e) at  $19 \pm 3.8$  VAC. For added reliability, the twelve cartridges are

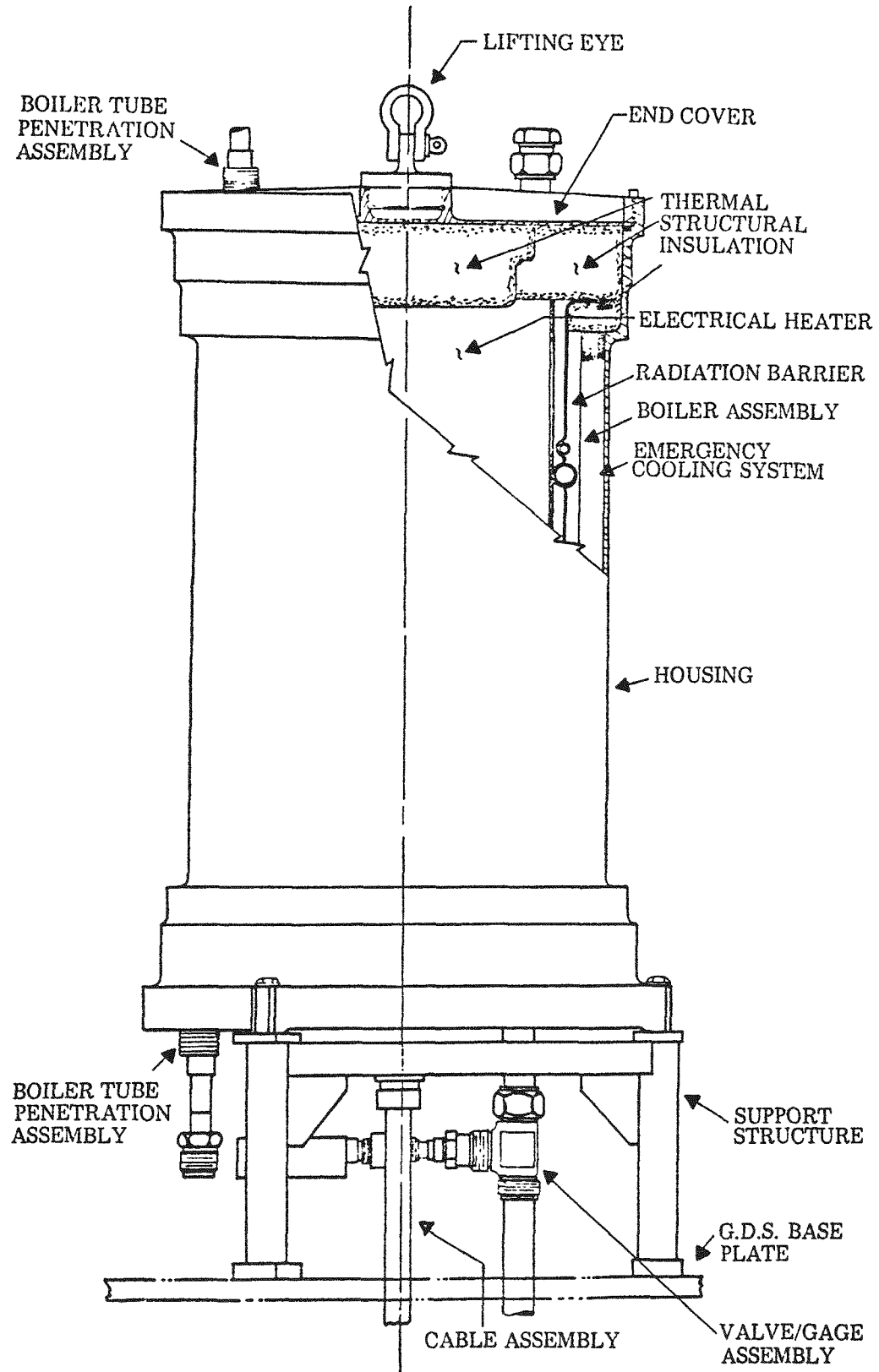


Figure 4-5 Electrical Heat Source Installation

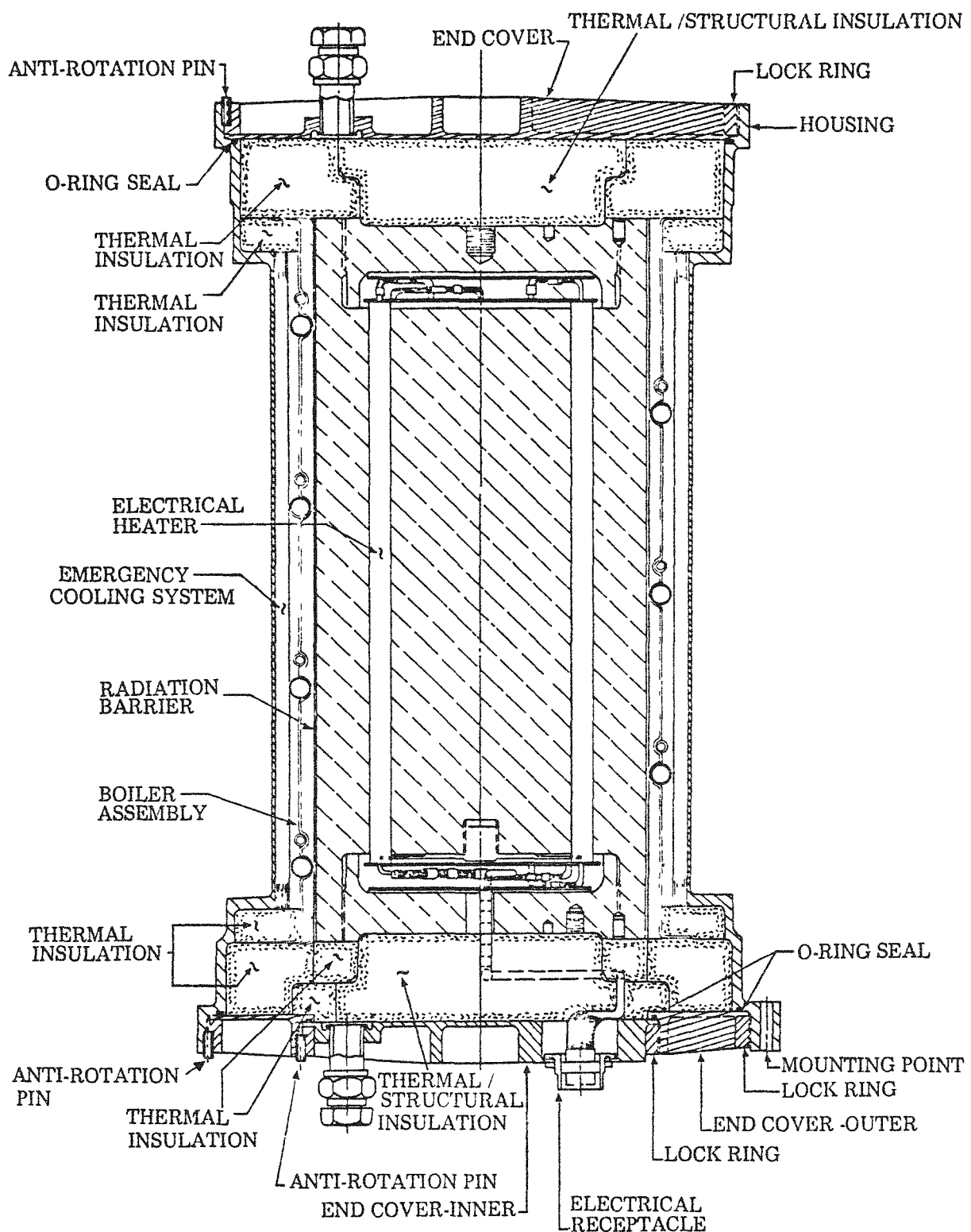


Figure 4-6 Electrical Heat Source Assembly

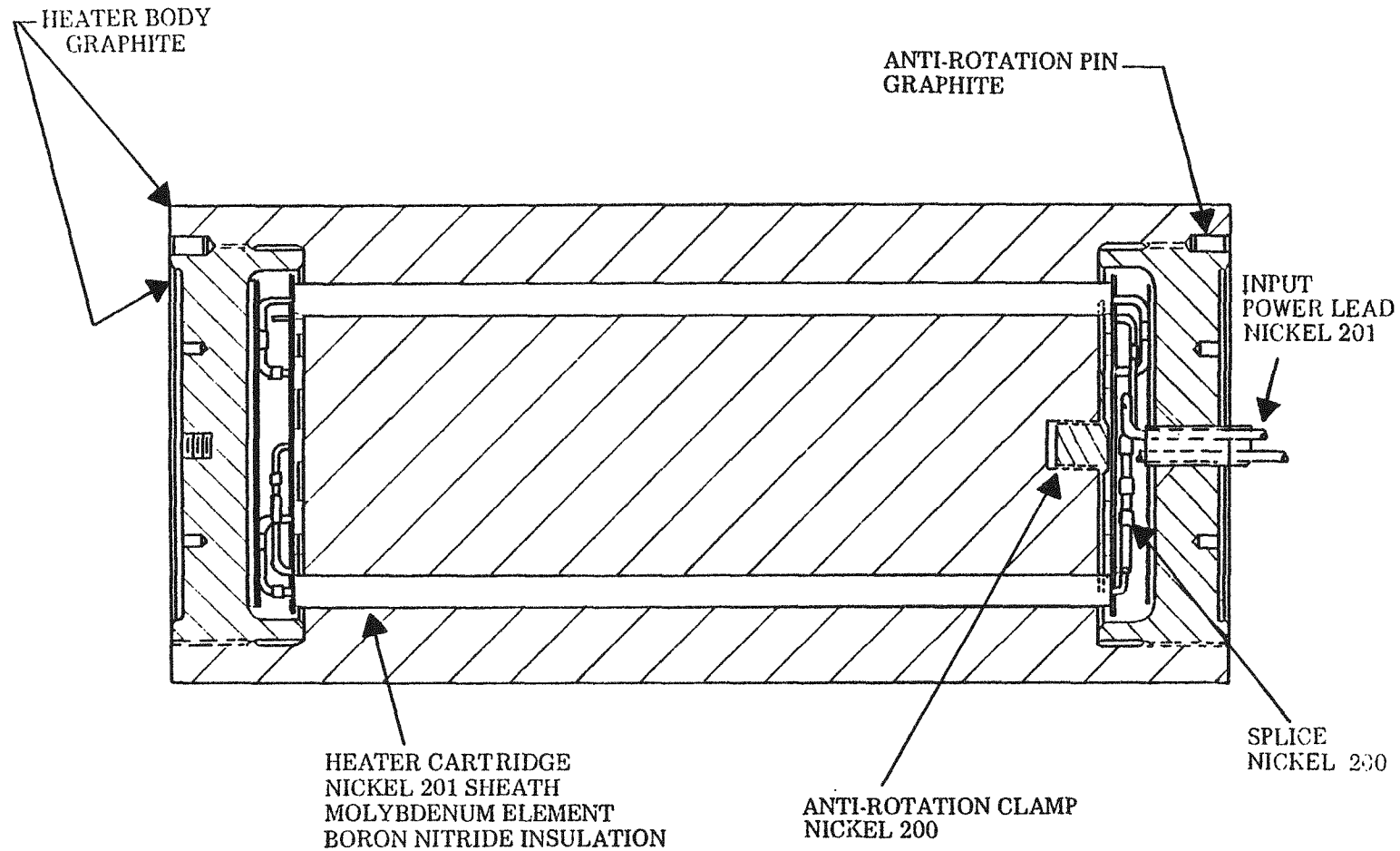


Figure 4-7 Electrical Heater

connected in two parallel circuits of six cartridges each. Therefore, one circuit could cease to function and the remaining cartridges would be capable of producing the design power of 2400 watts(e). See Figure 4-8.

The heater cartridges are manufactured by Watlow Electric Manufacturing Company, and measure 0.478 in. diameter by 12.75 in. long and have a heated length of 10.0 in. The heater element is molybdenum, internal insulation is tightly compacted boron nitride, the bare #10 AWG power leads and the sheath are nickel 201.

The solid power leads are crimped internally to the molybdenum heater element, and externally to the nickel 201 stranded input power leads using nickel 200 crimps. Each power lead is crimped to a pigtail lead coming from a Deutsch 26 pin receptacle. Sample crimp splices are made before and after the actual hardware splices are made, and are pull tested, to determine the quality of the crimp splice joint. Inside the electrical heat source, the power leads are insulated using ceramic ( $Al_2O_3$ ) beads. The wires and crimp splices are isolated from the heater body and end plugs by means of mica discs which rest on top of the wiring and the ends of the heater cartridges. There is also a layer (approximately 0.125 in.) of A-100 fibrous insulation between the mica disc and the end plug for additional isolation on each end of the heat source.

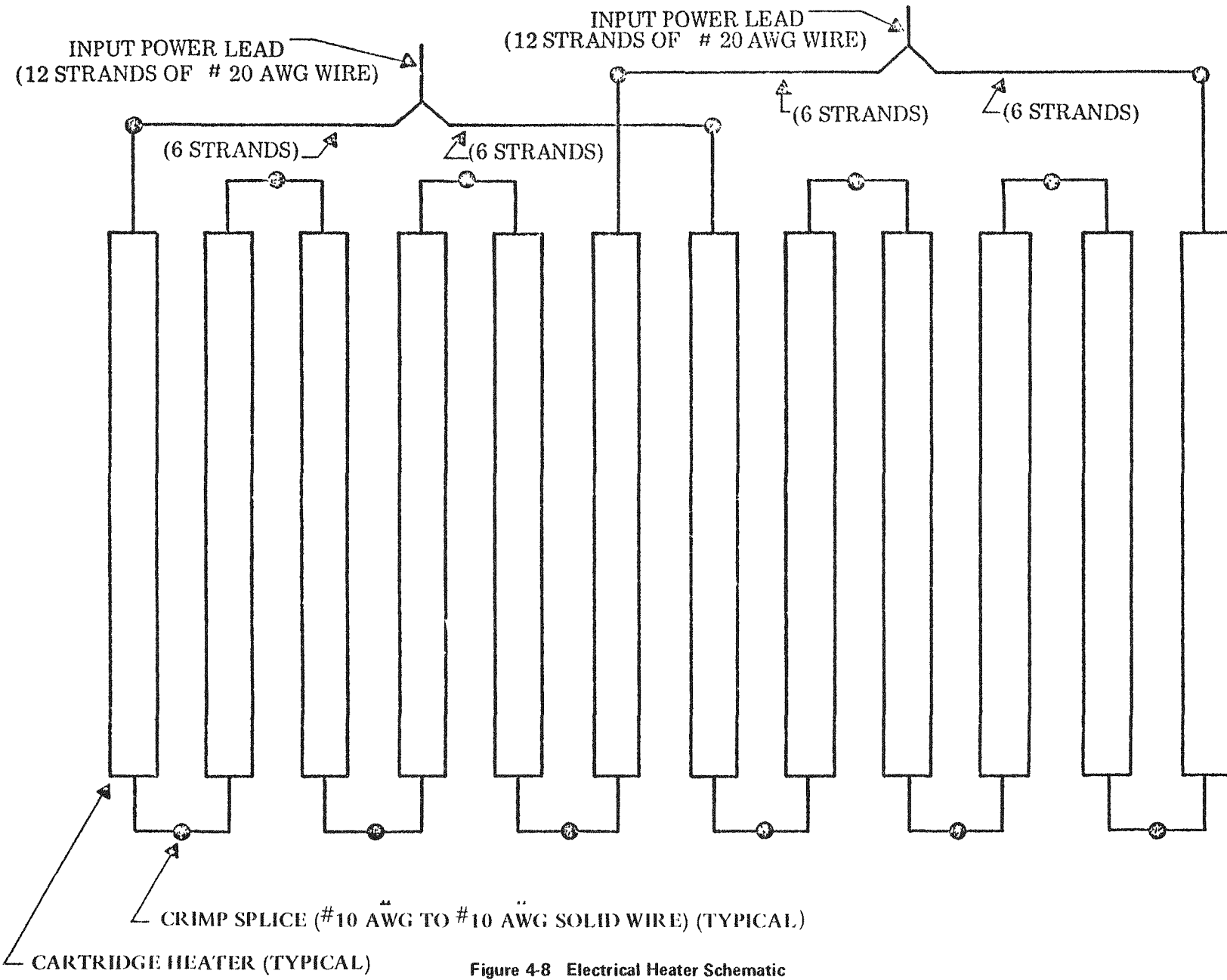
**4.2.1.1.2 RADIATION BARRIER:** The radiation barrier, which is located in the annular space between the heat source and boiler assemblies, is required in order to raise the temperature of the flight system isotope heat source during normal operation. It is required for the GDS because the proper heater block temperatures must be achieved in order to simulate flight system parasitic heat losses. The radiation barrier is attached to each end of the boiler assembly with five sheet metal screws.

The radiation barrier is a formed, thin wall, hollow right circular cylinder which measures 7.57 in. outside diameter by 0.010 in. thick by 16.53 in. long and is made from nickel 200 sheet. After forming, the two edges of the sheet, which are butted together, are seam welded along their entire length, to form a continuous cylinder. Each side of the cylinder is grit blasted with aluminum oxide grit to provide the desired emissivity characteristics.

**4.2.1.1.3 BOILER ASSEMBLY:** The boiler assembly consists of a 0.500 in. outside diameter by 0.035 in. wall stainless steel, copper plated tube which is wound in helical fashion around a 0.020 in. thick copper shell. A 0.250 in. outside diameter by 0.035 in. wall stainless steel, copper plated tube, for auxiliary cooling, is also wound around the shell. See Figure 4-9. The copper shell has helical grooves formed in it by spinning. The tubes are secured into these grooves by welding all along their lengths for the GDS units. The entire assembly is coated on the inside and outside diameter with an iron titanate coating which is intended to assist in controlling the heat source temperature.

The three GDS boiler assemblies are connected in series to form three fluid flow zones: subcooled, two phase and superheated. The inside of the 0.500 in. diameter tube, on each boiler, is fitted with a special insert which is intended to increase the film coefficient of the working fluid and to induce a high radial acceleration to maintain fluid contact on the tube wall even under the most extreme g loads. There is a different insert inside each boiler assembly.

The minimum inside diameter of the boiler shell is 7.63 in. and the maximum outside diameter, at the boiler tubes, is 8.81 in. The boiler assembly flange to flange length is 16.53 in. The boiler assembly fits in the annular space between the radiation barrier and the multifoil insulation system



414

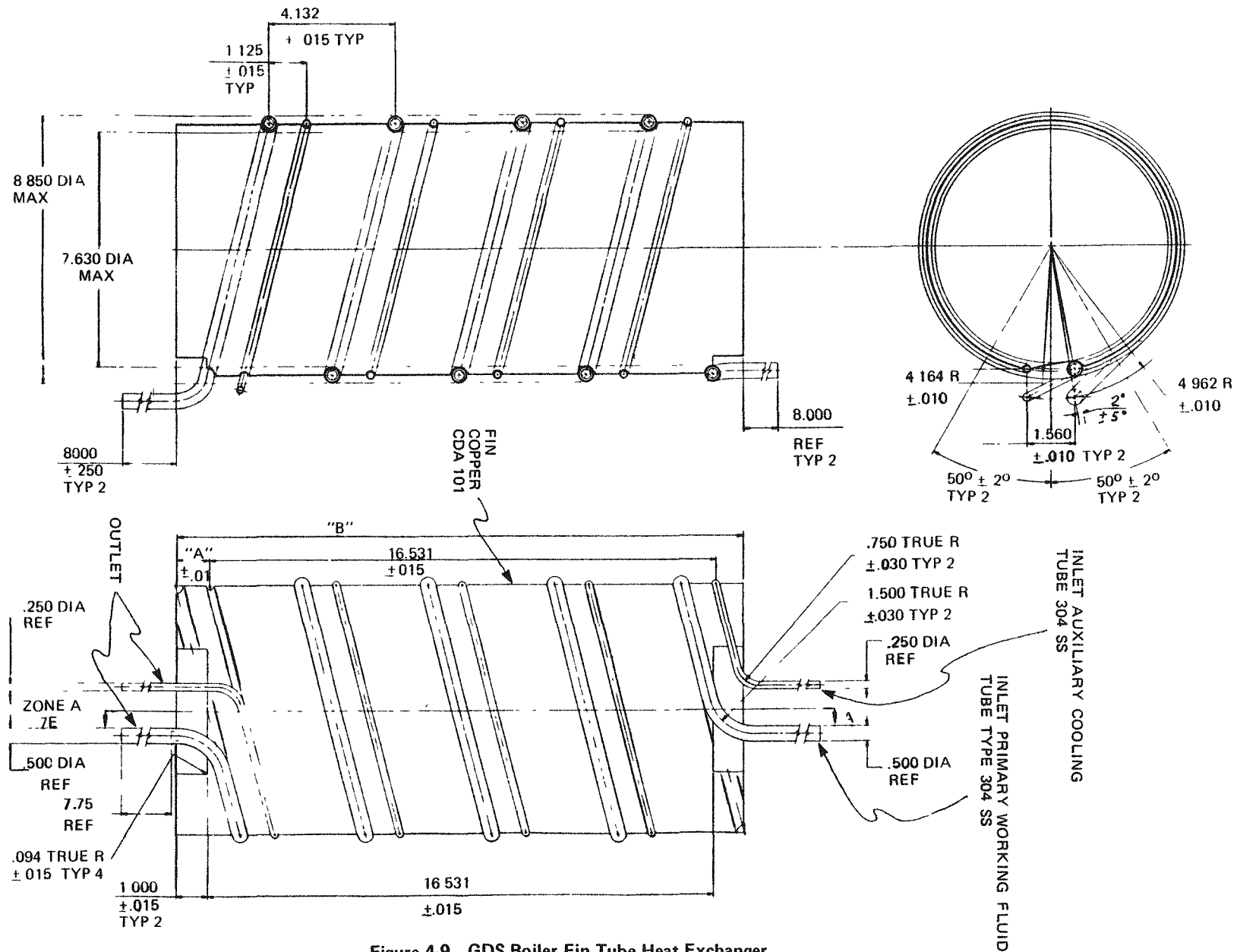


Figure 4-9 GDS Boiler Fin Tube Heat Exchanger

and is sandwiched between Min-K insulation at each end. The flanges are hand formed at assembly by making a series of cuts through the shell and bent to rest upon the Min-K.

The primary and auxiliary boiler tubes exit from each end of the boiler shell. They pass through the upper and lower end covers and through the penetration assemblies where they are terminated in special "vacuum-tight" (VCR-Cajon) fittings.

**4.2.1.1.4 EMERGENCY COOLING SYSTEM:** A multifoil insulation system is used in the flight system to assure that isotope heat source temperatures are maintained within tolerable limits, should Dowtherm cease to flow through the boiler assembly, by acting as an emergency heat dumping system. In such an accident situation, the heat source temperature would rise, resulting in the melting of the multifoil insulation, thereby allowing the heat source to radiate heat through the boiler assembly walls to the housing, thus maintaining tolerable heat source temperatures. Although an emergency cooling system (ECS) is not required for safety reasons for the electrical HSA as it is for the isotope HSA, it is required to simulate the same parasitic heat losses from the heat source assembly, and thus maintain the prototypicality between the two. The GDS electrical heat source temperature will always be within tolerable limits because of unique temperature controls which have been incorporated into the heater power supply. In addition to its ECS function the multifoil system (because of its excellent insulation properties) limits radial heat losses to the housing walls. The multifoil insulation system is located in the annular space between the outside of the boiler assembly and the inside of the housing.

The multifoil insulation system is a hollow right circular cylinder measuring 8.895 in. inside diameter by approximately 0.61 in. thick by 15.00 in. long. It consists of one continuous length of 0.001 in. thick type 1100 aluminum alloy foil loosely wrapped sixty times around an 0.010 in. thick type 1100 aluminum alloy foil can. Spacing between wraps is intended to be approximately 0.010 in. However, the GDS multifoil insulation systems were wrapped tighter and as a result, their final thickness was approximately 0.44 in. instead of 0.61 in. The foil material is lightly coated on one side with zirconium oxide ( $ZrO_2$ ). The primary purpose of the coating is to insure a separation between wraps of the foil. Aluminum was selected as the foil system material because of its compatibility with the boiler assembly operating temperature and its low density. The ECS for the GDS heat source assembly is identical to that proposed for the flight system.

**4.2.1.1.5 THERMAL/STRUCTURAL INSULATION:** Most of the insulation in an EHSA is Min-K TE-1400, and serves three purposes: to minimize longitudinal and radial heat losses to the housing/end covers, to provide sufficient end preload for the electrical heat source and to support the boiler assembly and multifoil insulation system. Min-K TE-1400 was selected because of its temperature, thermal conductivity and compressive strength properties. Since no binder is used in its manufacture, it is easily outgassed. Prior to use in the EHSA the insulation is vacuum outgassed at 1500°F for eight hours at a level of 1000  $\mu$  or less. After outgassing, air exposure is minimized.

**4.2.1.1.6 BOILER TUBE PENETRATION ASSEMBLIES:** The penetration assembly fittings have two functions: to minimize the heat losses from the boiler assembly tubes to the end covers (where the tubes penetrate the covers) and to form a vacuum tight closure between these tubes and the end cover. The penetration assembly consists of a type 321 stainless steel formed bellows welded to a type 304 stainless steel flange. Stainless steel was selected because of its compatibility with the type 304 stainless steel boiler assembly tube material and for its relatively low thermal conductivity properties. There are four penetration assemblies in each EHSA, two for the primary boiler tubes and two for the auxiliary boiler tubes. See Figure 4-10.

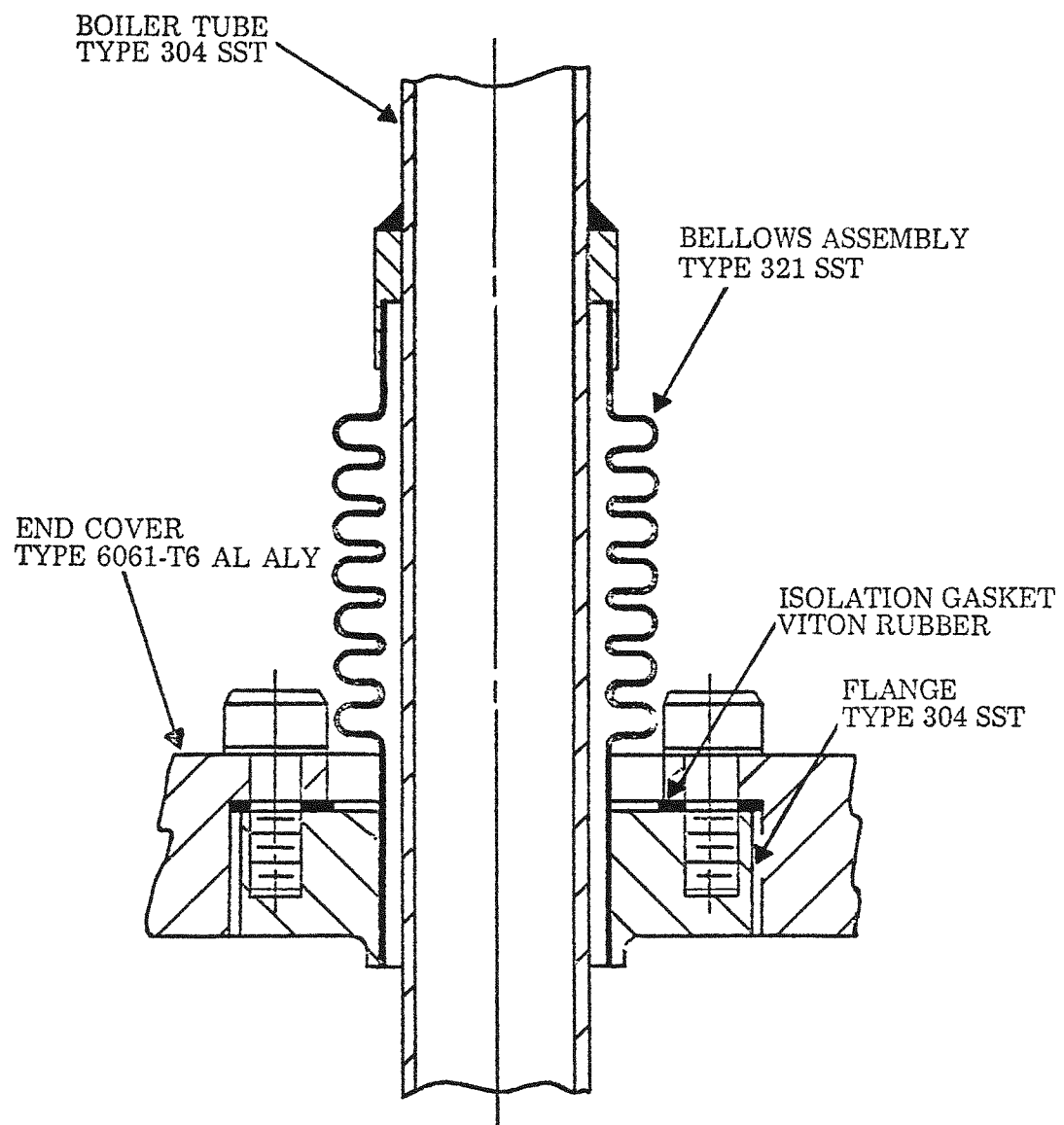


Figure 4-10 Boiler Tube Penetration Assembly Installation

4.2.1.1.7 END COVERS: Each of the end covers is machined from a disc of 6061-T6 aluminum alloy plate. Each end cover is circular shaped, with a flat, smooth underside to assist in the sealing and insulation preload process and has tapered ribs for added stiffness, machined as an integral part of the outside surface.

A single piece cover closes the upper end of the EHSA and contains the outlet connection fittings for the boiler assembly. The lower end of the EHSA is closed with an inner and outer cover which are locked together, by means of a specially machined lock ring, to form one integral assembly. The outer portion of the lower cover contains the inlet connections for the boiler assembly; the inner portion of the cover contains the electrical power input and instrumentation receptacles. The lower inner cover can be separated from the lower outer cover without having to remove the outer cover from the housing, thereby exposing a cavity of sufficient diameter to permit the electrical heat source to be installed/removed.

4.2.1.1.8 HOUSING: The housing is machined from a hollow tube, 6061-T6 aluminum alloy forging. In each end of the housing there is an Acme thread which allows each end cover to be attached by using a specially machined lock ring.

4.2.1.1.9 VENTING/GAS MANAGEMENT: The gas management system for the electrical heat source assembly consists of outgassing ports at each end of the EHSA, located on the covers. At the non-loading end the port is capped off for normal operations. At the EHSA loading end the outgassing assembly consists of a manual valve and a pressure/vacuum gauge. After outgassing, the EHSA is backfilled with an inert gas (argon) to a nominal pressure of 5 psig.

#### **4.2.1.2 Electric Heat Source Component Testing**

Heat source component tests were performed at the component level to confirm operational characteristics.

**HEATER CARTRIDGE TESTS:** After bake-out and burn-in, different heater cartridges were subjected to endurance tests, maximum power tests, thermal cycling tests and life tests, the latter group having operated for more than one year. The results of the life test indicate a gradual increase in resistance with time of about 8.3% in 7000 hours.

**HEATER BLOCK TESTS:** In these tests twelve heater cartridges were tested in a graphite block to determine performance capability. The whole block was tested in a thermal vacuum furnace with electric power applied. Changes in electrical resistance were low with time and the block thermal resistance was acceptable. In addition, no significant outgassing was noted.

**HEAT SOURCE TEST:** The total EHSA, comprising electrical heater block, radiation barrier, boiler heat exchanger, insulation and housing, was tested in a thermal vacuum chamber to evaluate performance and determine heat losses. Most EHSA component temperatures were measured at their nominal values. The heat losses were determined to be approximately 3.5% of the nominal input power.

**ACCEPTANCE TESTS:** All EHSAs were subjected to an acceptance test using Dowtherm before use in the GDS, to verify normal operating performance and heat loss.

**EMERGENCY COOLING MELTDOWN TEST:** A test was performed to confirm the acceptability of the multifoil emergency cooling system. A complete EHSA was brought to equilibrium

conditions in a thermal vacuum chamber with nominal Dowtherm flow. The flow was then abruptly stopped while maintaining the full 2400 watt electrical input and temperatures were recorded. After 45 minutes, foil meltdown was complete and after about four hours the components reached steady state conditions (< 1% difference from premeltdown temperatures). The final heater block temperature rose approximately 160°F above the premeltdown temperature of 1440°F and well within the allowable difference of 270°F. The most severe temperature rise was in the housing temperature which rose from 200°F to 820°F.

#### 4.2.1.3 GDS EHSA Compared to FSCD IHSA

The GDS HSA is the same as the FSCD HSA except for the minor differences delineated below:

- Isotope heat source compared to electric heat source
- Boiler tubes enter and leave from the same end on the FSCD, opposite ends on the GDS
- FSCD has single mount point, GDS has three mount points per HSA.
- The FSCD has an active Pressure Relief Device.

#### 4.2.2 RADIATOR

The GDS radiator assembly is an aluminum, welded/riveted assembly in the shape of a hollow right circular cylinder measuring 48.50 in. outside diameter by 111.75 in. long (at mounting feet) and weighs 80 lb. It has three mounting points which extend approximately 2.81 in. below the radiator skin in order to provide clearance for tubing connections to the outlet header assembly. See Figure 4-11. The complete radiator is shown in Figure 4-12.

The radiator employs a forced convection heat transfer loop. The organic fluid passes through sixteen vertical tube extrusions which are connected, at each end through an adapter fitting, to a common header, Figure 4-13. Each extrusion, Figure 4-14, serves three purposes: as a passageway for the organic fluid, as the required frontside and backside meteoroid armor protection and as vertical stiffening for the radiator shell. The headers are made from a 0.500 in. outside diameter by 0.062 in. wall tube which is formed to a circular shape. They are protected from meteoroid puncture by a shadow shield which is attached to the radiator structure.

The 0.025 in. thick radiator skin is spliced together at four places (because the available range of standard sheet widths is limited) by means of splice plates which are riveted in place. The extruded radiator tubes are seam welded to the skin prior to the sections being spliced together. Nine circumferential channel frames are riveted to the skin for structural support.

After the radiator has been fabricated and inspected, the exterior surfaces are coated with IITRI\* Z-93 thermal control coating. Z-93 is an inorganic type coating developed by IITRI which is composed of a zinc oxide (ZnO) pigment with a potassium silicate ( $K_2 SiO_4$ ) binder. The coating selected offers acceptable performance (material properties) coupled with ease of application, reproducibility, and ready repairability.

In the GDS design, there are two welds at each end of the flow tubes so that the number of welds, in fluid flow areas, in the radiator is at least  $N_{tubes} \times 4$ . For the GDS radiator, this amounts to 64 weld joints. The first weld attaches a saddle-like, 6061-T6 aluminum alloy adaptor fitting to each

\*Note: \*IITRI – Illinois Institute of Technology Research Institute

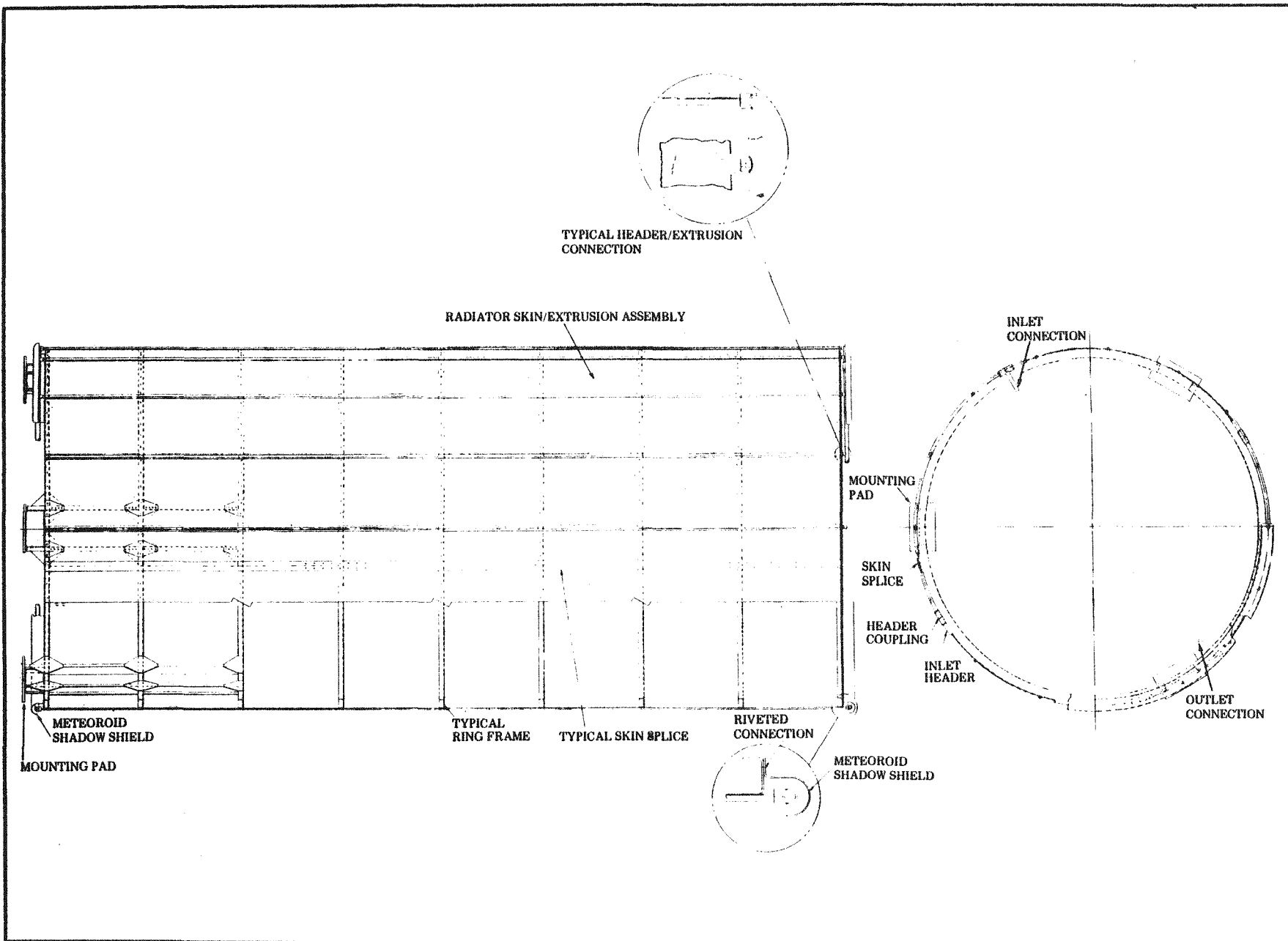
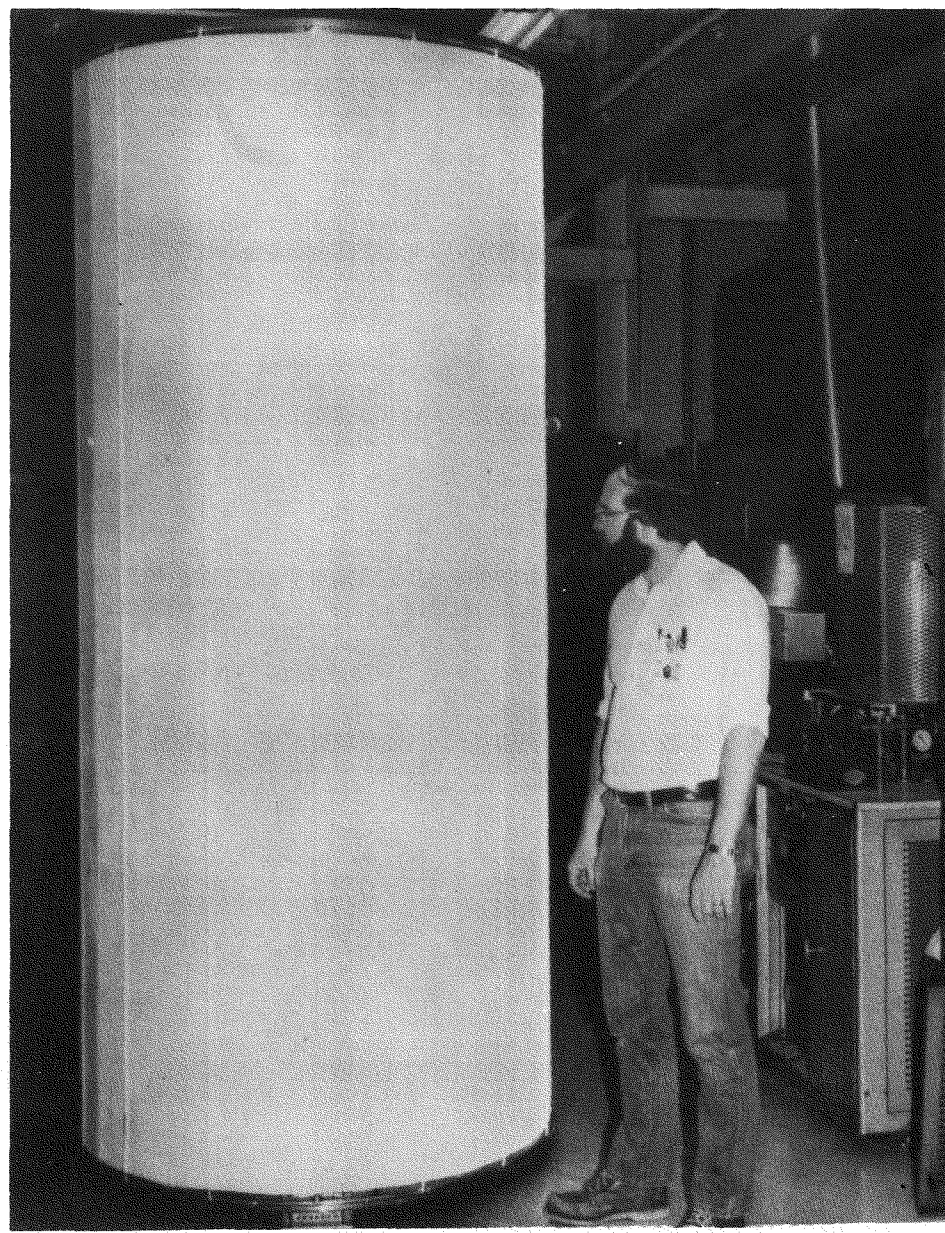


Figure 4-11 Ground Demonstration System Radiator Assembly



**Figure 4-12 GDS Radiator**

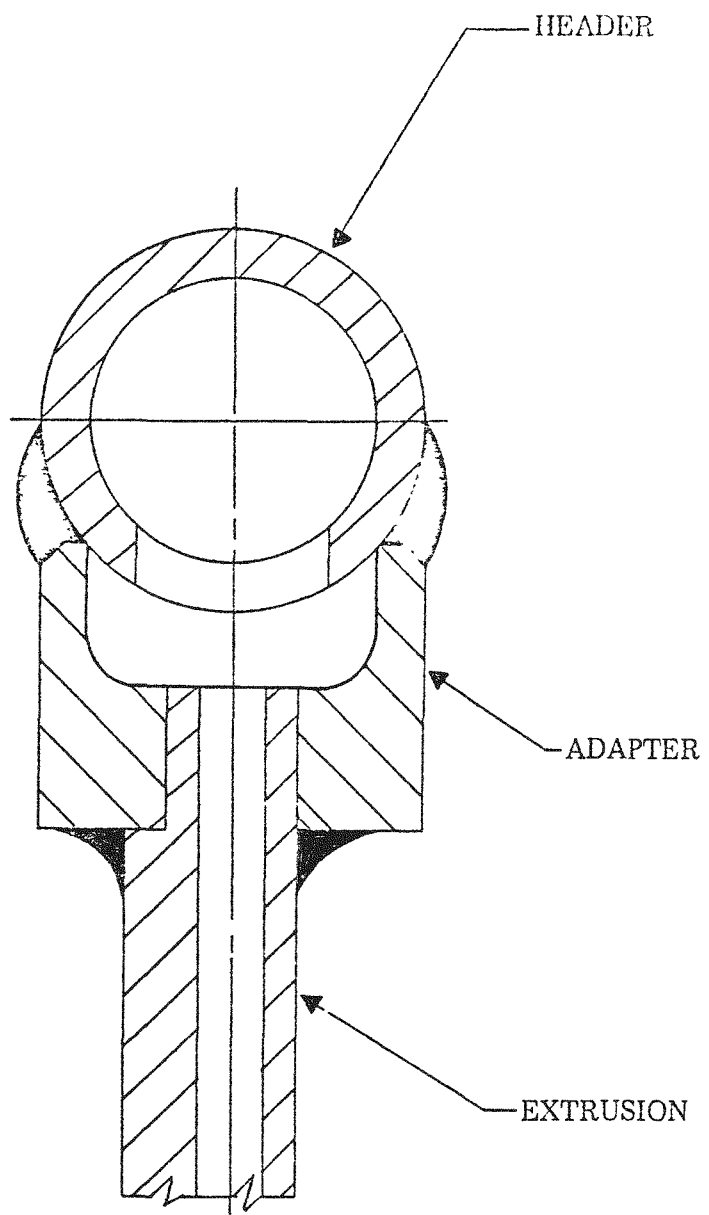


Figure 4-13 GDS Radiator Extrusion/Adaptor to Header Termination

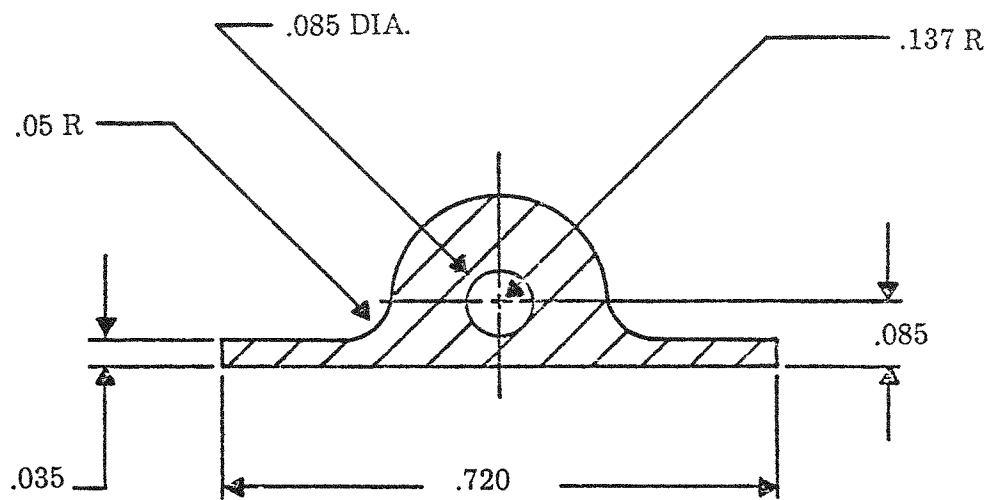


Figure 4-14 GDS Radiator Tube Extrusion

machined end of the 6063-T5 aluminum alloy extrusion (flow tube with meteoroid armor). The second weld attaches each end of the extrusion/adaptor subassembly to the 6061-T6 aluminum alloy header.

The inspection technique used during the GDS fabrication was a two stage technique involving each weld at two levels of assembly with 100% of the components subjected to inspection. The first assembly level involved welding the saddle-like adaptor to each end of the machined extrusion. This subassembly is physically easy to inspect, the flow tube opening can easily be checked for restrictions and assures that only acceptable components are seam welded to the radiator skin. The second assembly level involved the radiator header to extrusion/adaptor subassembly welds and could only be performed after the radiator was fully assembled.

Acceptance criteria for the tube/adaptor and adaptor/header welds was based on acceptable helium leak check data. A flight system radiator would require more elaborate non-destructive testing techniques. Therefore, to demonstrate this capability the radiator panel assemblies (extrusions/skin) and the completed assembly welds (header/adapter tube) were radiographed. Results show that radiography of these welds can be performed and should be considered as a valid non-destructive testing method.

The radiator design was based on obtaining the lowest weight radiator which satisfied all system performance requirements and other system design constraints as listed in Table 4-A. For the GDS radiator an additional consideration was that the design be capable of being manufactured and assembled without a costly manufacturing development effort.

Within those constraints listed in Table 4-A, the final design parameters selected for the GDS radiator are as follows:

Radiator diameter	4 feet
Radiator length	9.27 feet
Skin thickness	0.025 inch
Number of flow tubes	16
Flow tube inside diameter	0.085 inch
Flow tube frontside armor thickness*	0.094 inch
Flow tube backside armor thickness**	0.060 inch
Header inside diameter	0.375 inch
Header armor thickness	0.025 inch
Header bumper thickness	0.025 inch
IITRI Z-93 (ZnO/K <sub>2</sub> SiO <sub>4</sub> ) coating properties	$\epsilon_H = 0.90$ (EOM) $\alpha_S = 0.3465$ (EOM)

\* Original design based on  $P(o) = 0.973$  allocation subsequently changed for flight system to  $P(o) = 0.99$ .

\*\*Provided by method of construction, actual thickness required is less.

Table 4-A GDS Radiator Design Performance Requirements and Design Constraints

Dowtherm flow rates:	Minimum	—	0.159 lbs/sec
	Maximum	—	0.358 lbs/sec
	Nominal	—	0.249 lbs/sec
Waste heat load:	Nominal	—	18255 Btu/hr
Radiator Coating emissivity:	$\epsilon$	—	0.90 (EOM)
Solar heat load:	Geosynchronous Orbit Solar absorptivity (EOM) $\alpha_S = 0.3467$ Average solar load 48.89 Btu/hr-ft <sup>2</sup>		
Dowtherm inlet temperature:	Nominal	—	212°F
Reynolds number in flow tubes at exit $\geq 3000$ for nominal flow and higher			
Maximum fluid pressure drop $\Delta p = 20$ psi (at nominal flow)			
Meteoroid penetration criterion (total for radiator) — $P(o) = 0.99$			
Operations lifetime — 7 years			
Radiator diameter limit*	4 ft. minimum approximately		
Acoustic noise/spectrum	145 db overall		

\*To permit installation of PCS and heat sources within the radiator envelope.

#### 4.2.2.1 Radiator Meteoroid Protection

The radiator design is based on an overall probability of non-puncture by meteoroids of 0.99 for seven years in a synchronous geocentric orbit. The overall probability includes the probabilities of non-puncture for the frontside of the tube, the backside of the tube and the headers. The backsides of the radiator tubes are assumed to be protected by the radiator skin which acts as a so called "bumper." The tube backside vulnerability to meteoroids entering the open end of the radiator cylinder has not been considered in the weight calculations for the GDS radiator.

Required armor thicknesses, assuming 6061-T6 aluminum construction, are as follows:

Header	0.010 in. (with 0.025 inch bumper)
Tube frontside	0.094 in.
Tube backside	0.020 in. (with 0.025 inch bumper)

Armor weight is a strong function of non-puncture probability. For a given probability, however, it does not vary appreciably with small changes in design (shell diameter, number of tubes, etc.), particularly near the optimum 4 foot diameter 16 tube radiator design. The dominant weight is that of the tube frontside armor, since other required armor thicknesses are less than the minimum practical thickness of manufacture. Hence, it is possible to design to extremely high probabilities of no-puncture for the header and tube backside, with the tube frontside probability of no-puncture close to the desired overall value. The dependence of weight on non-puncture probability is illustrated in Figure 4-15.

#### 4.2.2.2 Radiator Component Tests

Various tests were performed on the radiator at the component level to confirm operating characteristics. These are summarized below.

**THERMAL COATING:** Evaluation of the IITRI Z-93 coating properties was performed by TRW Inc on samples sprayed at the same time as the radiator test panels. The solar absorptance ( $a_s$ ) and total hemispherical emittance ( $\epsilon_h$ ) were measured to be .25 for  $a_s$  and .92 to .94 for  $\epsilon_h$ .

**HYDRAULIC CHARACTERISTICS:** Numerous hydraulic tests were performed on the radiator tubes using heated Dowtherm. Tests were performed on separate tubes, a full length radiator panel and finally the full size radiator. In the latter tests, a radiator pressure drop of about 15 psi was measured.

**THERMAL CHARACTERISTICS:** The heat rejection capabilities were measured using a short radiator quarter panel in a cryogenically cooled vacuum chamber. Measured heat rejection rates showed that design requirements were met.

#### 4.2.2.3 GDS Radiator Compared to FSCD Radiator

The GDS Radiator is essentially the same as the FSCD with minor differences as outlined below:

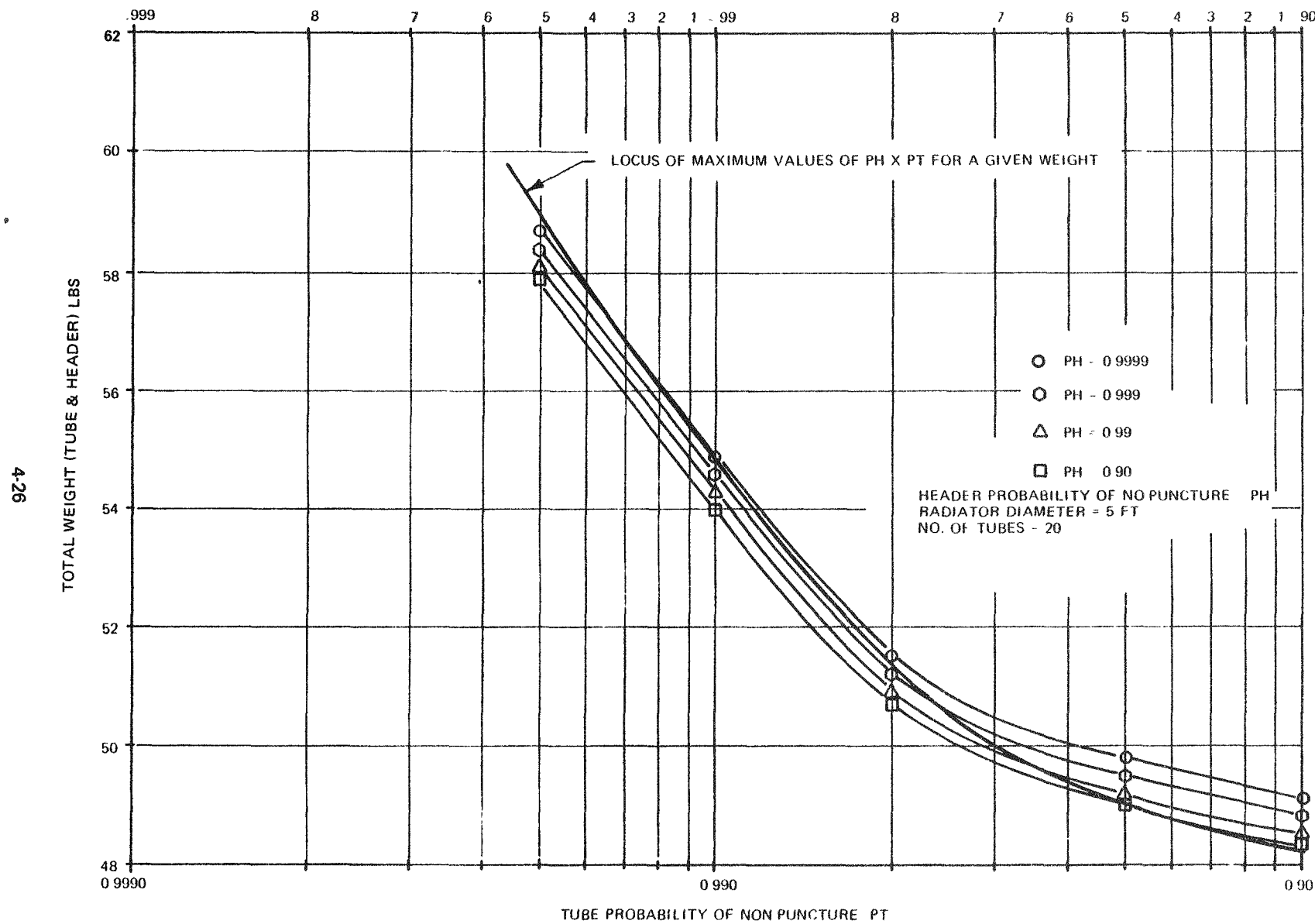


Figure 4-15 Relationship of Radiator Weight to Tube and Header Probability

- The FSCD radiator has 18 tubes while the GDS has 16 tubes.
- The FSCD radiator is shorter than the GDS resulting from backside radiation.

#### 4.2.3 GDS POWER CONVERSION SYSTEM

The Power Conversion System (PCS) comprises the components used to extract work from the superheated vapor and condense it to subcooled liquid. These components are the regenerator, jet condenser-accumulator, combined rotating unit, controls, associated hardware and plumbing. It was found during jet condenser component testing that if significant quantities of liquid were allowed to accumulate in areas where they may later be displaced, then jet condenser floodout could occur.

For this reason, and in order to simulate exactly the design of the FSCD, the PCS was designed to eliminate any possibility of condensation on cold surfaces. The resulting mechanical arrangement is essentially the same as that of the FSCD, except that in order to make use of existing hardware, the ducting that passes through the regenerator area splits the regenerator heat exchanger into two separate parts. This will not affect the operation of the regenerator.

Figure 4-16 shows a comparison of the flight system PCS to the GDS PCS. The obvious differences are in the packaging, removal of flanges and change in configuration of the accumulator. However, the basic configurations are operationally the same.

##### 4.2.3.1 GDS Regenerator

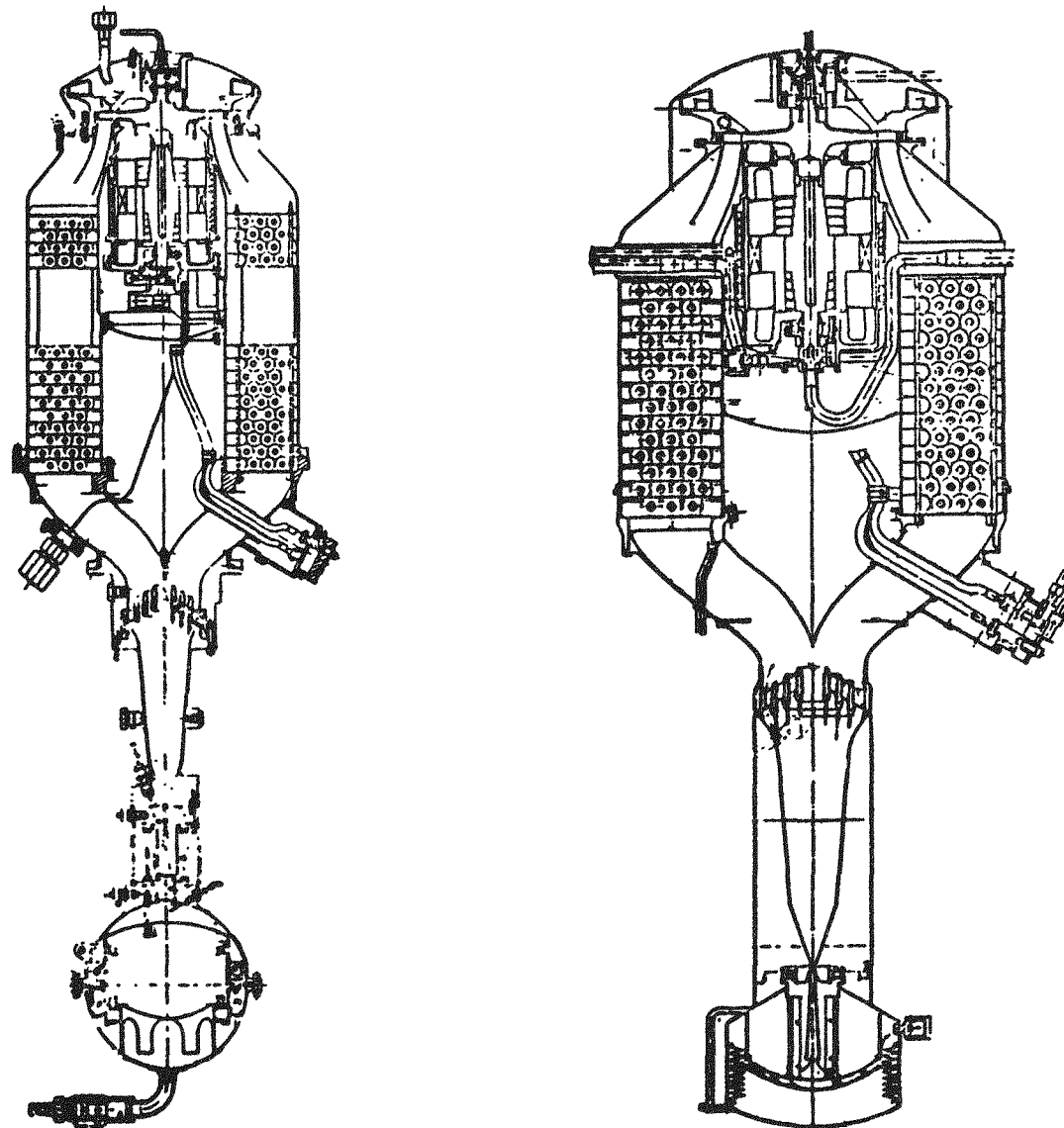
The heat exchanger configuration is the same as that of the FSCD; i.e. counter-flow finned tube, spirally wound in an annular arrangement around the combined rotating unit. Two mechanical arrangements have been used. The first employs all the finned tube coils in a continuous stack; this was used in the regenerator test rig and in the KIPS development test unit and is consistent with the FSCD. The second, used in the GDS, has the regenerator fin-tube assembly split into two separate stacks, in order to allow two ducts to pass through the regenerator shell walls to carry liquid plumbing lines. This was necessary to eliminate the possibility of condensation of the vapor on cold walls and yet use existing related hardware discussed in subsection 4.2.3. In both cases, the coils are supported by baffles and held together with tie bolts.

An electric preheater has been incorporated into the GDS regenerator flow circuit. This preheats liquid flow into the heat exchanger during the startup mode in order to prevent premature condensation which could cause jet condenser floodout. By doing so it permits faster, more repeatable startups.

The mechanical construction of the GDS regenerator is essentially the same as the FSCD with the exception that it has additional spacers to provide the gap for the plumbing ducts.

The test rig and development unit regenerator employed a brazed fin tube construction, while the GDS uses an integral fin-tube similar to the FSCD.

The adoption of the integral fin-tube construction for the GDS was based upon the greatly improved reliability that can be obtained. This results from the reduced number of joints and from the improved cleanliness qualities, since the potential presence of braze flux is a corrosion and fluid degradation risk statement.



(NOTE Not to same scale.)

Figure 4-16 System Comparison

The three regenerator configurations are shown in Figure 4-17.

#### 4.2.3.2 Condensing Heat Exchanger

The GDS injector is identical to the FSCD except that: (1) the ring end caps are brazed on the leading edge side rather than the trailing edge, (2) the orifices were made separate pieces from the injector body to facilitate testing of different orifice configurations. They were threaded into the injector body and then a bead of Epoxylite 6203 was placed around the base of the orifice to seal the threads, provide anti-rotation locking and aerodynamically fair the orifice to the injector body. Flanges and O ring seals were incorporated to facilitate the GDS development tests.

The vapor funnel for the GDS is identical to the FSCD except that flanges were incorporated on each end to facilitate testing. Instrumentation bosses were added to allow measurement of critical performance parameters. Wall thicknesses were left heavy in many areas for ease of manufacturing.

The GDS diffuser is identical to the FSCD except that wall thicknesses are larger to allow utilization of flanges, incorporation of instrumentation, and housing of an additional check valve. Figure 4-18 shows the two jet condensers.

Extensive rig testing has facilitated the formulation of a mathematical model with which it is possible to accurately predict the thermal performance (mixing chamber pressure performance) of a jet condenser.

The baseline GDS jet condenser incorporates 90 nozzles with 0.010 in. diameter injectors and 80 psia injection pressure. Initial GDS testing was performed with 45 nozzles having 0.0145 in. injectors.

In the GDS, thermal differential expansion between the jet condenser conical housing and the struts supporting the accumulator necessitated an expansion compensation bellows assembly located between the jet condenser and the accumulator. (The FSCD has fewer convolutions because of the redesigned support structure.)

The bellows assembly consists of two concentric bellows welded to common headers. The assembly is a redundant construction so that, if one of the bellows fails, it will not cause a system failure. The cavity between the bellows is evacuated.

The bellows is designed to meet a failure probability requirement of less than  $1 \times 10^{-9}$ . Each bellows was proof pressure tested and helium leak checked. The space between the bellows was then evacuated and sealed via an EBW process. The materials of construction are AM-350 for the laminations and 304L for the flanges.

#### 4.2.3.3 System Accumulator

The GDS system accumulator is compared to the FSCD accumulator in Figure 4-19.

The same rationale was used in selecting and sizing the accumulator for the FSCD and GDS. Because the GDS did not have a noncondensable gas removal system in its initial design, the amount of fluid in the accumulator was increased to keep the gas concentration in the system at an acceptable level for seven year mission. Also, the GDS accumulator has the extra capacity to keep the bearings lubricated in the event of jet condenser floodout during development of the system.

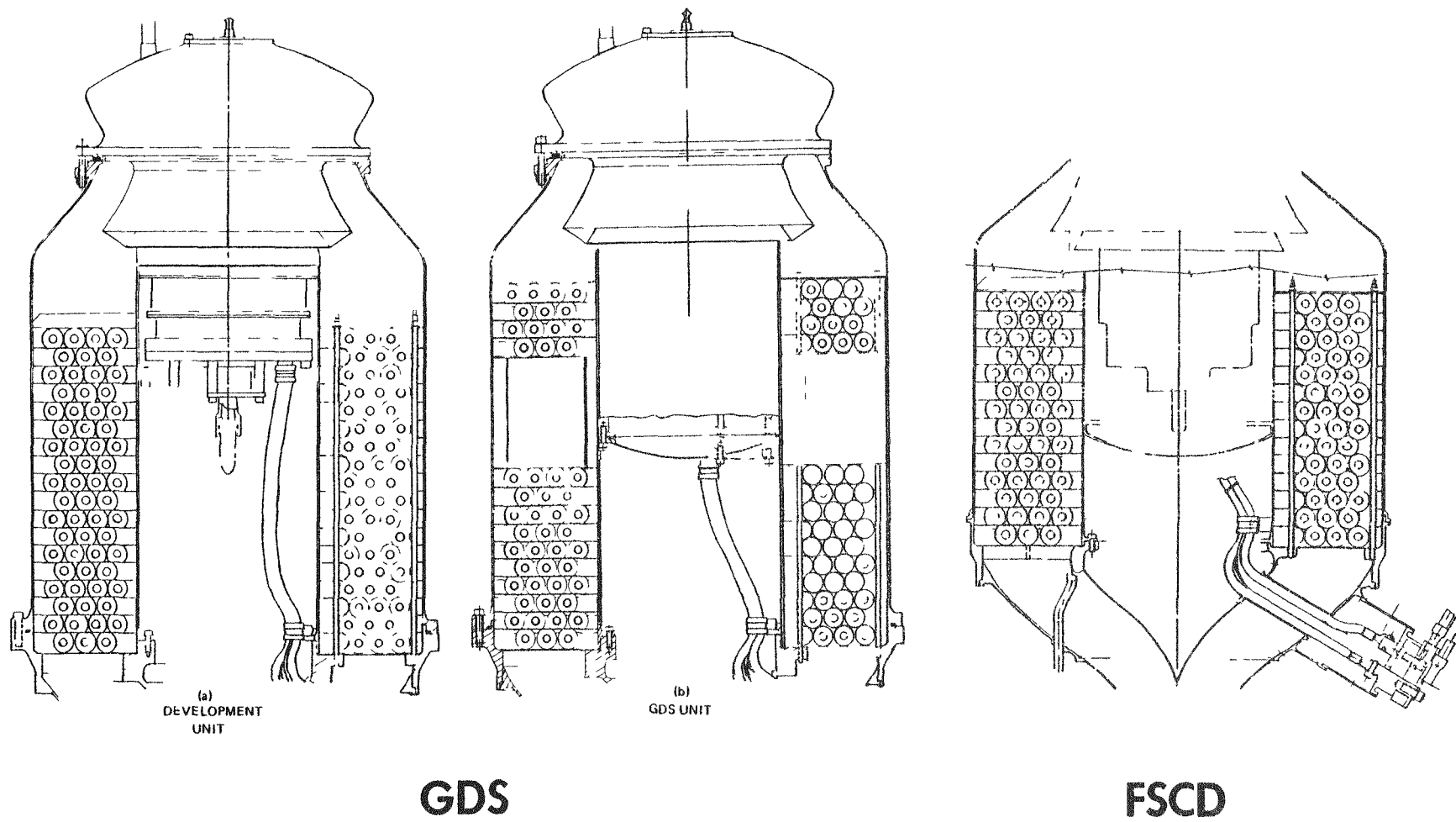
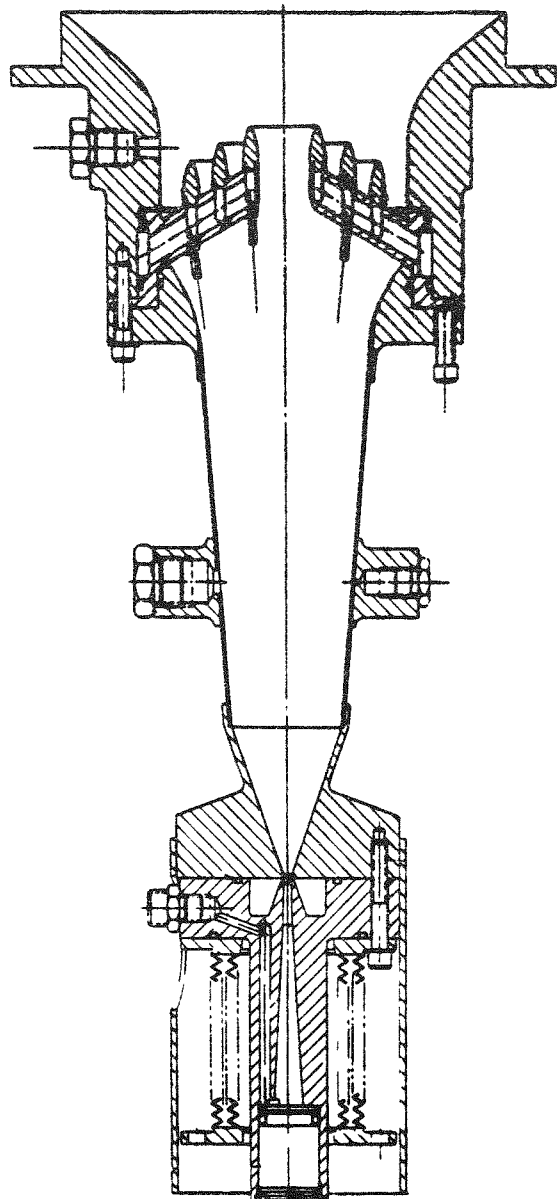
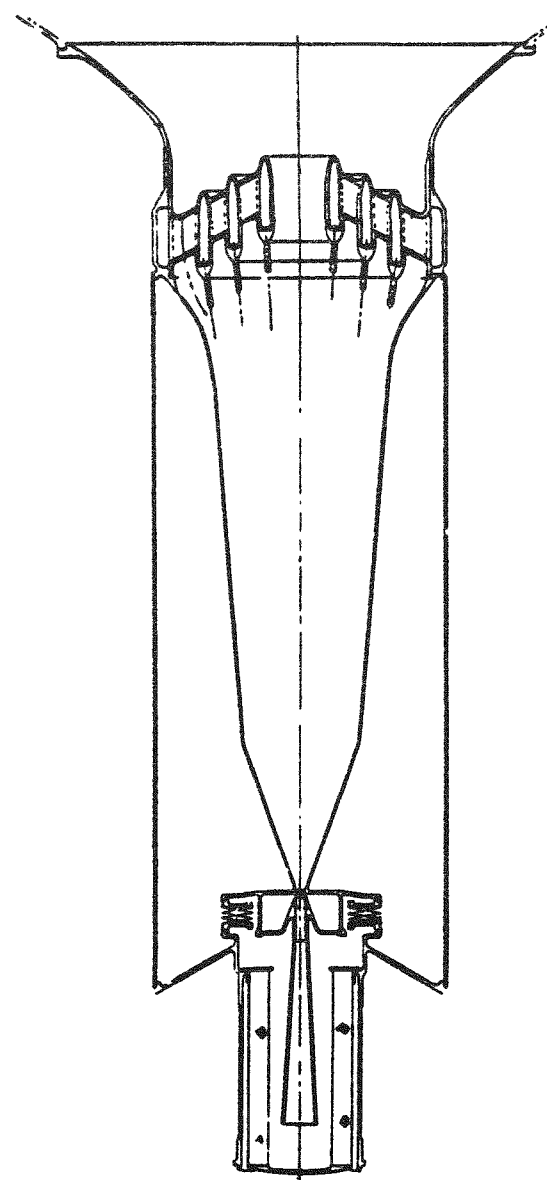


Figure 4-17 Regenerator Configurations



**GDS**



**FSCD**

Figure 4-18 Jet Condenser Configurations

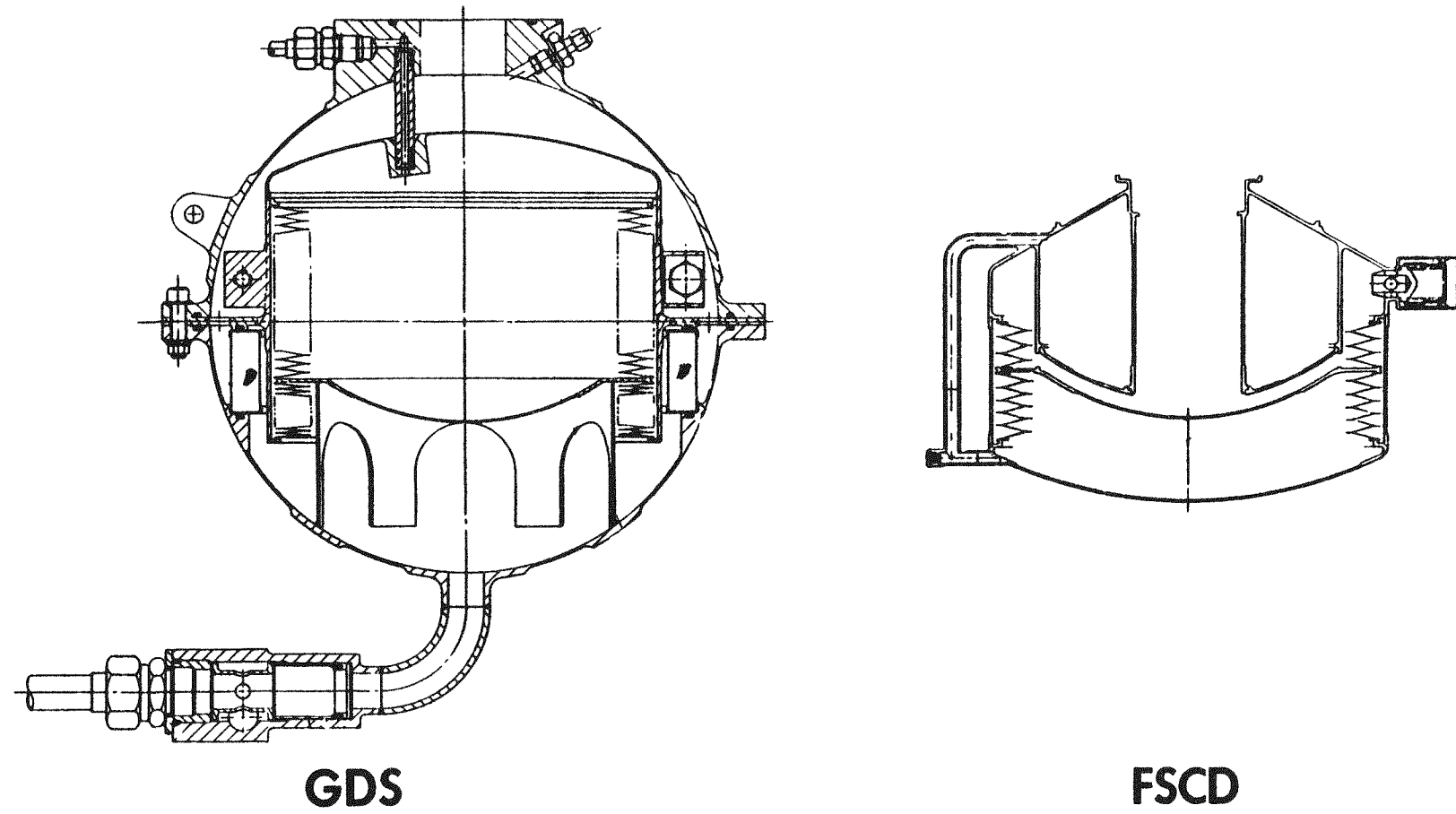


Figure 4-19 Accumulation Configurations

Because of these two reasons, the fluid volume was sized to be 185 cu. in. in the GDS. Taking advantage of the larger volume, the system filter in the GDS was made as large as the space would allow. Since the flight design is not restricted by the above considerations, it has a smaller volume.

The gas pressurization port was made accessible in the GDS to allow flexibility in setting jet condenser recovery during initial GDS testing.

The accumulator housings and the bellows assembly were stressed to meet a failure probability of less than  $1 \times 10^{-9}$ .

The accumulator housings were machined from 304L stainless steel. The bellows assembly was fabricated using AM-350 diaphragm material heat treated to the SCT 1000 condition, and 304L stainless steel material for the surrounding parts.

The bellows assembly was procured from Metal Bellows Company. All weld joints in the bellows assembly except those in the diaphragms were penetrant inspected. The final assembly was proof pressure tested and helium leak checked.

#### 4.2.3.4 Combined Rotating Unit

This subsection describes the combined rotating unit (CRU). Its function in the KIPS is to extract useful work from the Dowtherm and convert it into shaft power in order to produce electric power from the alternator and hydraulic power from the system pump. The term CRU results from having pump, alternator, and turbine on a common shaft. Figure 4-20 and 4-21 are photographs of the GDS CRU, while Figure 4-22 shows a comparison of the FSCD and GDS CRUs.

The GDS CRU is essentially the same as that of the FSCD described in subsection 3.2.3.4, apart from the pump size and difference in the turbine discussed in the FSCD section. The slight oversizing of the pump is necessary to provide sufficient pressure rise to overcome flow losses in instrumentation which will not be present in the FSCD.

**4.2.3.4.1 GDS TURBINE:** The turbine originally selected for the GDS incorporated the relatively long (wide chord), converging-diverging blade passage (supersonic) and was expected to be most efficient when used with the slightly merged nozzle ring. Rig test results indicated that this configuration was not as efficient as others tested. The configuration found to be highest in efficiency during rig testing was incorporated into the flight design and into the GDS retrofit CRU. The retrofit turbine has a narrower chord with constant area (subsonic) blade passages and achieves highest efficiency with slightly spaced nozzles. The turbine design is therefore essentially the same as that presented for the FSCD.

**4.2.3.4.2 SYSTEM PUMP:** The GDS system pump is shown in Figure 4-23. The pump design is the same as that of the FSCD (see subsection 3.2.3.4.2) except that the GDS pump was oversized to accommodate the most pessimistic predictions of component performance and to compensate for additional pressure drops associated with GDS instrumentation which would not exist in the FSCD.

Test results indicated a pump efficiency of 65%.

**4.2.3.4.3 ALTERNATOR:** The GDS and flight system alternator configurations are identical except for the four thermocouples placed within the armature windings of the GDS. The thermocouples' purpose is to monitor armature winding temperatures during ground demonstration tests only.

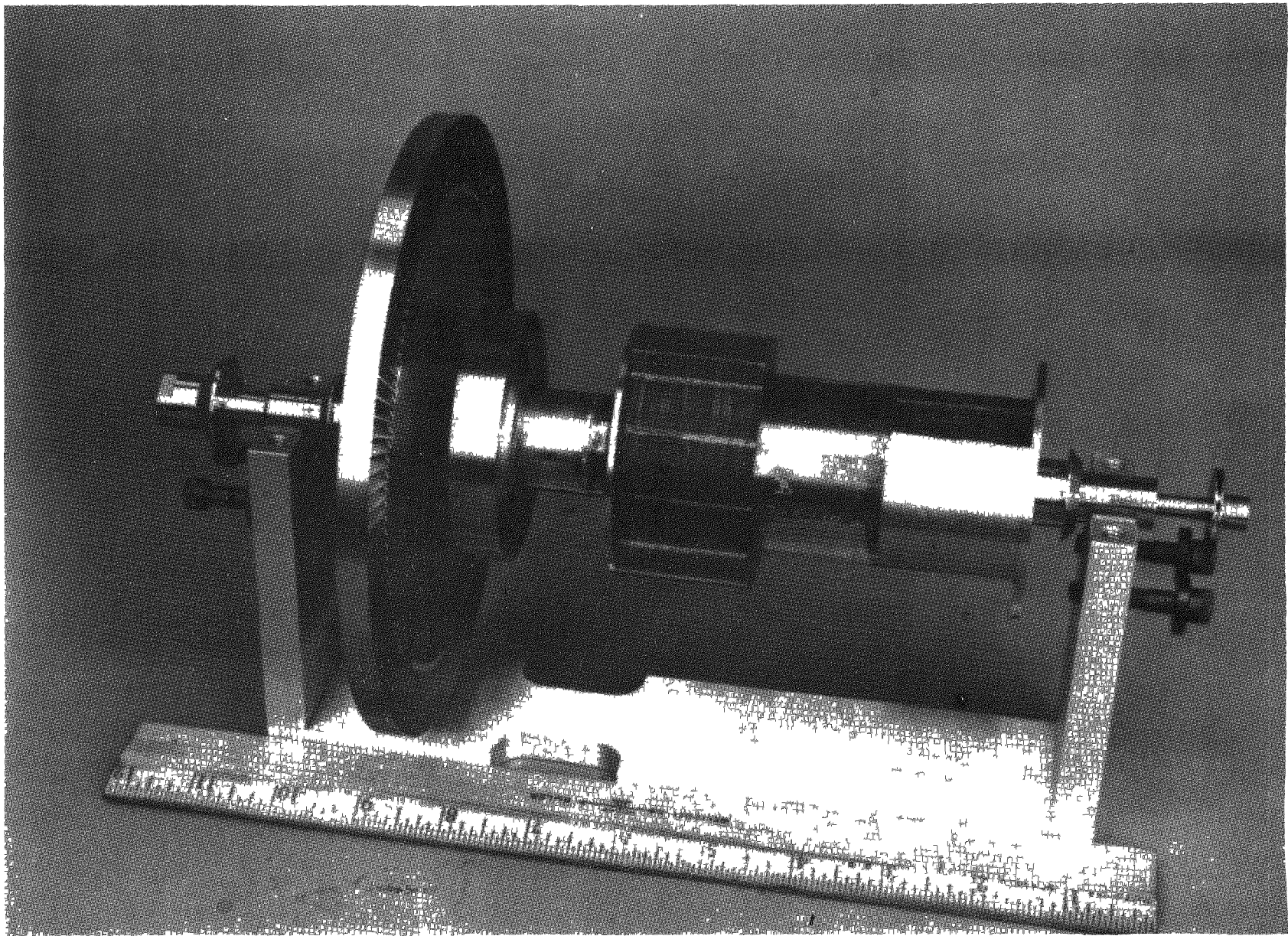
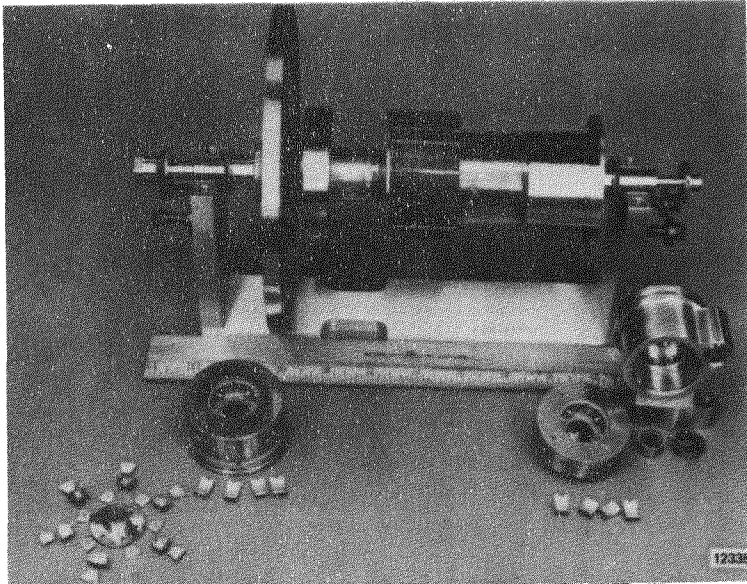
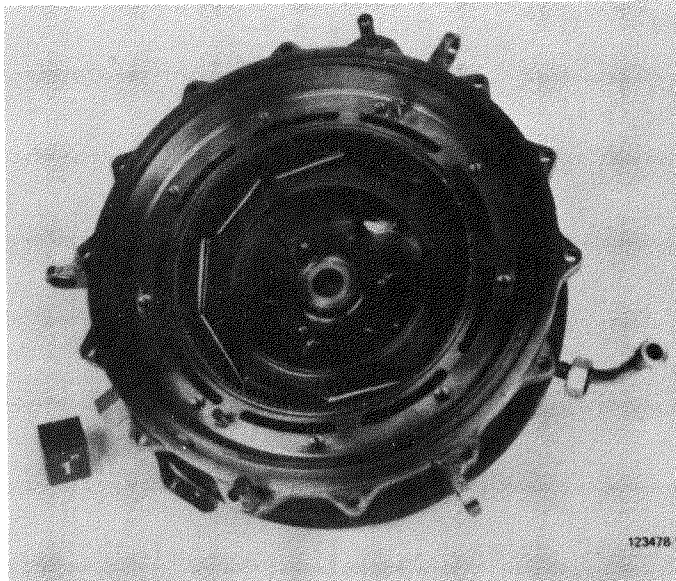


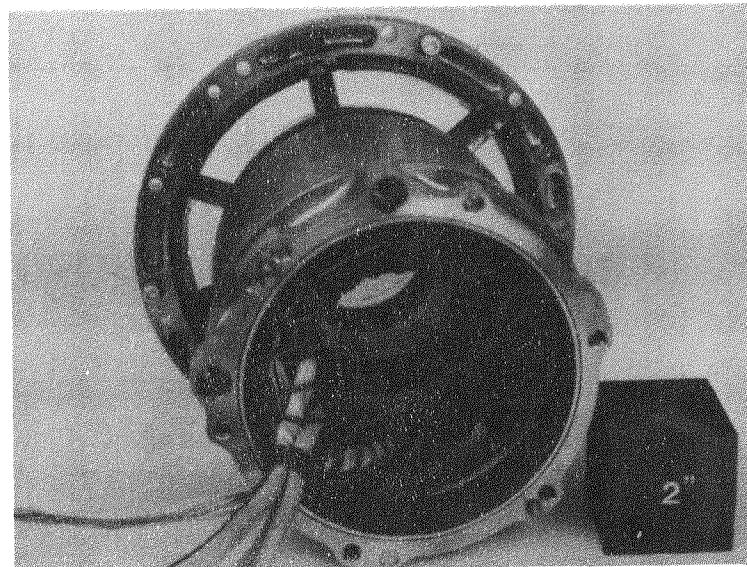
Figure 4-20 GDS Combined Rotating Unit



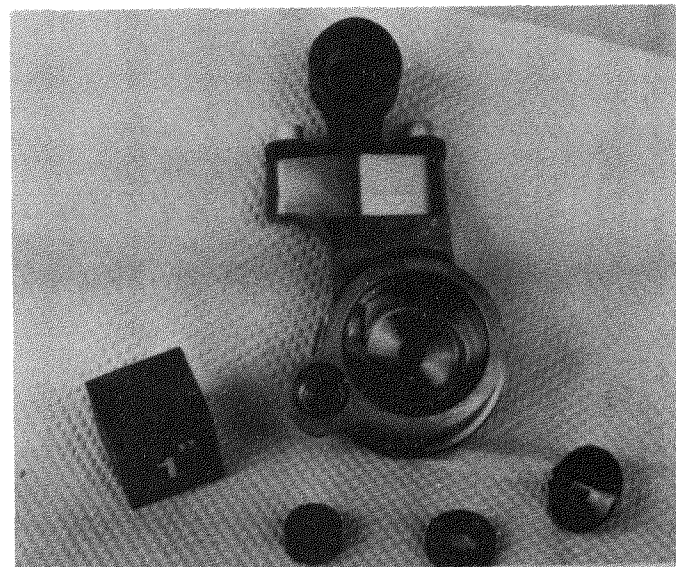
**ROTATING ASSEMBLY**



**NOZZLE HOUSING**



**ALTERNATOR STATOR**



**PUMP**

Figure 4-21 Combined Rotating Unit

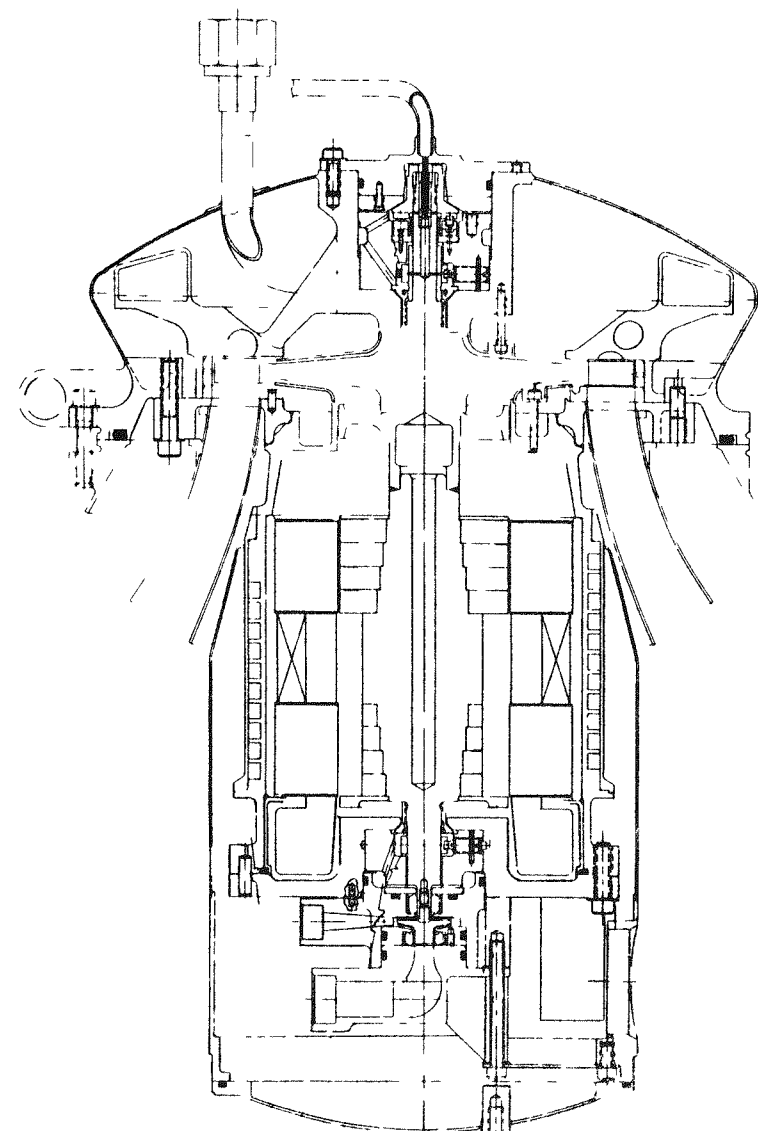
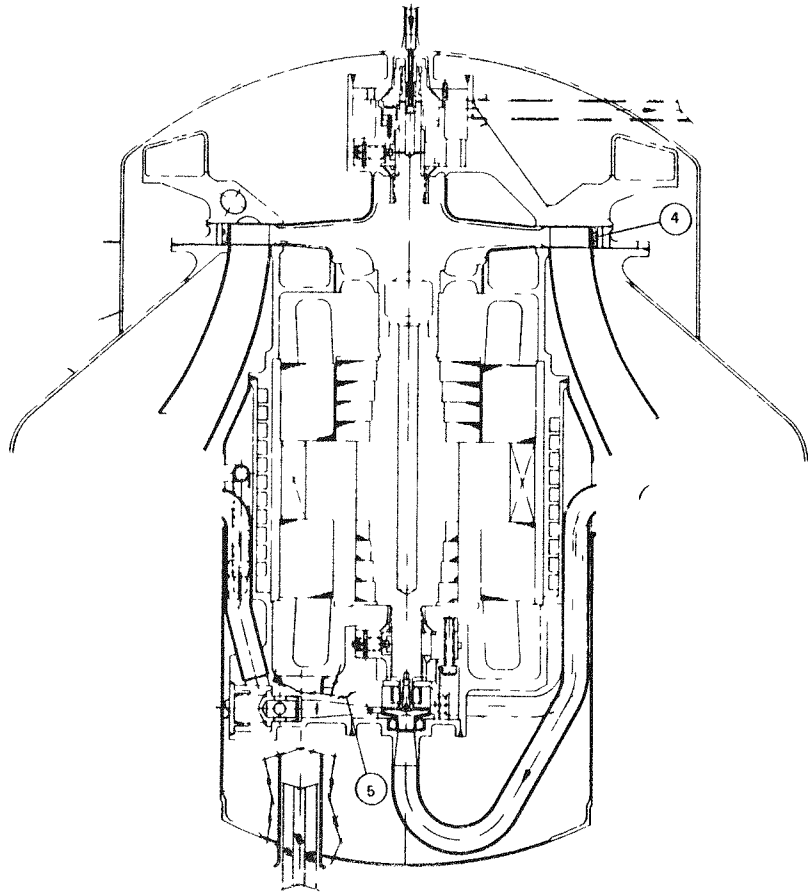
**GDS****FSCD**

Figure 4.22 Combined Rotating Units

(NOTE - Not to same scale)

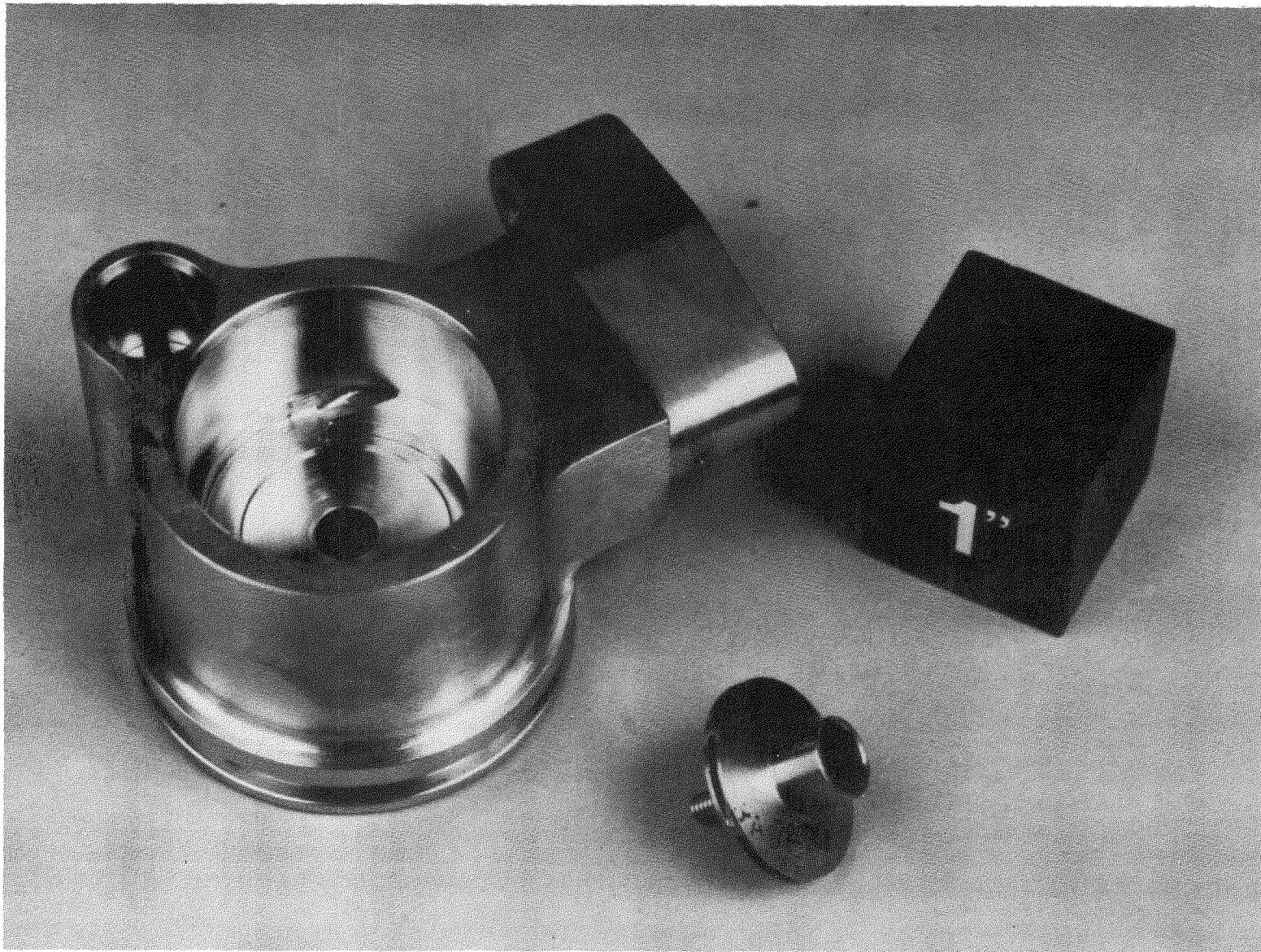


Figure 4-23 GDS Pump

4.2.3.4.4 BEARINGS: The GDS bearings are exactly the same as the FSCD bearings and are described in detail in subsection 3.2.3.4.4.

#### 4.2.3.5 GDS Control System

The GDS control system is identical to the flight control system with a hydraulic control valve pack for fluid loop control and a completely independent electrical controller to provide speed control, voltage regulation, overload protection, and power conditioning.

In the fluid loop valve pack, the radiator bypass valve and the turbine loop flow control have been tested as components and with the system, and perform as expected.

The electrical controller performs its speed control and overload protection functions as designed.

4.2.3.5.1 TURBINE FLOW CONTROL VALVE: The GDS version of the turbine flow control valve is functionally identical to the flight system version. The flexing flappers, bellows and nozzles are all identical as can be seen from Figure 4-24 where cross-sections of the two valve designs are shown. The only difference between the two versions is that the GDS unit is designed to use O ring seals on all components so they can be easily adjusted during system development and to permit inspection of the components at the completion of GDS testing. The flight version is of all-welded construction to meet the low leakage requirements of a seven year mission. This construction also reduces the valve weight.

The temperature sensors on the GDS were originally designed without fill tubes and were intended to be filled by evacuating the assembly and backfilling with NaK. This procedure proved to be unsuitable as the resulting sensors were "soft", indicating that a gas bubble had been trapped in the line during filling and sealing. The sensors were then modified to add fill tubes to permit "flow through" filling on both the GDS and flight designs, and satisfactory filling and operation have subsequently been demonstrated.

4.2.3.5.2 RADIATOR BYPASS VALVE: The GDS radiator bypass valve is identical to the flight valve. The valves installed in the flight and GDS housings are shown in Figure 4-25.

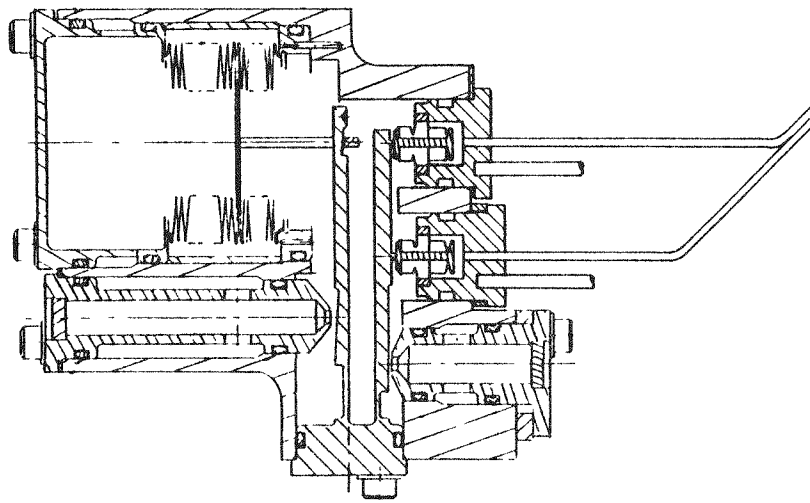
The predicted behavior of the bypass valve was demonstrated on a test loop. Data were accumulated to demonstrate the valve's linear bypass flow versus jet condenser inlet temperature characteristic. The acceptable limits on the valve's performance were established at two design points:  $60\% \pm 5\%$  bypass fraction at  $155^{\circ}\text{F}$ , and zero bypass flow at  $168^{\circ}\text{F}$ .

4.2.3.5.3 GDS ELECTRICAL CONTROLS: When the GDS controller was designed, the requirements were not completely or specifically defined in all aspects. Upon full definition of spacecraft requirements in Phase II, a controller can be designed to satisfy the requirements. The GDS controller is shown in Figure 4-26.

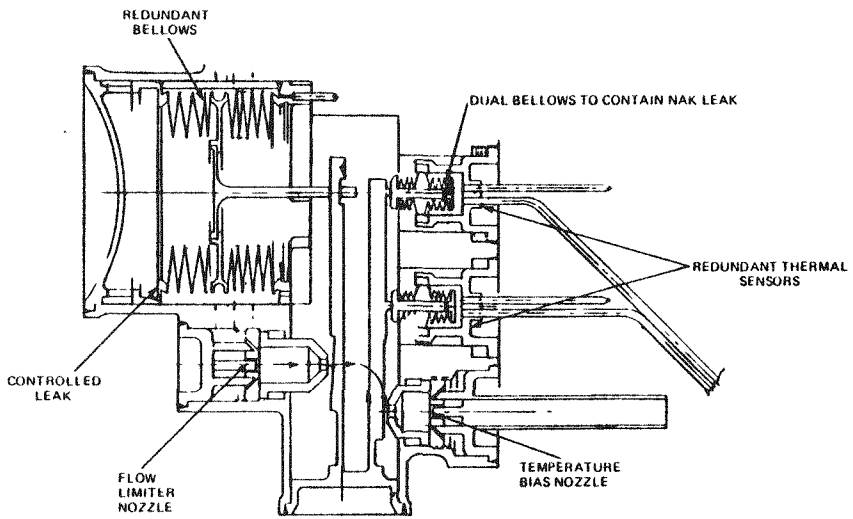
The circuits in the GDS controller are identical to those of the baseline flight system controller discussed in subsection 3.2.3.5.3. Minor differences occur in the reliability rating of components (JAN instead of JANTXV, for example) due to the longer lead times for the high reliability parts and the time constraints of the GDS schedule, but these differences do not affect performance.

The ripple content was not specified at the time of the GDS controller design, and a 2 volt RMS ripple was assumed to be acceptable for design purposes. The ripple content is at present specified

4-39



**GDS**



**FSCD**

Figure 4-24 Flow Control Valve

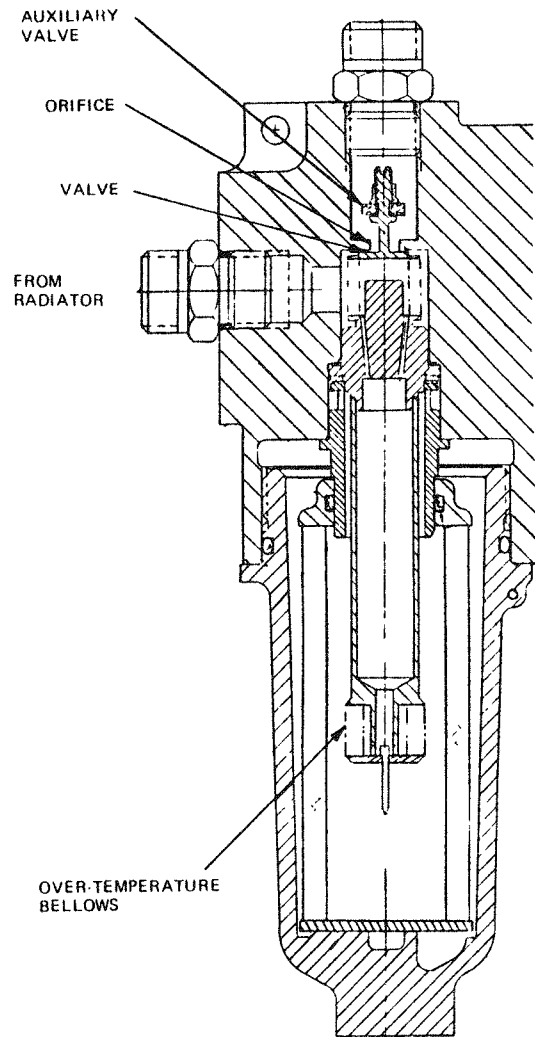
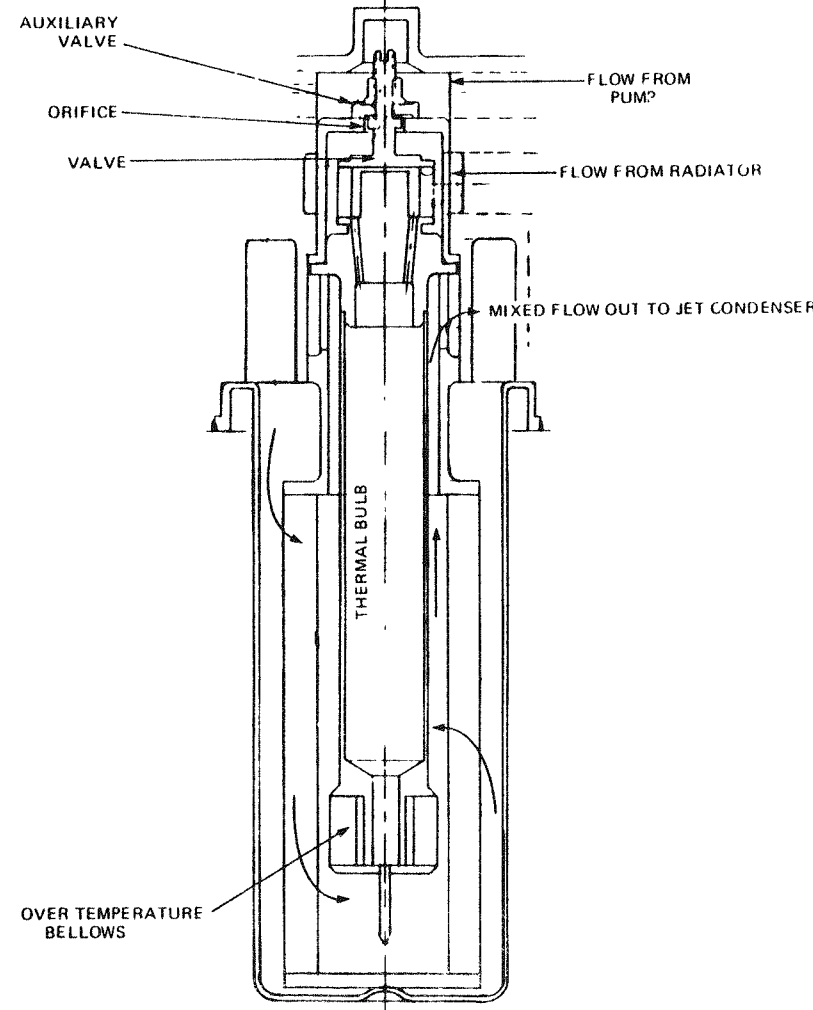
**GDS****FSCD**

Figure 4-25 Radiator Bypass Valve

(NOTE Not to same scale)

4-41

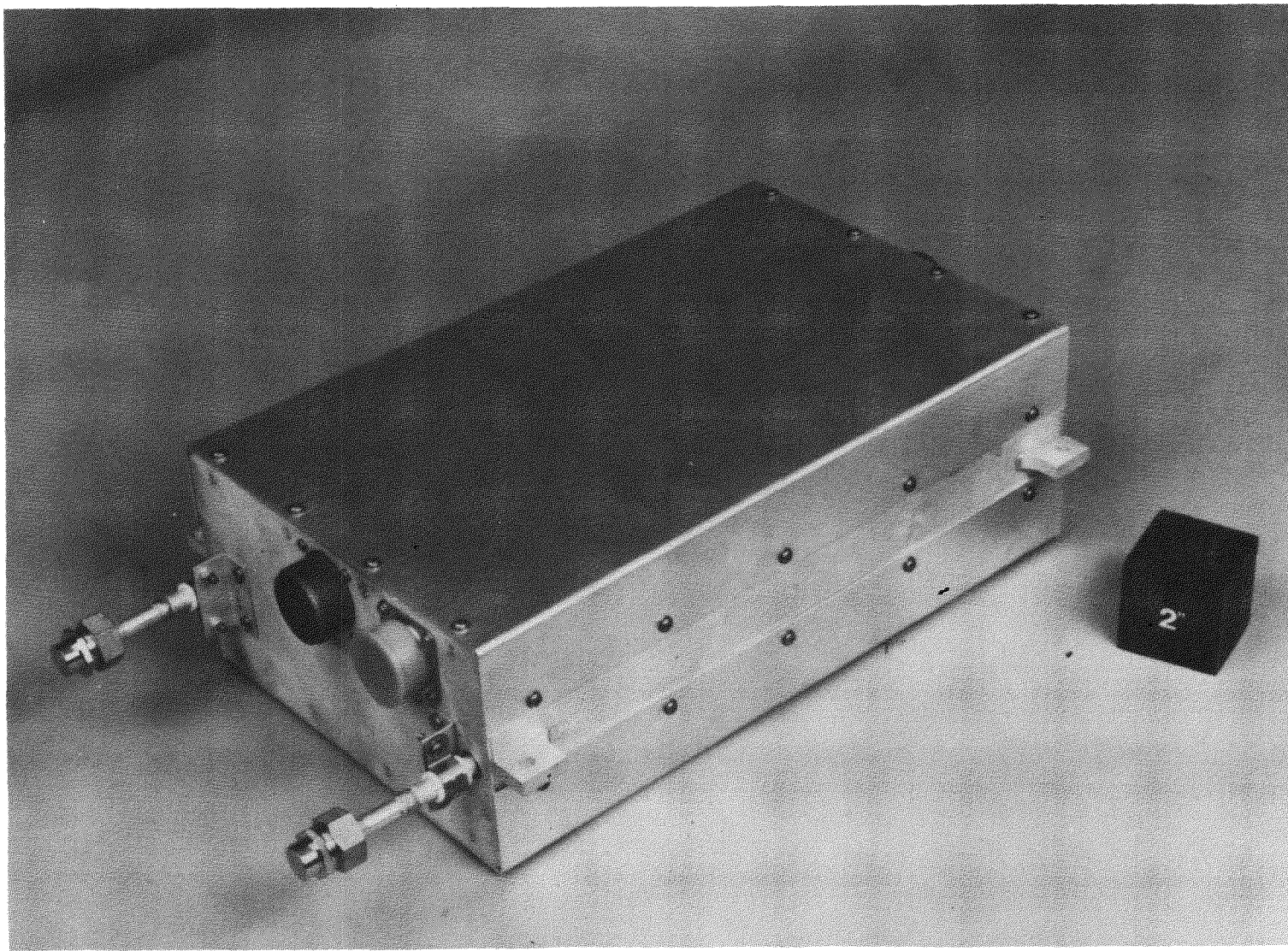


Figure 4-26 GDS Controller

at 0.1% RMS (0.028 volts RMS) for the flight system, requiring filter improvements over the GDS configuration.

The GDS controller includes instrumentation and test leads that are deleted in the flight controller.

Controller cooling is accomplished by means of a tube imbedded in the component mounting plate as in the flight version. This tube is cast into the plate in the flight version to reduce weight while it is clamped in place in the GDS version. A silver filled epoxy is used to fill the space between the tube and the clamp in the GDS for improved thermal contact.

The general configuration of the GDS controller is the same as the flight version, with power handling components mounted directly to the cold plate and low power components mounted on three printed wiring boards.

In its present configuration, the tuning capacitors are permanently wired into the circuit and have been found to cause excessive alternator self-excitation when running at the lower power levels typical of frequency wild operation. These capacitors are satisfactory for GDS testing, but a simple switch is incorporated for the FSCD.

The parasitic load resistor (PLR) is not the same as the flight design PLR since the GDS is to be tested on the ground only. The GDS uses a parallel assembly of wire-wound power resistors configured as three 1.1 OHM sections (power level at 28 volts is 2140 watts total). The PLR is located outside of the test chamber and dissipates the electrical load by convection. The flight design PLR will be a three section radiative heating element which is matched to the system requirements. This PLR is similar to the PLR described in NASA Report CR72436: "Design and Manufacture of Parasitic Load Resistors for Brayton Power Conversion System". The details of the PLR design for the KIPS program will be specified when the configuration analysis is complete; factors such as weight, reliability, mounting, and micrometeorite protection play important roles in this analysis.

#### 4.2.3.6 Miscellaneous Components

4.2.3.6.1 NONCONDENSABLE GAS REMOVAL SYSTEM: The GDS and FSCD noncondensable gas removal systems are both comprised of a palladium hydrogen diffusion cell and a noncondensable gas separator (NCGS).

The palladium diffusion cells for the GDS and FSCD are identical except that the GDS coil constraint assembly is built into a threaded plug which is installed to the GDS with an O ring seal. This is to facilitate assembly and removal during GDS testing.

The NCGSs for the GDS and FSCD are identical except that the GDS condenser heat exchanger shell is not an integral part of the valve pack housing as in the FSCD. This facilitates GDS component testing and checkout, permitting handling of the valve pack and NCGS independently.

4.2.3.6.2 CENTRIFUGAL SEPARATOR: The reasons for incorporating a centrifugal separator into the KIPS GDS are identical to the ones described for the Flight System Centrifugal Separator in subparagraph 2.3.3.6.2. The GDS separator is identical in configuration and operational characteristics to the FSCD centrifugal separator except for the addition of demountable fittings.

4.2.3.6.3 QUICK DISCONNECTS: There are four locations in the GDS where quick disconnects

are being used: accumulator gas pressurization port, accumulator bellows ullage cavity, accumulator outlet line and system pump outlet line. Their functions are as follows:

To allow hookup with minimum amount of air inclusion (0.002 cubic inch maximum)

To allow disconnect with minimum amount of fluid spillage (0.003 cubic inch maximum)

After disconnect, to keep the system hermetically sealed (leak rate less than  $1 \times 10^{-8}$  scc/sec He at 1 atmos.)

**4.2.3.6.4 FILTRATION:** The KIPS GDS has two filters in its loop. The function and need of these filters is the same as described in the FSCD section of this report. Refer to paragraph 3.2.3.6.4. The same rationale was used in selecting the micron rating of filters in the GDS as was used in the selection of the rating of filter elements in the FSCD.

The filter in the radiator flow loop is made per AN6235-4 configuration and the system filter is made similar to AN6236 configuration. The geometry is such that filters are removable and when installed, the joint is sealed with an O ring.

Both elements are of all stainless (304) construction. The filter mesh is welded to end rings via GTAW or EBW process. The filters are oversized to provide sufficient particle capacity. The stresses in these components are very low.

**4.2.3.6.5 GDS RADIATOR AUXILIARY HEAT EXCHANGER:** The GDS is operated without a radiator. Consequently, the auxiliary heat exchanger completely replaces the heat rejection function of the radiator, which is simulated hydraulically by an orifice in series with the heat exchanger.

The configuration of the heat exchanger is the same as for the FSCD except that, instead of being linear for mounting longitudinally to the inside of the radiator, it is bent into a semicircular shape and supported from the underside of the GDS support plate, in order to simplify packaging. The heat exchanger is connected to the coolant supply through 1/2 inch quick disconnect fittings.

The heat exchanger was sized for the complete 7200 watt heat rejection requirement and tube sizes were selected for Freon 21 as coolant in order to simulate the FSCD. Actual operation of the heat exchanger for the GDS employs water as coolant. The nominal operating conditions for water at design output power and zero radiator bypass flow are:

Flow	=	.87 gpm
T <sub>in</sub>	=	50°F
T <sub>out</sub>	=	96°F

In order to allow the heat exchanger to be bent into a semicircle, a helical wire separator was inserted between the inside and outside tubes. This prevented the inside tube from touching the outside tube and thus affecting heat transfer performance. After bending, the end caps were welded between the inside and outside tubes and all four fittings attached.

#### 4.2.4 GDS GROUND SUPPORT EQUIPMENT

The requirements for ground support equipment for the GDS are the same as those of the FSCD.

#### **4.2.4.1 Start Module**

The basic function of the GDS start module is the same as that of the FSCD, namely to supply liquid flow to the jet condenser, bearings, and turbine until the system pump can provide the required flow. However, additional functions have been added for convenience in conducting the test program. The major difference is the ability to deaerate the working fluid. Of secondary importance is the capability of evacuating the system liquid plumbing and of measuring the liquid inventory transferred into and out of the system. The start module is also used to provide the N<sub>2</sub> pressure reference for the system accumulator.

The GDS start module schematic is presented in Figure 4-27.

Deaeration of the working fluid is essential to prevent problems of jet condenser flood-out associated with brooming of the liquid jets when leaving the nozzles. The fluid is deaerated prior to introduction into the system. The deaerator can also be used during the initial operation of the system to remove any gases which may be generated by outgassing of various components, if the noncondensable separator is not installed.

#### **4.2.4.2 Heat Source Auxiliary Cooling**

The auxiliary cooling system provides heat rejection capability for the electric heat source assemblies (EHSAs) when the power conversion unit is not removing heat with the working fluid.

The start procedure for the GDS is similar to that of the FSCD and requires the boiler fin to be at design temperature before flow reaches the boiler assembly. This can be achieved by preheating the boiler and removing the heat with the auxiliary cooling system.

Whenever a KIPS shutdown occurs, whether planned or a safety shutdown, active cooling must be provided in order to prevent an overtemperature condition of the heat source assemblies. Even with heater electric power off, the thermal capacitance of the heater block requires active cooling for approximately three hours minimum to prevent overheating of the fin-tube, which would cause degradation of the Dowtherm.

Individual HSAs incorporate a 0.25 inch diameter coolant tube welded to the fin adjacent to the Dowtherm tube. Each HSA is connected in series with interconnecting tubes, thus providing a continuous flow path. The inlet to HSA No. 1 is plumbed into the temperature control system and the outlet of HSA No. 3 is vented to ambient. By flowing coolant through the boilers in a series fashion, the resultant fin temperatures are close to actual operating temperatures with Dowtherm flow and minimal temperature changes occur during the transition from nitrogen to Dowtherm flow.

The boiler fin temperature at the outlet of HSA No. 3 is sensed for controlling nitrogen flow. The error signal from the setpoint is used to activate a normally-closed ball valve in the nitrogen supply circuit in a bang-bang mode. The frequency is a function of the pressure setpoint; i.e., nitrogen flow through the cooling tubes. A backup 28 volts DC power supply is provided to operate the valves in the event of a facility power failure. In parallel with the normally closed valve is a normally open ball valve which provides constant flow in the event of a power failure or safety shutdown. The control has a nonoverride safety on the outlet fin temperature, with a maximum value of 800°F. This safety or any of the system safeties activate the normally open valve.

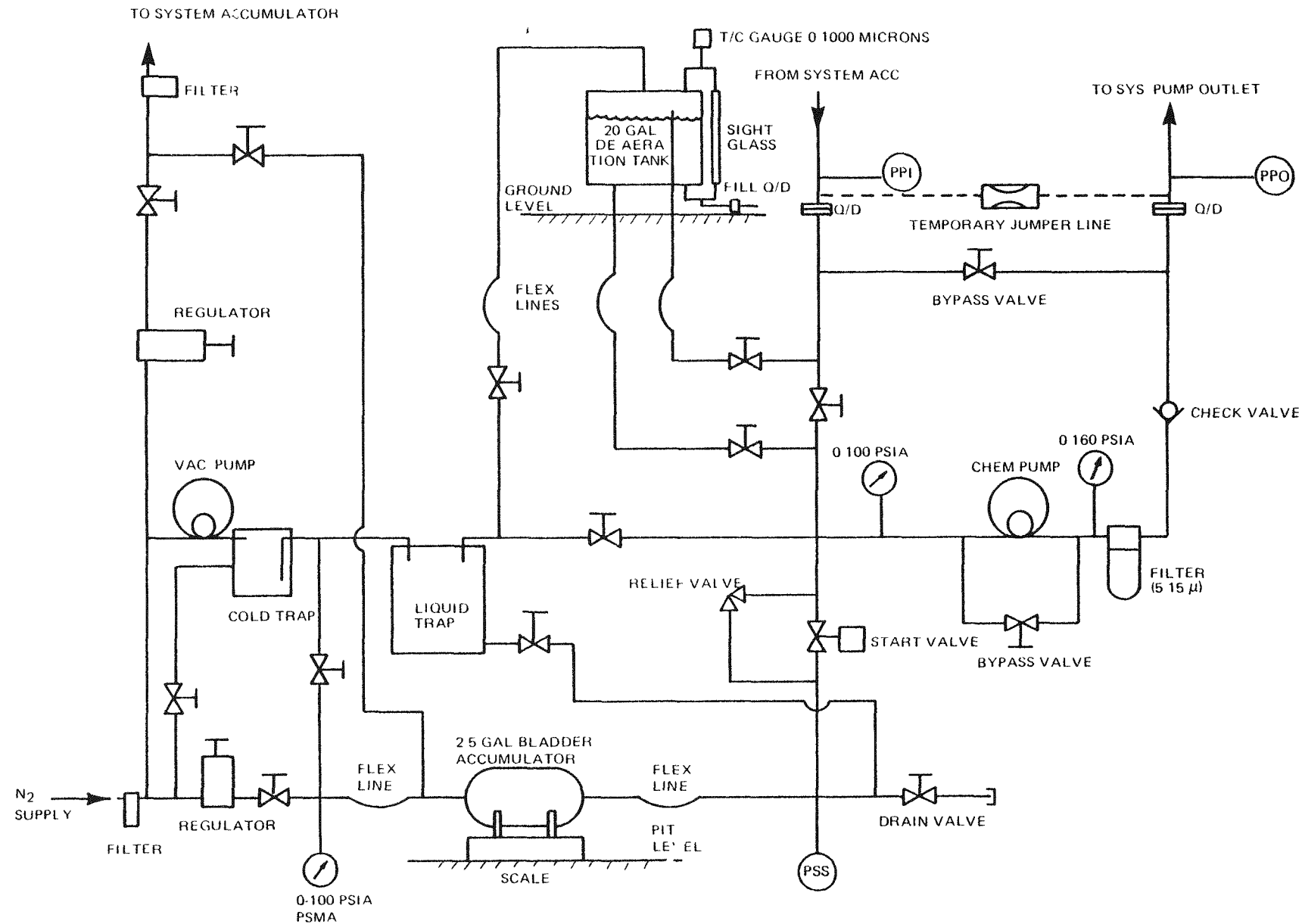


Figure 4-27 GDS Start Module Schematic

Backup nitrogen is provided by storage bottles in parallel with the facility nitrogen. If a nitrogen facility failure occurs, the backup supply automatically can supply flow. However, if the backup supply pressure drops below 2600 psig, the heater power is automatically turned off to allow the stored heat of the boilers to be removed before the backup supply is exhausted. Water is also plumbed into the nitrogen circuit to provide emergency cooling in the event of failure of both nitrogen supplies.

The schematic of the boiler temperature control system is shown in Figure 4-28.

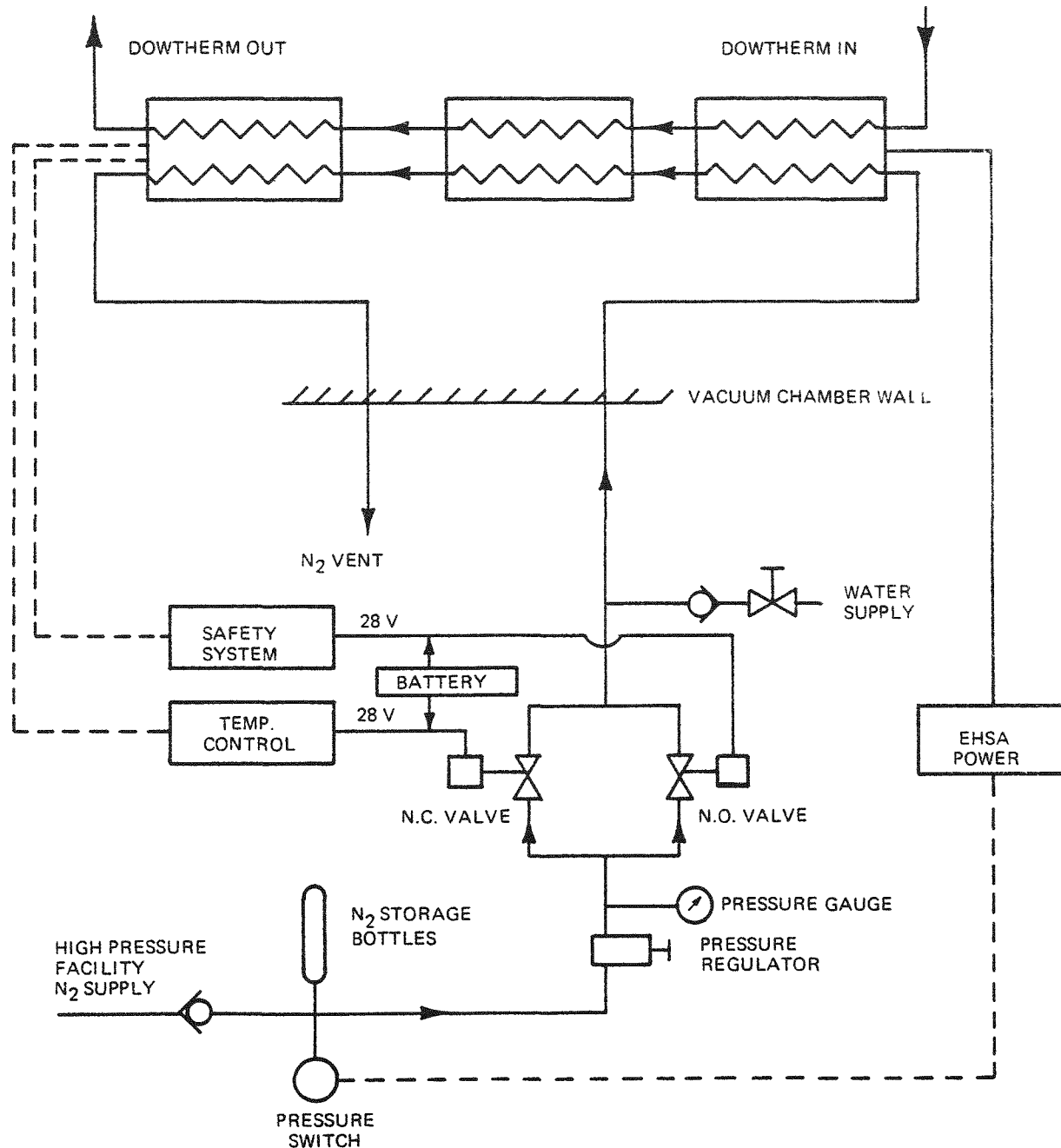


Figure 4-28 Heat Source Auxiliary Cooling Schematic

### 4.3 GDS TEST RESULTS

At the time of writing this report, the KIPS dynamic power system has been on test for approximately six months. In that time, system shakedown and development were performed on a development system. Higher performance components were retrofitted to the development system, yielding the Ground Demonstration System (GDS) configuration which closely simulates a flight design. Over 1100 hours of operation have been achieved on the GDS with more than 1600 hours on those components which were also run on the development system. System performance of greater than 15% overall efficiency has been demonstrated on the GDS and over 18% is achievable with further development. Table 4-B summarizes the major GDS test results.

Table 4-B Summary of KIPS Phase I Test Results

GROUND DEMONSTRATION SYSTEM	
Total Hours on GDS	1114*
System Efficiency (28 VDC Output)	15.15%
Number of Startup Cycles	29
DEVELOPMENT SYSTEM	
Total Hours on Development System	540**
System Efficiency (28 VDC Output)	11%
Number of Startup Cycles	118
NOTE: Total hours on components used in development system and GDS	1654
* Final GDS configuration with NaK sensor flow control valve had two continuous runs of 447 and 573 hours (total of 1020 hours). Intermediate shutdown was due to unscheduled plant power interruption. Intentional shutdown after 573 hours.	
** Longest continuous run was 470 hours. Intentional shutdown.	

**SECTION 5.0**  
**QUALITY, RELIABILITY, AND SAFETY**

## SECTION 5.0

### QUALITY, RELIABILITY, AND SAFETY

---

For the Phase I KIPS program, extensive quality controls were imposed by the DOE. The majority of the control requirements were inherent in Sundstrand's existing quality control system and the requirements unique to KIPS were readily implemented. Sundstrand prepared a Quality Assurance Program Plan, based on DOE Specification NRA-1, which was submitted to and approved by the DOE. This plan was followed during the Phase I program. During the last 6 months of this phase, a KIPS Quality Assurance Representative (from SANDIA Laboratories) was in full time residence at Sundstrand.

A Reliability Program Plan, based on DOE Specification SNS-2, was prepared, submitted to and approved by the DOE. This plan was followed during the Phase I effort. It was mandatory that the KIPS be designed to have the highest possible reliability in order to meet the design life goal of 7 years unattended operation.

Preliminary Ground Safety Assessment and Flight Safety Reports were prepared and submitted to the DOE. Detailing and expansion of these reports are planned for the Phase II effort.

**SECTION 6.0**  
**RECOMMENDED FOLLOW-ON PROGRAM**

## SECTION 6.0

### RECOMMENDED FOLLOW-ON PROGRAM

---

Two programs are presented here for consideration by the Department of Energy as follow-on effort to the KIPS Phase I Program. The first program proposed is for ground qualification of the system and the second is for technology verification and advanced development.

#### 6.1 GROUND QUALIFICATION PROGRAM

The Phase II program plan outlined here is a 30 month program, encompassing the flight design and fabrication of a system for ground qualification. Qualification will include testing with the MHW heat source as well as the electric heat source. The flight design will be based upon the technology obtained during the Ground Demonstration System design, fabrication, and testing in Phase I. Phase III would be the follow-on production phase for fabrication, acceptance test, and delivery of units in December of 1981 for flight test.

The objective of this Phase II KIPS program is to qualify an organic Rankine power system in the 500 to 2000 watt(e) output range for flight test in 1982. The program approach to meet this Phase II objective is:

- Designing and fabricating the proposed flight power system
- Conducting a development and a qualification program including both environmental and endurance testing, using an electrical and a radioisotope heat source
- Planning for flight test and spacecraft integration
- Continuing Ground Demonstration System testing to act as a flight system breadboard and accumulate life data

Phase II would consist of the ten tasks which are described in Table 6-A.

Table 6-A Phase II Task Summary

Task 1 — Program Management

- Program Direction
- Contract Administration
- Planning and Scheduling
- Evaluation of Progress and Performance
- Cost Planning and Control
- Document Control and Distribution
- Procurements
- Liaison with Other Program Participants and Potential User Organizations

Task 2 — Design and Analysis

- Heat Source Assembly
- Radiator
- Power Conversion System
- Ground Support Equipment
- Spacecraft Integration
- Component Specifications
- Design Reviews

Task 3 — Safety

- Launch and Flight Safety Analysis
- Ground Safety Analysis

Task 4 — Quality Plan

- Quality Assurance Plan
- Product Assurance Implementation
- Testing and Inspection Requirements
- Receiving, Source, and In-Process Inspection
- Non-Conforming Articles and Materials
- Material Review Board
- Ground Support Equipment
- Test Equipment

Task 5 — Reliability Plan

- Management
- Design Analysis
- Testing Evaluation

Task 6 — Fabrication and Assembly

- Assembly of Flight Qualification System (FQS)
- FQS Spares
- FQS Engineering Test Hardware
- GDS Upgrade
- System Mass Model
- Ground Support Equipment
- Component Sub-Assembly Tests
- Processes, Procedures, and Specifications

Table 6-A Phase II Task Summary (cont'd)

<p>Task 7 — Test Equipment</p> <ul style="list-style-type: none"><li>● FQS Testing</li><li>● GDS Testing</li><li>● Breadboard Stand Component Testing</li><li>● New Component Facilities</li></ul>
<p>Task 8 — Qualification Testing</p> <ul style="list-style-type: none"><li>● Test Plan</li><li>● Test Procedure</li><li>● GDS Testing</li><li>● Qualification Program Plan</li></ul>
<p>Task 9 — Component Development Tests</p> <ul style="list-style-type: none"><li>● Test Plans</li><li>● Heat Source Assembly</li><li>● Radiator</li><li>● Combined Rotating Unit</li><li>● Jet Condenser</li><li>● Other Components</li></ul>
<p>Task 10 — Reports &amp; Data</p> <ul style="list-style-type: none"><li>● Monthly Top Summary, Financial, Technical</li><li>● Topical and Special</li><li>● Final</li><li>● Phase III Program Plan</li></ul>

The time phasing of these tasks is shown on the Phase II schedule, Figure 6-1. The preliminary Phase III schedule is also included as part of this program plan as Figure 6-2.

## 6.2 TECHNOLOGY VERIFICATION PROGRAM

If the flight test of the KIPS is to take place later than 1982, it may be desirable to initially pursue a technology verification and advanced development program prior to ground qualification. In the Phase I effort, the KIPS demonstrated a system efficiency of 15.1 percent which is several percentage points short of the potential for an organic Rankine system of this size. Specific areas have been identified in which improvement in efficiency can be realized with further development. A system efficiency of over 18% is a realistic goal. Areas for efficiency improvement are in the dynamic seals, turbine, jet condenser and regenerator. This type of follow-on program could also address extended component reliability testing and a longer system endurance test.

The schedule, work definition and scope for this type program prior to ground qualification is directly dependent on the anticipated flight test date. If this program is desired, Sundstrand will work with DOE to develop the program plan.

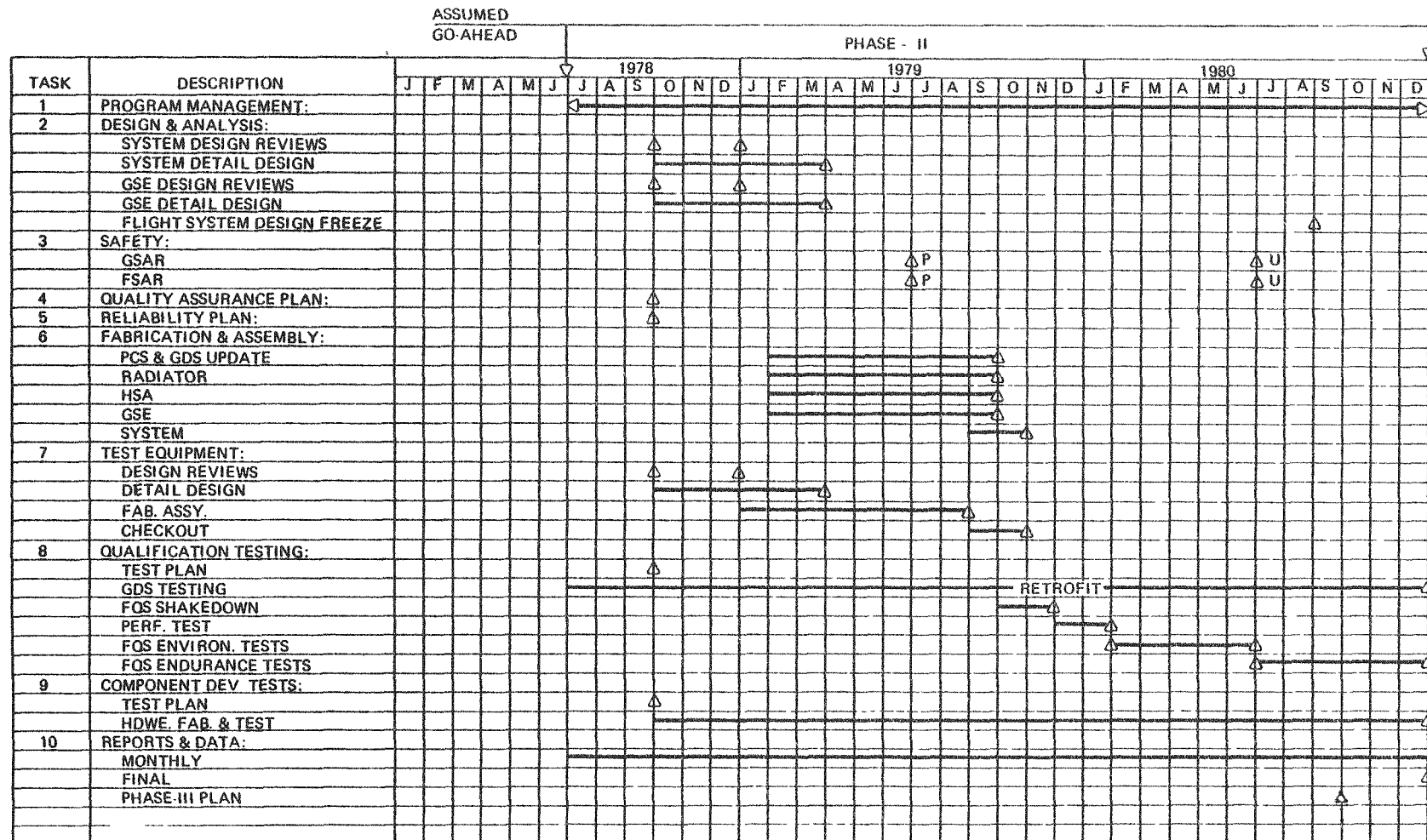


Figure 6-1 KIPS Phase-II Schedule

	PHASE III	1981											
		J	F	M	A	M	J	J	A	S	O	N	D
	FLIGHT SYSTEM												
1	PROGRAM MANAGEMENT												
2	FLIGHT SYSTEM SAFETY							▲					
3	QUALITY & RELIABILITY												
4	FLIGHT SYSTEM DESIGN/ ANALYSIS			▲									
5	FLIGHT SYSTEM FAB & ASSY								▲				
6	SYSTEM ACCEPT TESTS									▲			
7	FLIGHT SYSTEM DELIVERY										▲		
8	SUPPORT										▲		
9	REPORTS/DOCUMENTATION										▲		

Figure 6-2 KIPS Program Plan Schedule – Phase III